2010

RECAPITULATING OSTEOBLASTOGENESIS WITH ELECTROSPUN FIBRINOGEN NANOFIBERS AND ADIPOSE STEM CELLS AND ELECTROSPINNING ADIPOSE TISSUE-DERIVED BASEMENT MEMBRANE

Michael Francis
Virginia Commonwealth University

Virginia Commonwealth University

This is to certify that the dissertation prepared by Michael Paul Francis entitled RECAPITULATING OSTEOBLASTOGENESIS WITH ELECTROSPUN FIBRINOGEN NANOFIBERS AND ADIPOSE STEM CELLS AND ELECTROSPINNING ADIPOSE TISSUE-DERIVED BASEMENT MEMBRANE has been approved by his or her committee as satisfactory completion of the dissertation requirement for the degree of Doctor of Philosophy.

Dr. Shawn E. Holt, School of Medicine

Dr. Gary L. Bowlin, School of Engineering

Dr. Lynne W. Elmore, School of Medicine

Dr. Colleen K. Jackson-Cook, School of Medicine

Dr. Matthew J. Beckman, School of Medicine

Dr. Jerome F. Strauss, Dean of the Medical School

Dr. F. Douglas Boudinot, Dean of the Graduate School

February 9, 2010

RECAPITULATING OSTEOBLASTOGENESIS WITH ELECTROSPUN FIBRINOGEN NANOFIBERS AND ADIPOSE STEM CELLS AND ELECTROSPINNING ADIPOSE TISSUE-DERIVED BASEMENT MEMBRANE

A dissertation submitted in partial fulfillment of the requirements for the degree of Doctor of Philosophy at Virginia Commonwealth University.

by

MICHAEL PAUL FRANCIS

B.A. Philosophy, University of Akron, 2001

B.S. Biology, University of Akron, 2001

Major Director: Shawn E. Holt, Associate Professor
Department of Pathology, and
Department of Pharmacology and Toxicology, and
Department of Human and Molecular Genetics

Virginia Commonwealth University
Richmond, Virginia

February 2010

Acknowledgements

I would like to thank Dr. Shawn Holt and Dr. Lynne Elmore for the freedom to explore the regenerative medicine and aging research fields in your labs. Shawn has allowed me to make and correct innumerable mistakes in my work, allowing me to gain true expertise in my art, teaching me how to be a better scientist, while unquestionably making me a better science writer in the process.

I thank Dr. Gary Bowlin for sharing your extraordinary laboratory equipment and many exceptional and inspirational scientific ideas.

To Dr. Matthew Beckman, the straightest shooting scientist I have met, your frank office conversations have been a guiding light.

To my labmates Pat, Scott, Parth, Yas, Koyal, Michael, and Malissa, it has been an honor working and sharing ideas with you these past 3 years, and hopefully for years to come.

To Dr. Roy Ogle, your office and lunch conversations at UVA taught me more then all my graduate school coursework combined.

To Mom, Dad, Kevin and Crystal, your love and patience in supporting me through this tempestuous journey can only be described as heroic.

To my grandfather, Joseph Francis, boundless thanks are owed to you for infecting me with your curiosity and enthusiasm for life, and for teaching me perseverance.

Finally, I would like to thank the many enthusiastic friends, family and other non-scientist who would listen eagerly to my scientific visions and aspirations to help forge a better future, and return my excitement in kind.

Table of Contents

List of Tables

Page

List of Figures

Page

Abstract

RECAPITULATING OSTEOBLASTOGENESIS WITH ELECTROSPUN FIBRINOGEN NANOFIBERS AND ADIPOSE STEM CELLS AND ELECTROSPINNING ADIPOSE TISSUE-DERIVED BASEMENT MEMBRANE

By Michael P. Francis, B.A., B.S.

A dissertation submitted in partial fulfillment of the requirements for the degree of Doctor of Philosophy at Virginia Commonwealth University.

Virginia Commonwealth University, 2010

Major Director: Shawn E. Holt, Associate Professor
Department of Pathology,
Department of Pharmacology and Toxicology, and
Department of Human and Molecular Genetics

To repair, replace, or regenerate damaged or diseased tissue has been a long-standing, albeit elusive, goal in medical research. Here, we characterize patient-derivable mesenchymal stem cell types, termed adipose-derived stem cells (ASCs). These cells, which can be derived from liposuction fat and lipoaspirate saline, are sources for patient-derivable extracellular matrix (ECM), fibrinogen (Fg) and adipose tissue extracellular matrix, and may prove useful for synthesizing new bone tissue analogues *in vitro*.

Traditionally and rapidly isolated ASCs were thoroughly characterized as multipotent, having osteogenic, adipogenic, and chondrogenic differentiation potential, and they exhibited

comparable proliferative lifespans. These ASCs also shared an indistinguishable immunophenotype when compared to bone marrow-derived mesenchymal stem cells, suggesting that these cells are an excellent source for bone following tissue engineering experimentation.

In order to synthesize bone *ex-vivo*, electrospun scaffolds of fibrinogen (Fg), polydioxanone (PDO), and Fg:PDO blends were seeded with early passage ASCs, fibroblasts, or osteosarcoma cells and were maintained for 21 days in osteogenic or regular growth media. Constructs were analyzed both histologically and molecularly for evidence of osteoblastogenesis. Using SEM, the appearance of regular, mineralized-appearing structures were found in osteogenic-induced ASC seeded scaffolds beyond 14 days, only in the scaffolds containing Fg. Further, at 21 days of culture, Fg scaffolds with ASCs in osteogenic media became hard and brittle. Robust new collagen synthesis and matrix remodeling were observed on all Fg scaffolds, the levels of which were elevated over time. Pronounced mineralization was found throughout bone-induced ASC scaffolds, while control scaffolds (BJ foreskin fibroblasts) showed no mineral deposition (although they did demonstrate excellent cellularity). Analysis of gene expression (qRT-PCR) indicated that electrospun Fg supported osteoblastogenesis through the upregulation of alkaline phosphatase and osteocalcin gene expression. To confirm our gene expression results, osteogenic-induced ASCs on Fg scaffolds were also shown to secrete osteocalcin in the extracellular matrix, a key marker in osteoblastogenesis. Thus, electrospun Fg is an excellent material for ASC growth, proliferation, and osteogenic differentiation, providing an ideal system for furthering basic bone model-based research and for advancing regenerative medicine.

In addition to establishing Fg as a source of scaffolding, we developed and characterized a novel method for isolating and subsequently electrospinning adipose tissue matrix. Because

adipose ECM contains many primordial matrix proteins important for embryonic development and regeneration (such as laminin, type IV collagen, and fibronectin), adipose ECM may prove to be an autologous tissue engineering matrix and stem cell culture substrate. We show here that adipose tissue ECM can, in fact, be electrospun into a nanofiberous mesh, histologically shown to contain connective tissue, collagens, elastic fibers/elastin, proteoglycans, and glycoproteins in the newly synthesized matrix. We also show that this novel electrospun adipose tissue scaffold is capable of supporting stem cell growth. Taken together, experiments using ASCs cultured on extracellular matrices of electrospun Fg or adipose ECM present an excellent framework for future advances in regenerative medicine therapeutics and research.

-Chapter 1-

Background and Significance

Bone: Basic Biology

Bone, a seemingly simple tissue, carries out a lengthy list of functions in the body including, but not limited to, organ protection (skull and ribs), red and white blood cell production, mineral storage (phosphorous), and fat storage. Bone holds 99% of the total body calcium, a mineral critical for innumerable physiological processes. Bone is also crucial for locomotion, heavy metal detoxification, buffering the blood against excessive pH, and providing shape to the body, as well as being essential for sound transduction (hearing) (Lieberman and Friedlaender, 2005).

Bone is a special form of connective tissue, composed of microscopic crystals of phosphates and calcium within a matrix of collagen, primarily Type I, which is also the major structural protein in skin and tendons. This collagen is typically 300nm in length with regular 67nm banded fibrils in its fundamental unit and is as strong as steel, kilogram-for-kilogram (Haralson et al., 1995). Type I collagen is made up of a triple helix of three polypeptides tightly bound together, two of which are identical α_1 polypeptides, encoded by a single gene, with a separate gene producing the third chain, the α_2 polypeptide (Haralson et al., 1995).

Sufficient quantities of protein and minerals are essential for normal bone maintenance. Bone crystals, made mostly of inorganic mineral hydroxyapatite ($Ca_{10}(PO_4)_6(OH)_2$), measuring 20nm x 3-7nm, comprise 70% of the dry weight of bone (Lieberman and Friedlaender, 2005). Sodium and trace amounts of carbonate, magnesium, and other metals are also present in mature bone. Macroscopically, most bones are made of a compact outer layer, surrounding trabecular

bone and, in many cases, a bone marrow cavity. Trabecular, or spongy, bone is composed of bone spicules separated by open spaces or pores that undergo constant remodeling, the dynamic physiology of which is critical for maintaining healthy bone.

In the highly intertwined and dynamic process of bone remodeling, giant multinucleated cells, called osteoclasts, function to break down bone matrix. Osteoclasts become multinucleated by cell fusion and are believed to be derived from hematopoietic stem cells of the resident bone marrow. In an acidification process using hydrogen pumps (with Na+/K+ ATPase; HCO_3-/CL- exchanger; Na+/H+ exchangers), osteoclasts solubilize and erode bone crystals, followed by the release of enzymes to digest remaining bone proteins and the formation of resorption lacunae into which osteoclasts burrow (Liebschner et al. 2003). The growing resorption lacunae are followed by and partially filled with forming capillaries to supply nutrients to the bone cells. Once the lacuna acquires a certain depth, osteoblasts enter the formed cavity and fill it with osteoid. The more osteoclasts that are activated, the more bone is resorbed and the more calcium released. Trabecular bone becomes increasingly brittle as the number and depth of the resorption lacunae increases and the diameter of the remaining trabeculae decreases; whereas, conversely, healthy bone of athletes is typified by thick, dense trabeculate.

New bone is produced by osteoblasts, which are mononuclear cells arising from progenitors located in the marrow and the periosteum. Osteoblasts secrete large quantities of type I collagen, alkaline phosphatase, and other bone matrix proteins and typically fill resorption lacunae as they are created by protagonist osteoclasts. The new bone material, or osteoid, formed by osteoblasts is rendered hard through calcium phosphate crystal deposition. Once the osteoblast is incorporated into the bone matrix, it becomes quiescent and is known as an

osteocyte, occupying a small cavity or bone lacuna in the matrix. From the lacuna, osteocytes radiate "arms" through slender channels to communicate with neighboring lacunae. One of the more interesting histological features of mature bone is the relative scarcity of cells in the dense tissue matrix and the regular spiral patterning created by the bone remodeling process.

Only 5-20% of the bone typically undergoes remodeling at any time with the rest existing in a quiescent state. The local bone remodeling process begins with the activation of osteoclasts and concludes with new bone formation by osteoblasts, requiring 3-4 months to complete. In healthy individuals, 5-10% of the total bone substance is replaced annually (Liebschner et al., 2003).

Bone: Regeneration

Along with the liver and kidneys (nephrons), bone is one of the few tissues in adult mammals that can undergo true regeneration, complete with blastema formation and asymmetric cell divisions, rather than scarring for wound repair. Healing of a fractured bone in the body occurs through distinct yet overlapping stages (Lieberman and Friedlaender, 2005). The first is the *early inflammatory stage* where a fibrin-laced hematoma develops within the fracture. This hematoma is a blood clot that originates from lacerated blood vessels in the bone and the periosteum. Hematoma formation leads to the infiltration of inflammatory cells such as macrophages, monocytes, and lymphocytes, as well as osteoblasts to clean and resorb the necrotic bone and inflamed hematoma. Granulation tissue develops from cells of the periosteum and endosteum as the hematoma is resorbed, followed by an infiltration of pluripotent mesenchymal stem cells into the granulation tissue to begin repairs (Schindler et al., 2008). This

granulation tissue formation process is typical of an early stage wound in most mammalian tissue types, with the stimulation of an ingrowth of vascular tissues and recruitment of progenitor cells as key features.

In the second stage of healing, *the repair stage*, the progenitor cells differentiate into chondrocytes and later osteocytes, producing cartilage and bone, respectively. These differentiated osteocytes can be recognized by the upregulation of common bone-specific marker genes and proteins, such as osteocalcin, osteopontin, and bone sialoprotein protein (Liebschner et al., 2003). Recruited fibroblasts further lay down a mesh of stroma supporting vascular ingrowth in the granulation tissue, with the collagen matrix supporting the osteoid. A soft callus structure finally forms around the repair site that fills with woven bone made by the osteoblasts.

Fracture healing concludes in the *late remodeling stage*, where healing bone regains its original structure, shape and mechanical integrity. This remodeling occurs over months to years, shrinking the callus as the trabeculae form along stress lines, and thus, the late healing process is highly facilitated by mechanical stress placed throughout the bone to guide its reformation.

Bone: Diseases, Disorders and Clinical Repair Strategies

Failures of the bone organ can occur as the result of any number of clinical conditions, including cancers (osteosarcomas and as a target tissue of metastatic cancers), infections (commonly osteomyelitis), blunt traumas that may result in non-unions, and congenital defects (e.g. osteogenesis imperfecta). Many of these diseases will result in moderate to extreme pain and also partial or total loss of mobility. Furthermore, some bone disorders, while rare in the population, are even fatal, as in Osteogenesis Imperfecta Type II, or Brittle Bone Disease, a

disease linked to an absence of collagen in quantity and quality, which is seen in approximately 6 in 100,000 newborns (Lieberman et al., 2005).

Though fracture healing usually progresses smoothly, non-unions in bone are prevalent when regeneration fails. Non-healing unions are a problem in long bones that is more commonly seen with increasing age, and they often result in intense inflammation and pain in the elderly, with amputation as a possible consequence. Non-unions from combat related injuries in war have also become a major concern. To accelerate bone healing or the closure of non-unions, health care providers in many labs and clinics have implemented injecting a basic fibrinogen gel for guiding osteogenesis into the fracture, both with and without mesenchymal stem cells added to the mixture (Valbonesi, 2006). Fibrinogen-based gels and stem cells have proven to be extremely well tolerated and effective in animal models. In humans, most therapeutic strategies have relied primarily on progenitor cells derived from the bone marrow, which has patient morbidity associated with drilling a large hole in the iliac crest to harvest these cells. The use of mechanically unsound gels is also far from ideal especially with microscopic structures in the hundreds of microns scale, the latter of which are far from the native few hundred nanometer fiber diameters seen in naturally formed hematomas. This finding suggests that a rigid replacement tissue would be more clinically desirable (Tamer et al., 2008).

Among common bone disorders, postmenopausal osteoporosis is estimated to affect 1 in 3 women, while 1 in 12 men over 50 are believed to have osteoporosis worldwide. The mechanism behind osteoporosis is linked to an imbalance between bone resorption and bone formation (**Figure 1**), where bone mineral density decreases, the spicules of trabeculae become thin and break, and the amount and variety of non-collagenous proteins differ from a normal

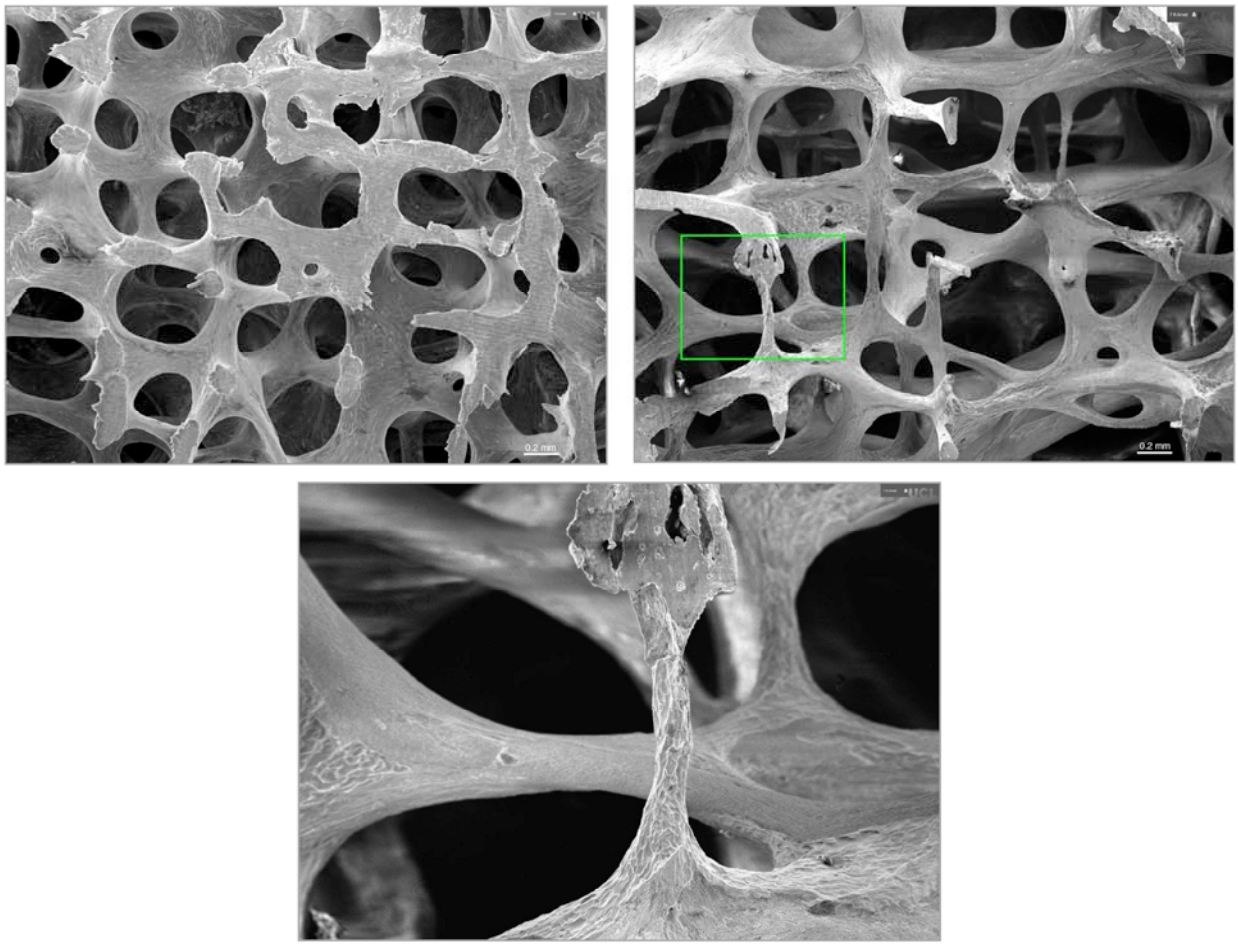

Figure 1. Healthy and Osteoporotic Trabecular Bone. A low power scanning electron micrograph (SEM) image of normal 3rd lumbar vertebra bone architecture from a 30 yr old woman (upper left, with marrow and cells removed), showing thick interconnected plates of bone, is compared to osteoporotic bone in the same region from a 71 yr old woman (with marrow and other cells removed), revealing eroded bone (by kind permission of Tim Arnett and the Bone Research Society).

healthy state. Osteoporosis is responsible for millions of fractures annually, mostly involving the hip, wrist, and lumbar vertebrae, with rib fractures also common in men. Annually, at least 250,000 hip fractures are attributed to osteoporosis in the U.S alone (Lieberman and Friedlaender, 2005). As the incidence of osteoporosis increases in the elderly, the incidence of bone fracture increases as well, often with little to no subsequent repair occurring; which can greatly affect life expectancy and the quality of life.

Along with a need for rejuvenating bone in the elderly, bone tissue and bone substitutes are needed for the treatment of several pathologies ranging from calvarial defects to non-healing fractures. In the U.S. alone, over 500,000 surgical procedures are performed annually, that require new bone tissue or bone analogues (Langer et al., 2003). While cadaveric bone grafts have proven highly effective clinically, donated bone tissue can have underlying infections or cause immunological rejection. Further, donor bodies for bone are rare, which has created a black market for stolen cadaveric bone tissue with thousands of stolen cadaver bones thefts being recently uncovered by one company alone (Powell et al., 2006).

Stem Cells

Stem cells are defined functionally as a cell type having the ability to self-renew with the capacity to form differentiated cells (Weissman et al., 2001). Most somatic stem cells are mortal, while embryonic stem cells are capable of extensive proliferation. Importantly, stem cells are said to be clonogenic, with single cells capable of creating more stem cells, both in the body and in culture. Stem cells exhibit variable potency including: (1) a totipotent or pluripotent embryonic stem cell that can differentiate into all cell types in the adult organism; (2)

multipotent mesenchymal stem cells that can form a handful of lineages; and (3) unipotent progenitor cells that only produce a single type of differentiated descendent.

The clonal nature of marrow cells was revealed over 45 years ago (Becker et al., 1963; Siminovitch et al., 1963). Friedenstein and colleagues later developed an assay for examining the clonogenic potential of these multipotent bone marrow-derived mesenchymal stem cells (BM-MSC) (Friedenstein et al., 1974 & 1976). MSCs are believed to be multipotent cells that are able to replicate as undifferentiated cells and are also well known for their potential to give rise to myocytes, adipocytes, chondrocytes, and osteoblasts. Thus, these cells appear to be capable of differentiating through complex, interrelated genetic pathways that only recently are becoming understood (Sensenstien et al., 2008). In osteoblast differentiation, for example, Runx2 expression is essential to initiate osteogenesis, along with osterix and other genes acting downstream of Runx2 to induce mature osteoblasts that express mature osteoblast markers, such as osteocalcin (Sensenstien et al. 2008).

Adipose-Derived Stem Cells

Where BM-MSCs have been the most widely studied of the MSC types, the existence of an analogous adipose stem cell source in human fat is becoming aparent (Zuk et al., 2001; Zuk et al., 2002). ASCs have gained considerable interest, in part, due to sharing a nearly identical transcriptome, immunophenotype (Katz et al., 2005), and differentiation potential (Izadpanah et al., 2006; Kern et al., 2006; Zuk et al; 2001 & 2002; Gimble et al., 2007) with their sister MSC cells from bone marrow.

In many ways, ASCs appear to be an advantageous cell type relative to BM-MSCs, since

they are 1,400 times more abundant (Izadpanah et al., 2006, Kern et al., 2006) and a more readily accessible tissue source relative to bone marrow. Liposuction also offers greatly reduced patient morbidity relative to tapping into the bone marrow. Although controversial, some evidence suggests that ASCs may be an immune-privileged (Rodriguez et al., 2005), or at least an immunomodulatory cell type that repels host immune cells (Hoogdujin et al., 2007). Additionally, ASCs are able to restore lethally irradiated bone marrow and fully re-populate the hematopoetic system (Chamberlain et al., 2007), suggesting the potential for allogeneic ASC transplantation. Furthermore, ASCs are reported to secrete potent growth factors in high quantities, such as basic fibroblast growth factor (bFGF), insulin-like growth factor 1 (IGF-1), hepatocyte growth factor (HGF), and vascular endothelial growth factor (VEGF) (Wang et al., 2006). These factors are crucial for tissue development and regeneration and will likely prove to be essential for constructing many artificial tissues.

Mesenchymal Stem Cells in the Clinic

Therapeutic use of mesenchymal stem cells for skeletal tissue regeneration, repairing bone fractures and treating congenital bone-related diseases is flourishing and appears to be an area of research with encouraging results (Arthur et al. 2009). Their multipotency, immune-modulatory properties, and secreted paracrine factors make ASCs ideally suited for regenerative medicine purposes, and their clinical use, along with BM-MSCs, has been well investigated over the past 2 decades.

In a healthy individual, MSCs within skeletal tissues contribute to the repair and normal remodeling process by providing a pool of osteoblasts to create the mineralized matrix of bone

(Bielby et al., 2007), yet anomalies such as non-union fractures, osteoarthritis, osteosarcomas, osteoporosis, and infections can interfere with the natural regenerative process. While it may seem obvious that ectopic transplant of MSCs to a bone defect site may aid in healing, regenerating 3D tissue, such as bone, is complex with a number of elements that are critical for coordinating the formation of a functional tertiary structure (Menicanin et al., 2007). While administering stem cells alone provides some degree of benefit in neuronal, hematopoietic, and cardiac regeneration, stimulating skeletal regeneration is proving to be most effective when using stem cells along with the mechanical and structural support provided by a scaffold (Arinzeh, 2005; Mastrogiacomo et al., 2006; Kanxsler and Oreffo, 2008).

In large animal studies, transplanting MSCs alone or in porous ceramic scaffolds made of hydroxyapatite significantly stimulated new bone growth in a non-union fracture model, with treated animal bones becoming as strong as uninjured control bones 8 to 32 weeks after treatment (Kon et al., 2000; Liu et al., 2008). In analogous human trials, 16-, 22- and 41-year old patients with non-union fractures having 4-7cm critical size defects were treated with autologous MSCs seeded in defect-sized hydroxyapatite scaffolds (Quarto et al., 2001). All 3 patients regained function of the injured limb without side-effects and with callus formation within 2 months. Patients reached a recovery stage within a few months that traditionally would take 1-1.5 years to attain using traditional bone grafting methods (Quarto et al., 2001).

In treating craniofacial defects, Lendeckel and colleagues (2004) reported a case study where a 7-yr old girl who had suffered widespread calvarial defects with complicating chronic infection was treated with autologous ASCs, using an autologous fibrin glue to retain the stem cells in the defects. Three months after reconstruction, extensive new bone formation and nearly

complete calvarial continuity was observed, with total repair occurring by 24 months. ASCs were used in this treatment partially because autologous bone from the iliac crest was limited, making sufficient BM-MSCs unavailable for treatment.

The first MSC trials addressing osteogenesis imperfecta (OI) in children (Horwitz et al., 1999, 2001, 2002) demonstrated that un-manipulated, HLA-matched sibling bone marrow and MSCs were safe and effective when administered by intravenous infusion. In these studies, the transplants were well tolerated, lacking any apparent immunological response. Osteoblast engraftment from donor tissue was observed in all patients, and bone mineral volume and overall growth was noted, along with a reduction in fracture frequency relative to age-matched controls. Subsequent studies demonstrated the feasibility of culture expansion and modification of cells prior to treatment of OI as well (Horwitz et al, 2002).

Collectively, these advantages make ASCs an excellent stem cell source, an ideal bone progenitor cell, and a cell type with significant therapeutic potential. However, stem cells do not exist or repair tissue in a vacuum; rather, they are dependent on an intricate, three-dimensional extracellular matrix network.

Extracellular Matrix:

Basic ECM Biology, Functions and Types

Traditionally thought of as merely the structural component for cell and tissue support, extracellular matrix (ECM) has been established as being of utmost importance throughout biology the past 30 years. Four major classes of macromolecules—collagens, structural glycoproteins, proteoglycans, and elastin—collectively comprise the ECM of animal cells, being

both widely distributed and multifunctional throughout the body **(Table 1)**. ECM is constantly synthesized, secreted, oriented, and modified by the cellular components that they support. All ECM molecules, apart from elastin, contain families of related proteins derived from uniquely arranged gene products. Members of each family and class of ECM molecules exhibit a degree of tissue-specific distribution, implicating the ECM in development and tissue function. Additionally, specific cell surface receptors have been identified on ECM components, linking the biology of the cell with its ECM interactions.

Some of the more critical known functions of native ECM include:

(1) Contributing mechanical and Structural Support
(2) Providing Cell Anchoring Sites
(3) Aiding Cell-Cell and Cell-Matrix Communications
(4) Directing Cell Orientation
(5) Controlling Cell Activity
(6) Maintaining or Inducing Differentiation
(7) Establishing Microenvironment (Sequesters & Presents Regulatory Molecules)
(8) Guiding Embryonic, Fetal, and Somatic Tissue Development
(9) Providing Provisional Wound Healing Substratum
(10) Forming Tissue Barriers
(11) Selectively Inhibiting or Promoting Cell Migration or Proliferation

The ECM is believed to influence cells through at least two families of cell surface receptors: integrins and syndecans. Cells have been shown to produce extracellular matrix based on a delicate interaction between regulatory signals from growth factors and cytokines, vitamins and hormones, and cell-to-cell contact (Lutolf and Hubbell, 2005). Furthermore, many of the biological effects attributed to cytokine and growth factor effects on a cell are nearly identical to the effects imparted by ECM itself on cells, such as a modification in the state of differentiation, metabolic responses, and growth.

Table 1: Major ECM Components, Their Functions and Localizations.[#]

Component	Functions	Localization
Collagens (Types I - XVIII)	Tissue architecture, tensile strength, cell-matrix interaction, matrix-matrix interaction	Widely distributed (skin, tendon, ligament, cornea, lung, bone, basement membrane, etc.)
Elastin	Tissue architecture, elasticity	Tissues requiring elasticity (lung, blood vessel, skin)
Proteoglycans	Cell-matrix interaction, matrix-matrix interaction, cell proliferation, cell migration	Widely distributed (cell surface, neural tissues, liver, basement membrane)
Glycosamino-glycans	Cell-matrix interaction, matrix-matrix interaction, cell proliferation, cell migration	Widely distributed (synovial fluid, connective tissue, etc.)
Laminin	Type IV collagen interactions, cell binding, cell development, migration, differentiation, wound healing, morphogenesis, angiogenesis	Basement membranes and widely in developing embryo and fetus
Fibronectin	Cell differentiation, proliferation and migration, tissue architecture, cell-matrix interaction, matrix-matrix interaction	Widely distributed (Plasma, produced by fibroblasts, epithelial and endothelia cells, platelets, etc.)
Fibrinogen	Blood clotting, cell proliferation, cell migration, hemostasis	Blood and wound healing

[#]Adapted from Palson et al., 2004

The function and fate of a cell is largely orchestrated by extrinsic and intrinsic factors, suggesting that the new cellular paradigm holds that beyond genetic programming, four major types of interactions—growth factors/cytokines, hormones/vitamins, cell-to-cell contact, and the ECM—regulate the growth, shape, differentiation state, biochemical responses, and development of the cell. Each of these interactions are translated through specific cytoplasmic or cell surface receptors and affect changes in gene expression, which in turn alter ECM expression itself in a phenomenon called "mutual reciprocity" (Palson et al., 2004). Complicating this whole process is the observation that ECM, with its extensive binding sites present on its surface, is specifically associated with many cytokines and growth factors (Rapraeger, 1993; Vlodavsky et al., 1993). Thus, it is becoming clear that the extracellular matrix plays a pivotal role in a cell's biological phenotype, especially related to its normal development/function and its pathological responses.

ECM in Development

Throughout embryonic and fetal development, extracellular matrix interactions orchestrate such activities as cell migration and proliferation, stem cell differentiation, tissue patterning, and morphogenesis (Campbell et al., 2005, Flaim et al., 2005, Haylock et al., 2005, Kihara et al., 1998, Naugle et al., 2006, Suzuki et al., 2003). The ECM interacts directly with cell surface receptors, acting as a reservoir for growth factors and morphogenetic proteins, or simply providing a scaffold for cell attachment and cell migration. Even cell morphology is determined by contact with the ECM, which may be associated with cell differentiation and proliferation. For example, floating type I collagen gel can induce functional differentiation of precursor cells into mammary glands, mediated through changes in cell shape, thereby allowing branching

morphogenesis to occur (Bissel et al., 1987). Further, laminin-I is expressed in developing mouse lung by epithelial and mesenchymal cells where it is essential for branching morphogenesis (Schuger et al., 1991). The biomechanics of the scaffold also plays a crucial role in development. For example, the rigidity of the ECM substrate alone can induce the differentiation of precursor cells into hepatocyes and direct their morphogenetic pattering in the developing liver (DiPersio et al., 1991).

Basement membranes are common to tissues of nearly all multicellular metazoans, and their gene products are highly conserved and among the most ancient (Exposito et al., 2002; Hutter et al., 2000). Basement membrane (or basal laminae) proteins are the first ECM materials to appear during embryogenesis, with laminin being the first detectable ECM protein that appears shortly after morula differentiation. In what can be called the first true tissue to form in development, the morula consists of the inner cell mass, trophectoderm, and primitive endoderm (Martin and Timpl, 1987, Miner et al., 2004).

Assembled basal laminae are the earliest ECM recognized as a distinct structural entity. Throughout development of the embryo and fetus, basement membrane and other ECM materials assemble in nearly all tissues, having a profound effect on their developmental fate. Loss of phenotype studies in *C. elegans* (Kramer, 2005) have shown that several basement membrane components, including type IV collagen, laminin, perlecan, and possibly osteonectin/SPARC, are necessary for tissue organization and structural integrity, the latter of which is essential for the completion of embryogenesis. Type XVIII collagen and nidogen, while not critical for embryonic or fetal viability, play primary roles in organizing the nervous system. All of these proteins further have a role in gonad development (Kramer, 2005).

The Stem Cell Niche

The stem cell niche concept holds that a highly specialized microenvironment is responsible for sustaining a stem cell pool in every tissue and organ system (Scadden, 2006). This specialized microenvironment consists of the local ECM, its stored growth factors, and the 3D ultra-structure of the niche, including the cell-cell contacts and the signals shared with parenchymal cells in the environment surrounding the stem cells (Haylock and Nilsson, 2005; Moore and Lemischka, 2006).

The ECM in particular has proven to play a critical role in niche formation, being first recognized to support the hematopoietic stem cell (HSC) niche through binding heparan sulfate proteoglycans (Daley et al., 2007; Gupta et al. 1998). Additionally integrin-ß1 has proven to be a potent stem cell marker that aids in restricting stem cells to the epidermal stem cell niche through MAP kinase signaling (Jensen et al., 1999; Zhu et al., 1999). The integrins, readily bound by numerous ECM binding sites, are key in communicating extracellular signals to stem cells, regulating cell proliferation, cell survival, and cell migration out of the niche (Leone et al., 2005), and even for niche-to-niche homing through extensive microenvironment interactions (Lapidot et al., 2005).

For HSCs, the bone surface lining, or endosteum, is identified as their major niche with resident osteoblasts maintaining HSCs in a quiescent state (Arai et al., 2004). Additionally, in the HSC niche, the phosphorylated glycoprotein osteopontin, secreted by osteoblasts, incorporates in the ECM and interacts with a vast array of integrins and CD44 on HSCs surface to inhibit stem cell expansion (Nilsson et al., 2005; Stier et al., 2005). In neural stem cell migration, laminin alone has been found sufficient *in vitro* for initiating neural stem cell outgrowth from a 3D

neurosphere (Flanagan et al., 2006). Interestingly, the ECM alone is able to induce osteogenesis with laminin-332 stimulating MSC osteogenic differentiation through ERK signaling (Klees et al., 2005).

Osteogenesis can also be induced through collagen type I or vitronectin contact, mediated through ERK-1/2 stimulation and the early stage osteogenic transcription factor Runx2 (Salasznyk et al., 2007). Cytoskeletal tension imparted from the ECM is also reported to induce osteogenic differentiation of MSCs, perhaps through RhoA/ROCK signaling (McBeath et al., 2004). Human MSCs are also inducible into many other cell types through contact with the ECM. Recent work suggests that endothelial cell matrix induces gene and protein marker expression, as well as functional gains of genuine vascular cell phenotype, with the endothelial cell matrix found to be an essential substrate for inducing vascular cell differentiation in MSCs (Lozito et al., 2009).

REGENERATIVE MEDICINE:

Basic Theory & Principles

Regenerative medicine, now synonymous with tissue engineering, is a rapidly expanding interdisciplinary field involving biological sciences (embryology and wound healing, cell biology, and physiology), medicine (surgery and transplantation, pathology, immunology, and radiology), and engineering (materials science, mechanics, fluid dynamics, chemical kinetics, and transport phenomena). This field employs a staggering number and range of biotechnologies (Langer and Vacanti, 1993). As such, regenerative medicine is revolutionizing the way scientists and clinicians improve the health and quality of life for millions of people worldwide through

restoring, maintaining, and/or enhancing organ and tissue function while confronting aging as a treatable disease. Beyond therapeutic applications, engineering tissues *ex vivo* has great potential for clinical applications, where synthetic tissue can be used to test drug metabolism and uptake, toxicity, and pathogenicity (Langer and Vacanti, 1999).

In practice, regenerative medicine is a field closely associated with any application used to replace or repair portions of or all of a tissue, ranging from blood vessels, cartilage, heart, bone, bladder, and other tissues. The recent, rapid explosion of stem cell biology advances has only further stoked the enthusiasm for the tissue engineering field, while creating potential raw material sources previously unavailable. Because many somatic cell types have been extremely difficult to isolate and expand in sufficient numbers to regrow or repair damaged tissue, stem cell biology is likely to eliminate this as an obstacle. While significant research is in progress under the umbrella of tissue engineering, we are particularly interested in the creation of biomimetic scaffolds that resemble native ECM relevant to our studies.

From the inception of the regenerative medicine field, three major strategies have dominated therapeutically: 1) a purely cellular approach that injects cells alone into the patient, directly or indirectly into the diseased or defective tissue; 2) a cell encapsulation system for cell support; and 3) the *ex vivo* growth and development of cells in a supporting scaffold prior to implantation (Nussbaum et al., 2007). Since almost all tissues and organs in the body appear to contain parenchymal (functional) and progenitor or stem (support) cells situated within a dynamic supporting ECM microenvironment, the third approach has gained considerable favor. In producing a supporting scaffold for tissue repair or replacement, the biomimicry of actual

bodily tissue matrices is a natural, logical approach, especially given the importance and influence of the ECM.

Since the ECM has been shown to be crucial for orchestrating developmental, regenerative, and wound repair/healing cues, it is logical to incorporate related natural ECM components in any engineered scaffold design, with biologically relevant nanofibers, cytokines, and cell binding sites available for cell growth, migration, and differentiation. While crudely injecting stem cells alone has some therapeutic promise in certain situations, application of the cells in a controllable manner directly to the target site has clear advantages. This has driven the tissue engineering field for developing bioscaffolds for cell delivery such that countless materials and material forming methods have been examined to address the many challenges of creating an idealized biomimetic, biocompatible, degradable, and semi-rigid matrix for natural cell growth and development.

Common gels, such as the mouse sarcoma-derived Matrigel and denatured collagenous gelatin, have proven very useful *in vitro* but are far less effective clinically due, in part, to the associated immune response and lack of mechanical integrity (Song et al., 2006). Other scaffolds based on natural materials, such as decellularized tissue (Gilbert et al., 2006), while tedious to create and complicated by lack of available starting materials, have shown significant promise, both at the bench and bedside. A more elegant and pliable scaffold building process has long been needed, and one such emerging process is electrospinning.

SCAFFOLD FABRICATION

Electrospinning

In its basic form, electrospinning involves the application of a 15 to 30kV DC electric potential to a polymer solution or melt, which is held in a syringe separated from a grounded or oppositely charged target. This creates an electrostatic field that when sufficiently high in strength allows the electric potential to overcome the solution surface tension resulting in the ejection of a small jet (via a Taylor Cone) of intertwined polymer chains. This stream whips around in space towards the target as driven by the charge repulsions between and within the jet. The solutions of charged polymers are typically dissolved in an organic solvent, and with optimized polymer concentration and jet travel distance, the solvent evaporates as the polymer flies to its target/mandrel and leaves a dry polymer fiber that collects as a non-woven fibrous mesh (Barnes et al., 2007) **(Figure 2)**. Electrospun fiber sizes and scaffold porosity parameters can be crudely tailored as desired through altering starting polymer concentrations. The fibrous mat can be further customized through target translation and rotation speed changes to orient the fibers in a controlled manner, from paralleled, aligned fibers to a randomly oriented mesh.

The recently evolved electrospinning technique for bio-scaffold construction is rapidly gaining favor in the tissue-engineering field due to its numerous advantages over conventional scaffold methods. Natural matrix materials, such as collagen, laminin, elastin, and fibrinogen with or without supporting synthetic blends, can be spun into scaffolds of nearly any shape and microscopic properties. Electrospun scaffolds highly resemble native extracellular matrices in geometry, fiber size, and material composition. While conventional polymer processing techniques for producing fibers generally create fibers 10 micrometers or larger in diameter, the

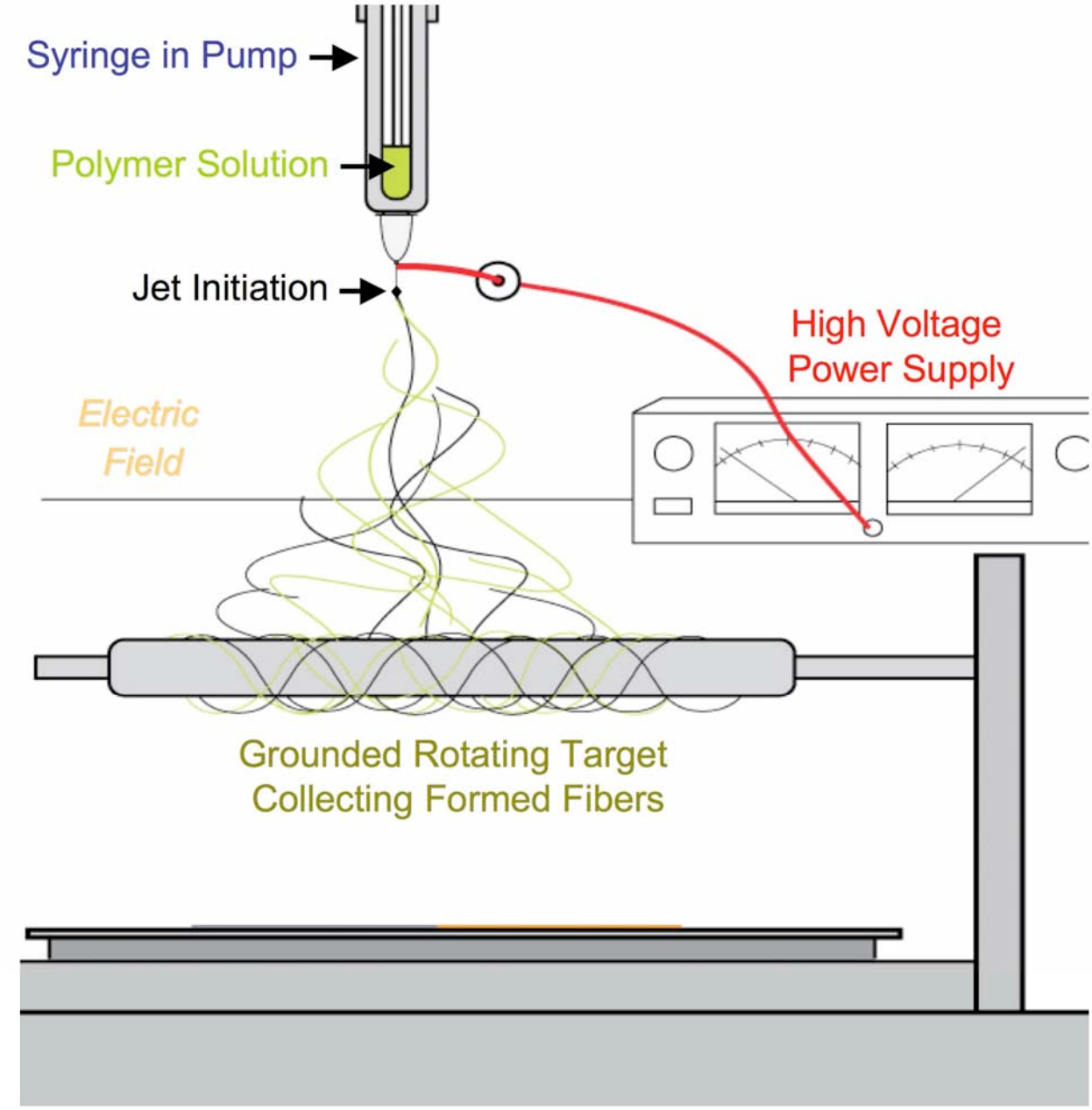

Figure 2. Electrospinning Apparatus Schematic. The elements of a basic electrospinning setup are shown, with a high voltage power supply connecting to the needle of a syringe filled with matrix polymer, for electrospinning fibers of the polymer material through the generated electric field, with fibers collecting on a rotating mandrel that is connected to ground.

nanofibers generated from electrospinning are capable of mimicking the sub-micron diameter and geometry typical of endogenous tissues.

Cross-Linking

Chemical cross-linking is commonly applied to tailor degradation rates and biomechanical characteristics of a tissue engineering scaffold, typically to match the properties of the target tissue for regeneration. However, many of these cross-linking chemicals can reduce biocompatibility, to the point that even the more popular cross-linking agents, such as glutaraldehyde (GLUT), formaldehyde, and epoxy compounds, have proven cytotoxic. This toxicity is likely due to the reactive moieties covalently coupled between adjacent collagen fibrils (Koob, 2004; Jayakrishann and Jameela, 2006; Badylak, 2002; Khor, 1997).

Many electrospun natural materials, such as collagens and elastin, shrink and disintegrate upon hydration in any aqueous solution. Therefore, cross-linking has been required to maintain structural integrity of many scaffolds. However, even natural electrospun scaffolds cross-linked in GLUT have a tendency to gel and lose their most important feature, their nanofibrous architecture, by fusing the fibers into a thick mat.

As fibrinogen is actively broken down by thrombin and other serum proteases, it was reasoned in prior work that electrospun fibrinogen should be cross-linked for cell-based studies in order to maintain scaffold integrity *in vitro* and *in vivo* (McManus et al., 2006 & 2007). Electrospun fibrinogen exhibits excellent bioactivity, yet was reported to exhibit poor mechanical integrity after a few days in culture (McManus et al., 2006, 2007, 2009). Ideally, a suitable cross-linker would slow the degradation rate of fibrinogen while not affecting the

bioactivity of the scaffold. Although fibrin clots have native factor XIII (transglutaminase) cross-linking, which forms a covalent bond between the lysyl and glutamyl residues of adjacent fibrin molecules (Achyuthan et al., 1988; Dickneite et al., 2002; Mosesson et al., 2005), this compound (transglutaminase) is cost prohibitive. Other agents may prove more cost effective while supplying similar biologic properties. To bypass chemical cross-linking, our laboratory has successfully electrospun blended natural materials with synthetic polymers (Barnes, 2005), which is a highly promising practice.

Among candidates for cross-linking fibrinogen (and possibly for adipose tissue ECM), GLUT is the most commonly used cross-linker for collagen tissue fixation (Olde Damink et al., 1996; Sung et al., 2003). GLUT is cost effective and fast acting, and it cross-links over varying distances while reacting with numerous amino groups in target proteins (Jayakrishnan and Jameela, 2006). GLUT, however, exhibits increased cytotoxicity and material calcification over time (Olde Damink et al., 1996; Sung et al., 2003).

The hetero-bifunctional carbodiimide 1-ethyl-3-(3-dimethylaminopropyl) carbodiimide hydrochloride (EDC) has been successfully used to cross-link electrospun elastin (McClure et al., 2007) and type II collagen (Barnes et al., 2007). EDC has the advantage of not being incorporated into the target macromolecule, known as a zero-length cross-linker, which in turn reduces the potential for cytotoxicity (Olde Damink et al., 1996; Sung et al., 2003).

Genipin, which is derived from the fruits of *Geninpa Americana* and *Gardenia jasminoides Ellis*, is a naturally occurring cross-linker that has been used for collagenous tissues (Sung et al., 2003). Genipin is effective in increasing material tensile strength and toughness while being far less cytotoxic then GLUT (Tsai et al., 2000), making it an ideal cross-linker for

fibrinogen where high mechanical strength is important. Our studies have determined the effectiveness of these cross-linkers for electrospun fibrinogen scaffolds. A particular goal of this study was to determine which cross-linker increases the mechanical properties, slows degradation, and, importantly, maintains the high level of bioactivity inherent in fibrinogen.

SCAFFOLD DESIGN

MATERIAL SELECTION: Fibrinogen

Fibrinogen is an integrin-spanning glycoprotein produced in the liver that binds collagen, fibrin, and heparan sulfate. Clinically used since at least 1944, fibrinogen is applied widely as a fibrin glue sealant or gel, used for treatment of burns and wounds, congenital cardiopathies, peptic ulcers, cardiac bypass surgeries, and especially in plastic surgery and many other applications (Mosesson, 2005). Fibrin(ogen) contains a ß15-42 sequence for binding heparin, allowing for active cell-matrix interactions. Fibrinogen has been shown to mediate endothelial cell spreading and fibroblast proliferation, capillary tube formation and proliferation, and is a von Willebrand factor releasing agent (Valbonesi, 2006). Conveniently, it uses binding site/factors that are also germane to ASCs (Katz et al, 2005).

Additionally, fibrinogen actively binds fibroblast growth factor-2 (FGF-2, bFGF), a crucial stem cell signaling molecule, as well as vascular endothelial growth factor (VEGF). Both of these functions may potentiate endothelial cell proliferation and may contribute to the healing response. Of note, ASCs have been shown to secrete high levels of VEGF (Katz et al, 2005), again making the pairing of ASCs and fibrinogen highly synergistic. As VEGF, TGF-ß1, and PDGF are normally linked to wound healing but are absent in purified fibrinogen or fibrin glue

as supplied, using ASCs to secrete these factors into scaffolds or wounds may be yet another advantage to our cellular approach.

Structurally, fibrinogen molecules are composed of two matched sets of disulfide-bridged α-, ß-, and γ-chains, each with two outer D domains connected by a coiled-coil segment to a central E domain. Fibrin forms from fibrinogen in the coagulation cascade process, where the zymogen prothrombin is activated to the serine protease thrombin, which cleaves fibrinopeptide A from the fibrinogen α-chain, thereby inducing fibrin polymerization. Fibrin is then cross-linked by factor XIII, forming a clot. Factor XIIIa further stabilized fibrin, incorporating the fibrinolysis inhibitors alpha-2-antiplasmin and thrombin activatable fibrinolysis inhibitor procarboxypeptidase B (TAFI). TAFI further allowing for the binding of several cell adhesive proteins (Mosesson, 2005).

Fibrinogen has the advantage of being an autologous matrix, that can be purified in as little as 20 minutes in a minimally-equipped lab or hospital setting, needing only a centrifuge, freezers, and cryoseal bags (Valbonesi, 2004). It is a rare patient-derivable scaffold source. Additionally, fibrin glue and fibrin gel-related products have been approved for clinical use in concert with mesenchymal stem cells. For instance, MSC implants are coupled with autologous fibrin-platelet glue in maxillofacial surgery to promote wound healing and bone regeneration (Giannini et al., 2004), creating bioengineered ocular surfaces for corneal epithelial stem cells to differentiate upon (Han et al., 2002) and form a dermal matrix with live fibroblasts for skin grafts (Meane et al., 1998).

Lastly, fibrinogen has been shown to be amenable to the electrospinning process (Matthews et al., 2002, McManus et al., 2007) to form a biomimetic, biocompatible, and

biodegradable matrix for tissue engineering applications. The ability to readily modify the average fiber diameters of electrospun fibrinogen to mimic the biologic fibrinogen fiber range of a few hundred nanometers **(Table 2)**, depending on clot architecture (Collet et al., 2000; Moen et all, 2003), further makes it an excellent starting material for tissue engineering.

MATERIAL SELECTION: Polydioxanone

Polydioxanone (PDO) is a crystalline, colorless biodegradable poly(ether-ester) polymer exhibiting good flexibility and mild shape memory. PDO is formed through ring opening of p-dioxanone monomers by heat and an organometallic catalyst (such as diethylzine, zinc L-lactate, or zirconium acetylacetone) to form polydioxanone polymers **(Figure 3)**. PDO has been applied for many biomedical uses including orthopedics, cardiovascular and plastic surgery applications, and drug delivery. Most notably, PDO is extruded into fibers for a degradable suture material, one that loses half of its mechanical strength in about 20 days *in vivo*, yet can take up to 6 months to fully degrade.

PDO has the distinct advantage of exhibiting a low inflammatory response compared to other polymers used in sutures (Wainstein et al., 1997). Though it has many biological benefits as a suture material, PDO retains shape memory, a major drawback for the suture application. The shape memory may, however, prove a valuable mechanical property in engineering tissue scaffolds, as has been proposed (Boland et al., 2005). Along with its biocompatibility, the absence of an immune response, and its ability for simple degradation by hydrolysis into safe byproducts make it an ideal candidate for tissue engineering and in many ways possibly superior to competing synthetic materials (Molea et al., 2000). Additionally, our work has shown that

Table 2: Average Fiber Diameter and Pore Size of Native/Uncross-linked Electrospun Fibrinogen Scaffolds[#]

	80 mg/ml Fibrinogen	110 mg/ml Fibrinogen	140 mg/ml Fibrinogen
Average Fiber Diameter	120 nm	316 nm	608 nm
Average Pore Size	1.3 μm^2	7.3 μm^2	13.1 μm^2

[#](adapted from McManus et al, 2006)

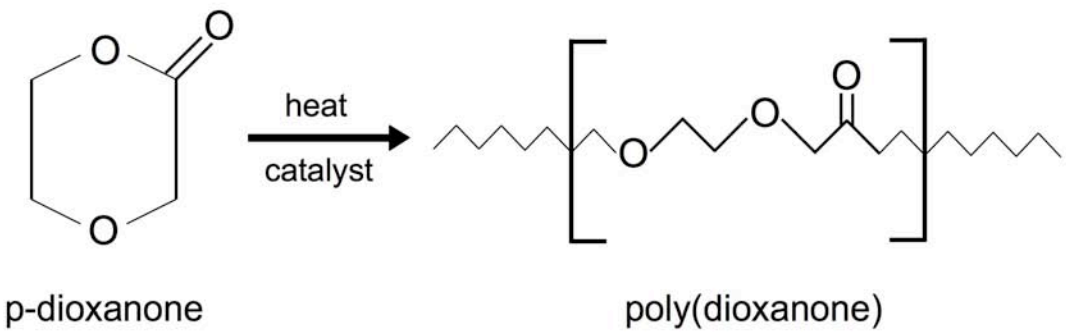

Figure 3. Polymerization Reaction of p-dioxanone to Polydioxanone. The chemical transition of p-dioxanone, through addition of heat and a catalyst, to the polydioxanone polymer is shown.

electrospinning of PDO produces micron to submicron diameter fibers, and it will readily co-electrospin with fibrinogen, collagen, and other natural matrix materials, again making it a suitable polymer for tissue engineering applications. Blending natural matrices with a synthetic, like PDO, has the advantage of alleviating the need for additional chemical cross-linking to prevent gelling or to slow dissociation of the natural polymer, as the blending itself stabilizes the electrospun mesh.

MATERIAL SELECTION: Adipose Extracellular Matrix

Adipose tissue is extracellular matrix-rich, densely composed of collagens Type I, III, IV, V, and VI, laminin, and fibronectin (Nakajima et al., 1998). In fact, the amounts of these proteins have been shown to match or exceed the levels of ECMs in tissues known to be rich in such materials, such as capillaries, arteries, and perimysium from skeletal muscle **(Table 3)**. Interestingly, using radiolabeled antibodies, investigators have shown that adipose cell precursors that differentiated into mature adipocytes *in vitro* heavily secrete collagens Type I, III, IV, V and VI, laminin, and fibronectin. These pre-adipocytes cultured in adipogenic differentiation media show an 8- to 15-fold upregulation in deposition of ECM materials in the extracellular spaces compared to the same cells cultured in normal growth media (Nakajima et al., 2002).

Incidentally, the ECM composition of Matrigel (BD Biosciences), a highly important mixed matrix derived from mouse sarcomas that has been shown to be crucial for supporting pluripotent stem cells and a wide array of other cell types, is comprised of 56% laminin, 31% collagen type IV, and 8% entactin. Furthermore, Matrigel (not growth factor reduced) contains

Table 3: Quantification of ECM Proteins from Dissected Skeletal Tissue, Matrigel and Adipose Tissue[#]

ECM proteins	Adipose Tissue	Capillaries and Small arteries	Matrigel
Type I Collagen	+	+	-
Type II Collagen	low	low	low
Type III Collagen	+	low	-
Type IV Collagen	+	low	+
Type V Collagen	+	low	-
Type VI Collagen	+	+	-
Elastin	+	+	-
Fibronectin	+	+	low
Laminin	+	+	+
Proteoglycans, Glycosoaminoglycans & Glycoprotein	+	+	+

[#]Adapted from Nakajima et al. 1998 and BD Bioscience product sheet data.

relatively high levels of EGF (1.3ng/ml), TGF-ß (2.3ng/ml), and PDGF (12pg/ml) with trace amounts of bFGF (0.1pg/ml), all of which are secreted by ASCs and can strongly bind the ECM molecules of adipose tissue. Because mouse-derived Matrigel has limits on its application clinically, derivation of a highly analogous ECM from human fat tissue has far reaching implications for translating a number of studies using Matrigel to potential clinical models.

Along with fibrinogen, and due to its extraordinary matrix composition, adipose tissue ECM may also prove to be a highly ideal, patient-derivable scaffolding source material for regenerative medicine and basic stem cell biology research. Currently, no established protocols exist for harvesting fat ECM from patient-derivable liposuction in quantities suitable for regenerative medicine applications. Moreover, fat ECMs have only been scarcely referenced and rarely studied in the field. Classic ECM papers of the 1940's through the 1970's set no precedent for fat ECM extraction, and, in fact, within their initial steps, ECM extraction protocols usually direct one to carefully remove all fat from the target tissue for discard (Haralson and Hassell, 1995). Needless to say, adipose tissue matrix has yet to be tested as a viable matrix for electrospinning, likely due to the absence of a suitable extraction methodology. While it is widely accepted that a biomimetic and autologous matrix source is therapeutically ideal, a plentiful autologous matrix source is still lacking. Because it is readily patient-derived and has rich matrix composition with high biological activity, adipose tissue matrix, along with plasma borne fibrinogen, may prove to be invaluable autologous matrix materials.

Study Rationale

With the ability to regenerate bone potentially having undergone 560 million years of refinement in vertebrates, it seems logical to look to nature for guidance in generating bone cells and bone tissue analogues for clinical and basic science needs. Given that a primordial matrix of fibrinogen forms in damaged bone leading to the recruitment of mesenchymal stem cell progenitors for subsequent stages of regeneration, we have chosen fibrinogen and adipose-derived mesenchymal stem cells as our starting template for modeling osteoblastogenesis *ex vivo*. While bone marrow-derived MSCs are also an excellent cell source, ASCs have shown distinct advantages over BM-MSCs; most notably that they are easily accessibility, very abundant with a stem cell pool well beyond the numbers of cells isolated for BM-MSCs, are capable of robust osteoblastogenesis and have a proven clinical record.

While collagen type I may be an excellent material for modeling and stimulating osteoblastogenesis, with type I collagen being the native and predominant ECM of mature bone, collagen is typically only available from rat-tails or bovine sources, which are problematic therapeutically. Human collagen, which would be far less immunoreactive, is not readily available or cost effective, and autologous collagen I is not currently harvested in large quantities without extreme patient morbidity associated with removing significant amounts of skin. Fibrinogen, however, can be readily harvested from the patient through simple blood collection and is potentially available in large quantities through blood/plasma clinics, as fibrinogen is generally removed from donated blood/plasma prior to use and than is ultimately discarded. Additionally, liposuction material rich in basement membrane ECM is discarded, and this ECM can be readily isolated for therapeutic and basic research use. Thus, the potential exists for the

use of frequently discarded medical waste that can be appropriately applied to regenerative medicine.

While many techniques for forming a biomimetic tissue scaffold exist for regenerative medicine apart from electrospinning, few approaches produce scaffolds with fibers rather then sheets and even fewer produce biologically relevant nanoscale fibers. Only electrospinning offers an elegant, affordable, and diverse method for creating nanofibrous scaffolds with modifiable mechanical properties and the mixed material composition needed for a wide array of tissue engineering needs.

In this study, we explore the potential of biomimetic and exclusively patient-derived regenerative matrices generated via the electrospinning of fibrinogen and adipose ECM as a substrate for ASC growth and differentiation. ***We hypothesize that*** electrospun fibrinogen nanofibers, alone or blended with PDO, are capable of supporting stem cell attachment, proliferation, and osteoblastogenic differentiation, thereby forming a mineralized scaffold containing cells expressing osteoblast-specific markers and proteins. Further, ***we hypothesize that*** a basement membrane-rich ECM can be derived from human adipose tissue that can: 1) be electrospun in its pure form; 2) be blended with a synthetic material, PDO, and then electrospun; 3) maintain its material composition through the electrospinning processing; and 4) support the attachment and cultivation of ASCs. These tissue generation and original scaffold material derivation experiments will lay a foundation for a wide range of uses in regenerative medicine, cell biology, cancer research, and other applications, whereby the natural healing process can be more thoroughly studied *in vitro*. The tools discovered here may further prove useful for developing better therapies for wound healing and safer drug development, while potentially

being used as a model for creating better artificial tissues *ex vivo* by following the recipes supplied by nature.

-Chapter 2-

Results: Isolating Adipose-Derived Mesenchymal Stem Cells from Lipoaspirate Blood and Saline Fraction

Preface: The following section has been published in Organogenesis, January 2010, Vol. 6, Issue 1, 10-14.

ABSTRACT

Isolation of adipose-derived stem cells (ASCs) typically involves 8+ hours of intense effort, requiring specialized equipment and reagents. Here, we present an improved technique for isolating viable populations of mesenchymal stem cells from lipoaspirate saline fractions within 30 minutes. Importantly, the cells exhibit remarkable similarities to those obtained using the traditional isolation protocols, in terms of their multipotent differentiation potential and immunophenotype. Reducing the acquisition time of ASCs is critical for advancing regenerative medicine therapeutics, and our approach provides rapid and simple techniques for enhanced isolation and expansion of patient-derived mesenchymal stem cells.

INTRODUCTION

The original, pioneering work on the isolation of adipose-derived stem cells (ASCs) from liposuction waste involves 8-10 hours of continuous intense effort (Zuk et al. 2001; 2002), making it a labor-intensive endeavor and increasing the risk of culture contaminations due to excessive handling. Based on recent reports (Crisan et al., 2008), we originally postulated that the blood/saline portion of lipoaspirate waste would prove to be a rich source of ASCs due to their association with the perivascular space. In addition, because of the violent nature of liposuction and the ultrasonic procedure used to obtain these samples, we expected to find significant number of ASCs in the blood and saline fractions of the lipoaspirate waste.

We present an enhanced method for isolating and quickly expanding a robust population of mesenchymal stem cells (MSCs) derived from lipoaspirate in less than 30 minutes. This isolation process yields an abundant population of ASCs (~100,000 cells per 100ml of blood/saline collected from sonicated lipoaspirate) with differentiation potential, characteristic cell surface markers, and proliferative lifespan indistinguishable from MSCs extracted from bone marrow (BM-MSCs) or conventionally processed ASCs (Zuk et al., 2001; 2002).

RESULTS

As outlined in **Fig. 4**, a viable population of adherent ASCs is easily obtained from the blood and saline phase that carries over with liposuction surgical refuse. This layer is located below the floating, more buoyant adipose tissue and is processed though a simple 5-step process. First, the blood/saline phase is isolated and cells pelleted (10 minutes). Second, the resulting pellet is gently re-suspended in NH_4Cl for red blood cell lysis (2-5 minutes). Third, the cells are

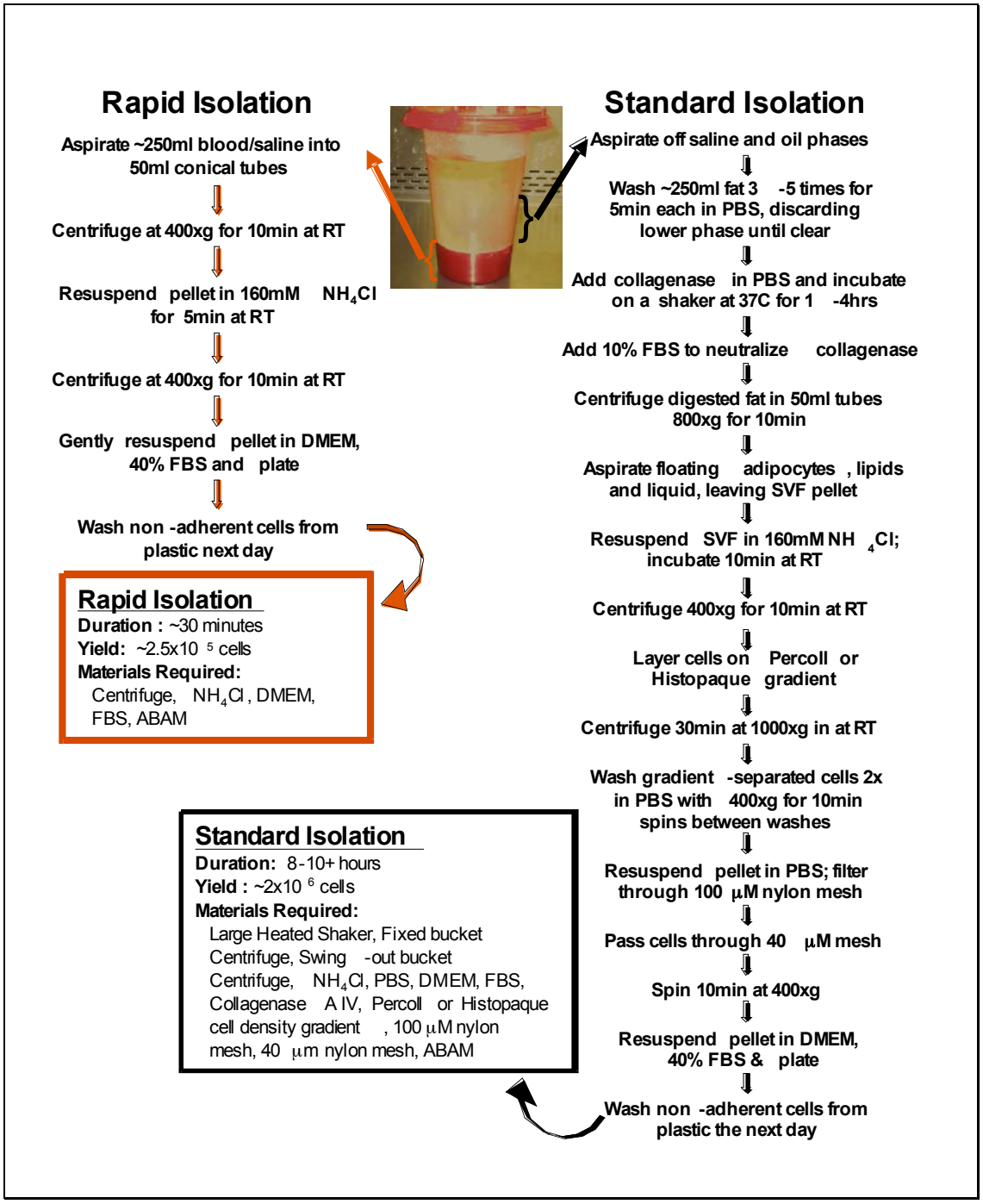

Figure 4. Adipose-Derived Stem Cell Isolation Techniques Flow Chart. The wide variance in the time, materials, and effort for obtaining ASCs via the Standard Isolation and our Rapid Isolation techniques is shown. A highly viable population of around 250,000 ASCs can be derived from 250ml of blood/saline fraction of the liposuction waste in as little as 30 minutes, as compared to 8-10 hours to obtain ASCs using the traditional isolation method. SVF – stromal vascular fraction; ABAM – antibiotic/antimycotic, FBS – fetal bovine serum.

pelleted again (10 minutes). Fourth, the cell pellet is gently re-suspended in DMEM with 40-50% fetal bovine serum (FBS), followed by plating the cells (2-5 minutes) and incubation overnight. Finally, the non-adherent cells and debris are washed away with phosphate-buffered saline (PBS), and the 30 minute ASC cultures are grown. This isolation method not only requires less than half an hour to complete but uses only standard tissue culture materials and equipment without the need for collagenase digestion, Percoll gradients, or extensive washing. Use of this isolation technique allows for the straightforward establishment of both patient-specific ASCs for regenerative medicine and disease-specific cell strains for scientific discovery.

Beyond sharing a mesenchymal morphology with other MSCs, the ASCs isolated in this streamlined manner were shown to share multipotent differentiation potential and an immunophenotype with the traditionally isolated ASCs (shown in **Figure 5A-I** for differentiation, **Table 3** for flow cytometry, performed as reported previously, Zuk et al., 2001; 2002; Katz et al., 2005), characteristics that are also indistinguishable from BM-MSCs (not shown). Rapidly isolated ASCs have a $CD14^-$, $CD29^+$,$CD31^-$, $CD34^{low/+}$, $CD45^-$, $CD73^+$ and $CD105^+$ immunophenotype **(Table 3)**, consistent with classically isolated ASCs (**Table 3**) and BM-MSCs (not shown). In agreement with previous reports on ASCs and BM-MSCs (Zuk et al., 2001; 2002; Izadpanah et al., 2005; Kern et al., 2006; Yoshimura et al., 2006), rapidly isolated ASCs also have undetectable levels of telomerase, as assessed either by a TRAP assay or RT-PCR for the catalytic subunit of telomerase, hTERT (not shown). Because rapidly isolated ASCs are nearly identical to both BM-MSCs and ASCs isolated in the traditional long protocol in terms of important MSC characteristics, ASCs isolated using our accelerated protocol warrant the same adult stem cell classification.

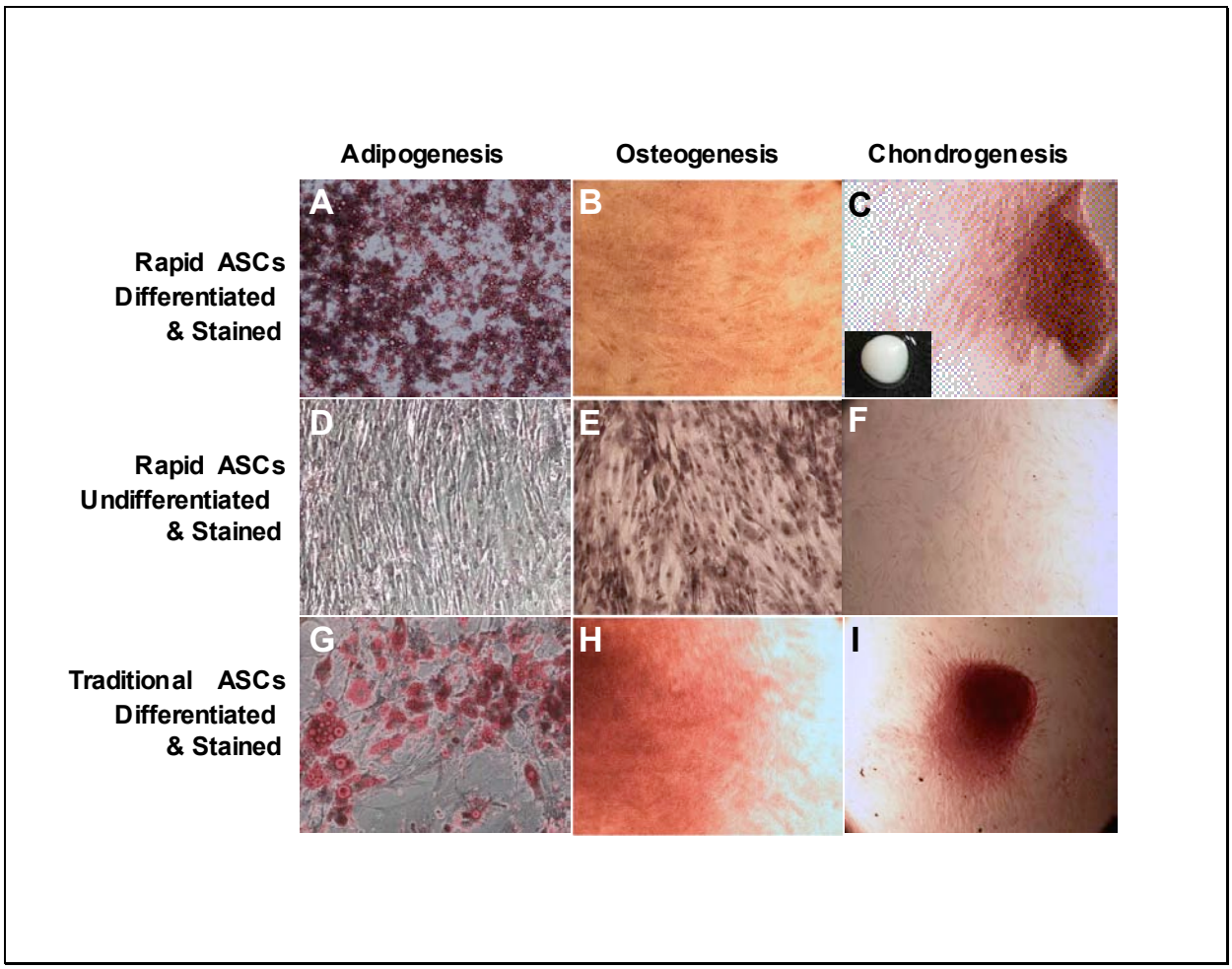

Figure 5. Characterization of ASC Differentiation. The differentiation potential of ASCs isolated in the streamlined, rapid protocol were compared to ASCs isolated using the standard protocol (traditional ASCs). Cells were induced to differentiate into adipocytes **(A)** for rapid ASCs and **(G)** for traditional ASCs; **(D)** rapid ASCs grown for 2 weeks without adipogenic media as control; all stained with oil red O and hematoxylin), osteocytes **(B)** for rapid ASCs and **(H)** for traditional ASCs; **(E)** rapid ASCs grown 2 weeks without osteocyte induction media as control; all stained with Alizarin red S and hematoxylin, and chondrocytes **(C)** for rapid ASCs and **(I)** for traditional ASCs, both in a micromass (solid micromass pellet, **insert, (C)**; **(F)** unpelleted rapid ASCs grown 4 weeks in induction media as control; all samples stained for Safranin O.

Table 4: Immunophenotype of ASCs Isolated using the Rapid and Standard Protocols

Cell Type	CD14	CD29	CD31	CD34	CD45	CD73	CD105
Rapid ASCs	-	+	-	low	-	+	+
Traditional ASCs	-	+	-	low	-	+	+
HL60 (controls)	+	nt	+	nt	+	nt	nt

nt = not tested.

We also show that the addition of epidermal growth factor (EGF) to the regular ASC growth media elicits a marked enhancement to the proliferation rate for ASCs with no effects on proliferative lifespan or differentiation potential (**Table 5**). ASC cultures supplemented with EGF show a sharp increase in proliferation rate and an increased senescence population doubling (PD) timing compared to unsupplemented ASCs (**Table 5**). With EGF added to normal growth sera, doubling times, as measured over a 120 day span, were calculated at 28 hours for EGF supplemented cells, compared to 65 hours for unsupplemented cells. Importantly, EGF-ASCs still undergo robust differentiation and appear otherwise unchanged compared to ASCs under standard conditions, apart from the enhanced proliferation rate and increased senescence timing, which is consistent with a recent report suggesting ASCs have functional EGF receptors (Baer et al., 2009).

We have detailed a simple, rapid, and effective method for isolating adipose-derived stem cells from the blood/saline fraction of lipoaspirates. These ASCs exhibit somatic progenitor (i.e. stem cell traits) and phenotypic properties indistinguishable from ASCs isolated using the labor-intensive traditional protocol and the gold-standard BM-MSC. We have also observed that EGF supplementation increases proliferation rates of ASC cultures. Thus, the methods described here mutually facilitate the autologous stem cell extraction process and the ability to generate a large number of cells, both of which have been longstanding hurdles for basic regenerative medicine research and therapeutics.

Table 5: EGF Supplemented ASC Media Enhances Growth

Cell Type	Growth Rate (PD/week)*	Avg. Senescence PD
ASCs (-EGF)[#]	2.58	38.5
ASCs (+EGF)	6.05	46.5

*PD – population doubling
[#]EGF – epidermal growth factor

METHODS

Traditional and Rapid ASC isolation

ASC isolation was carried out as previously described with slight variations (Zuk et al., 2002). Briefly, oil from the top of the lipoaspirate was immediately removed from freshly harvested fat, followed by the isolation of the saline/blood fraction (see Figure 4). For the traditional isolation, 200ml aliquots of fat were washed 3-4 times with equal volume PBS and incubated in 50% volume 150μg/mL collagenase (Sigma-Aldrich) with 1% ABAM (Invitrogen) for 60min at 37°C shaking at 250rpm. Collagenase was inactivated with 10% FBS, followed by redistribution of mixture into 50ml conicals and centrifugation at 1000xg for 10min to separate the oil and remaining fat lobules from the stromal vascular fraction (SVF). The pelleted SVF was treated with 160mM NH_4Cl at room temperature for 10min to lyse red blood cells, and applied to a Percoll gradient (Sigma-Aldrich) to purify the mononucleated cells.

The rapid isolation protocol involves multiple steps at room temperature including centrifugation of the saline/blood fraction at 400xg for 10min, followed by red blood cell lysis with 160mM NH_4Cl for 5min, and a final centrifugation for 10min at 400xg.

For both traditional and rapid protocols, the final pelleted fraction of mononuclear cells was then resuspended in 25ml DMEM:F12 media (Invitrogen) supplemented with 40% FBS (Invitrogen), ABAM, and 10ng/mL EGF (BD Biosciences) incubated overnight to select for adherent cells. The remaining floating cells were aspirated off the following day, and the plate was washed with PBS to remove any remaining debris. ASCs were maintained on DMEM low glucose supplemented with 10% FBS, 1% ABAM, with or without 10ng/ml EGF at 5% CO_2 at

37°C. For quantification of growth, cells were maintained on 100mm dishes and split at confluence at a ratio of 1:4 until a senescent state was achieved.

Osteocyte Differentiation

Cells are plated and grown until approximately 75% confluent, followed by osteogenic differentiation in DMEM with high glucose, 10% FBS, 0.01μm 1.25-dihydroxyvitamin D3 (Sigma-Aldrich), 50μm ascobate-2-phosphate (Sigma-Aldrich), 10mM β-glycerophosphate (Sigma-Aldrich), and 1% ABAM. The cells were cultured for 2 weeks and then washed and fixed in 4% paraformaldhyde. The cells were then stained using Alizarin Red S (Sigma-Aldrich), which specifically stains calcium deposits, and whole field light microscopy images were then captured at 10x.

Adipocyte Differentiation

Cells that were fully confluent were treated with adipogenic media containing DMEM low glucose, 10% FBS, 0.5mM isobutyl-methylxanthine (Sigma-Aldrich), 1μM dexamethasone (Sigma-Aldrich), 10μM insulin, 200μM indomethacin (Sigma-Aldrich), and 1% ABAM. The plates were maintained for 2 weeks until lipid droplet formation was observed, followed by fixation in 4% paraformaldehyde. Fixed cells were stained with Oil Red O (Sigma-Aldrich), which specifically stains lipid droplets, and whole field light microscopy images where captured at 10x.

Chondrocyte Differentiation

At total of 2 x 10^5 cells were pelleted in a 2ml V bottomed tube and placed in the incubator at 37°C with 10% CO_2 in chondrogenic media, which contained DMEM low glucose, 1% FBS, 6.25μg/ml insulin, 10ng/ml recombinant TGFβ3 (R&D Systems), 50nM ascorbate-2-phosphate, and 1% ABAM. After 1 week, the pellets were transferred to a 10 cm dish and cultured in the same media formulation for another 2wks. The pellets were fixed in 4% paraformaldehyde and stained with Safranin O (Sigma-Aldrich), which specifically stains GAG proteins present in chondrocyte extracellular matrix. The micromass pellets were imaged with a 1mm scale bar to indicate gross anatomy and size.

Flow Cytometry

Both traditional and rapid ASCs were trypsinized and counted in order to obtain 5 x 10^5 cells for primary antibody or 2 x 10^5 cells for secondary antibody only and no antibody controls. These cells were centrifuged at 100xG for 1min at 4°C and resuspended in 75μl of FACS buffer (PBS, 2% FBS) and incubated on ice for 10 minutes. The primary antibody was added (CD14, CD29, CD34, CD45, CD73, CD105, InVitrogen; CD34, Millipore, 100mg/ml) and incubated with rotation at 4°C for 30min, followed by centrifugation and 3 washes with FACS buffer. The secondary antibody (Alexa 488 goat anti-mouse; Invitrogen)) was then added at a dilution of 1:400 and incubated in the dark at 4°C with rotation for 30min. The washes were then repeated, and the resulting pellet was resuspended in 500μl PBS and forced through a 35μm mesh filter to remove any cell clumps. Immunolabeled cell suspensions were kept on ice until cytometric analysis, which was performed using a Coulter Epics XL-MCL.

-Chapter 3-

Results: Electrospinning Adipose Tissue-Derived Basement Membrane for Stem Cell Culture and Regenerative Medicine Applications

ABSTRACT:

We describe a robust method for purifying the extracellular matrix (ECM) from adipose tissue and the use of this adipose tissue ECM (At-ECM) for electrospinning and adipose stem cell (ASC) culture. The matrix composition of this purified and electrospun adipose tissue ECM was assessed histochemically, showing basement membrane, connective tissue, collagen elastic fibers/elastin, glycoprotein and proteoglycans staining. Each of the histochemical stains was positive for fat tissue, purified fat ECM, and for electrospun fat ECM samples, while staining slightly positive blended with a synthetic biomaterial, polydioxanone (PDO). Protein analysis also revealed the presence of collagen type I in purified adipose tissue ECM. Immunolabeling for collagen type IV directly indicated its presence in fat tissue, in purified fat ECM, and in electrospun fat ECMs. We also assessed the ability of electrospun adipose ECM, alone and blended with polydioxanone (PDO), for supporting adipose stem cell attachment and growth, showing that electrospun adipose ECM scaffolds fully support the cultivation of ASCs. These studies show for the first time that adipose ECM can be isolated and electrospun as a tissue engineering matrix capable of supporting stem cells, providing the groundwork for an array of future regenerative medicine advancements.

INTRODUCTION:

Originally thought of as merely the structural component for cell and tissue support, extracellular matrix (ECM) has been established as being important throughout biology. Four major classes of macromolecules—collagens, structural glycoproteins, proteoglycans, and elastin—collectively comprise the ECM of animal cells, being both widely distributed and multifunctional throughout the body **(Table 1) (**Palsson et al., 2004). ECM is constantly synthesized, secreted, oriented, and modified by the cellular components that they support. Members of each family and class of ECM molecules exhibit a degree of tissue-specific distribution, implicating the ECM in development and tissue function. Additionally, specific cell surface receptors have been identified on ECM components, linking the biology of the cell with its ECM interactions.

Throughout embryonic and fetal development, ECM interactions orchestrate such activities as cell migration and proliferation, stem cell differentiation, tissue patterning, and morphogenesis (Campbell et al., 1985; Flaim et al., 2005; Haylock et al., 2005; Kihara et al., 2006; Suzuki et al., 2003). The ECM interacts directly with cell surface receptors, acting as a reservoir for growth factors and morphogenetic proteins, as well as simply providing a scaffold for cell attachment and cell migration. Even cell morphology is determined by contact with the ECM, which may be associated with cell differentiation and proliferation. For example, floating type I collagen gels can induce functional differentiation of precursor cells into mammary glands, mediated through changes in cell shape, allowing branching morphogenesis to occur (Bissell et al., 1987). Further, laminin-I is expressed in developing mouse lung by epithelial and mesenchymal cells, where it is essential for branching morphogenesis (Schuger et al., 1991).

Basement membranes are common to tissues of nearly all multicellular metazoans, and their gene products are highly conserved and are among the most ancient in nature (Exposito et at., 2002, Hutter et al., 2000). Basement membrane (or basal laminae) proteins are the first ECM materials to appear during embryogenesis, with laminin being the first detectable ECM protein that appears shortly after morula differentiation (Martin and Timpl, 1987; Miner and Yurchenco, 2004). Throughout development of the embryo and fetus, basement membrane and other ECM materials assemble in nearly all tissues, having a profound effect on their developmental fate. Loss of phenotype studies in *C. elegans* have shown that several basement membrane components, including type IV collagen, laminin, and perlecan, are necessary for tissue organization and structural integrity, and essential for the completion of embryogenesis (Kramer, 2005).

While the basal laminae has proven to be an important ECM throughout biology, a suitable human source of this basement membrane ECM, especially engineered as biomimetic nanofibers, has been sorely lacking. If a basement membrane analogue of human origin could be derived and engineered with biologically relevant fibers sizes, there exist many potential applications for this material in basic research and clinical therpies.

A material of human origin that could possibly take the place of commonly used xenogenic basement membranes in research, such as Matrigel®, which would have great potential for rapid clinical translation, is autologous adipose tissue ECM (At-ECM). Adipose is an extracellular matrix-rich tissue densely composed of collagens Type I, III, IV, V, and VI, laminin, and fibronectin (Nakajima et al., 1998). In fact, the amounts of these proteins have been shown to match or exceed the levels of ECMs from tissues known to be rich in such materials,

such as the perimysium from skeletal muscle (Nakajima et al., 2005, Abberton et al., 2008). Interestingly, recent studies have shown that adipose cell precursors differentiated into mature adipocytes heavily secrete collagens Type I, III, IV, V, and VI, laminin, and fibronectin *in vitro*. These preadipocytes cultured in adipogenic differentiation media exhibit an 8- to 15-fold upregulation in deposition of these ECM materials in the extracellular spaces when compared to the same cells cultured in normal growth media (Nakajima et al., 2002).

Markedly few established protocols exist for harvesting purified fat ECM from patient-derivable liposuction in quantities suitable for regenerative medicine applications (Haaralson et al., 1995). Moreover, as fat ECMs have only been scarcely referenced and rarely studied in the field, it is not surprising that adipose tissue has yet to be tested for its ability to be electrospun into a nanofibrous tissue engineer matrix.

The electrospinning technique for bio-scaffold construction has rapidly gained favor in the tissue-engineering field due to its numerous advantages over conventional scaffold fabrication methods (Barnes et al., 2007). Electrospinning involves maintaining a polymer solution at the tip of a needle at its surface tension by way of a syringe pump. As sufficiently high voltage is passed through the needle, the polymer's outer layers receive a charge, pulling them from the needle and towards a grounded collection through the electric field. As the polymer leaves the needle, the solvent evaporates, leaving dry polymer fibers for collection. Natural matrix materials, such as collagen, laminin, elastin, and fibrinogen, and synthetic materials such as the suture material polydioxanone (PDO), can be electrospun into scaffolds of numerous shapes and microscopic properties, resembling native extracellular matrices in geometry, fiber size, and material composition (Barnes et al., 2007, Matthews et al., 2002; Wnek

et al., 2003; McManus et al., 2007; Boland et al., 2005). While conventional polymer processing techniques generally create fibers 10μm or larger in diameter, the nanofibers generated from electrospinning are capable of mimicking the sub-micron diameter and geometry typical of endogenous tissues.

While it is widely accepted that a biomimetic, autologous matrix supply is therapeutically desirable, an abundant source for regenerative medicine applications is still lacking. We show that adipose tissue ECM (At-ECM) is a valuable autologous ECM material, one that can be procured from a readily accessible source and is amenable to the electrospinning process. This newly synthesized material produces biomimetic nanofibrous scaffolds that are rich in basement membrane components that are further capable of supporting ASCs.

MATERIALS AND METHODS:

Adipose Stem Cell Primary Isolation and Culture

In accordance with Virginia Commonwealth University's IRB, lipoaspirate was obtained as surgical waste from patients undergoing elective, cosmetic surgery using standard techniques, and characterized as described previously (Francis et al., 1010, Zuk et al., 2001; Zuk et al., 2002). The cells were cultured in low glucose DMEM (Gibco) with 10% FBS (Hyclone), 10nM recombinant human EGF (Sigma), and 1% ABAM, and maintained at 37°C with 5% CO_2. Cells were verified to be multipotent and to exhibit a mesenchymal stem cell immunophenotype as we previously reported (Francis et al., 2010).

Microscopy

To determine scaffold topography and fiber diameter of electrospun adipose tissue ECM scaffolds, SEM was performed. Constructs were fixed in gluteraldehyde and processed by standard methods in the VCU Microscopy Core (Crawford et al., 2004). Samples were then gold sputter coated and analyzed by a Zeiss EVO 50 XVP (Nano Technology System Division, Carl Zeiss), with images taken at 20kV, and at least 3 representative fields captured for evaluation. For fluorescent microscopy visualizing of ASCs grown of electrospun At-ECM, scaffolds were stained with 4',6-diamidino-2-phenylindole (DAPI) and mounted in Vectashield (Vector Lab H-1000). An Olympus IX70 inverted fluorescent microscope was used for capturing phase and fluorescent images using QCapture Pro software (QImaging).

Adipose Tissue ECM Extraction

All steps were performed at 4ºC to maintain matrix integrity and prevent enzymatic digestion of the adipose tissue extracellular matrix (At-ECM). Around 200ml of lipoaspirate (n=16) was washed extensively in cold PBS to remove contaminating red blood cells and enzymes. The washed lipoaspirate was cycled through extensive freeze-thaw cycles with liquid nitrogen and a RT water bath. The upper oil/lipid phase from lysed adipocytes was drawn off, and the processed stromal tissue was then thoroughly digested in 20x volumes of 0.5M acetic acid at pH 2.5 for 48-72hrs with vigorous stirring, and tested with or without a 1:10 diluted pepsin (Sigma)-to-ECM blend. Remaining undigested floating tissue (albeit minimal) was filtered out with cheesecloth. The digested matrix was centrifuged at 8,000 x g for 10min and the undigested tissue pellet discarded and any remaining oil drawn off. The opaque supernatant was dialyzed 3 times in 12-14,000MW dialysis tubing against 0.5M acetic acid changed daily, then against 3 daily changes of pure deionized water. The resulting opaque and condensed matrix within the dialysis tubing was frozen at -80ºC and minimally lyophilized, with the resulting yellowish, fluffy matrix material weighed and stored at -20ºC. Samples were tested for solubility in organic solvent (1,1,1,3,3,3-hexaflouro-2-propanol, HFP, or triflouroacetic acid, TFA, Sigma or TCI America, Portland, OR). If procured At-ECM was not soluble in HFP or TFA, they were re-dissolved in 0.5M glacial acetic acid with a repeat of the dialysis process as above, again with only the minimal amount of lyophilization to prevent undue crosslinking. The samples are then and rechecked for solubility.

Electrospinning Adipose ECM

Separately, 60, 80, 100, 120 and 140mg/ml of adipose matrix material were dissolved in HFP or TFA organic solvents for roughly 15min with mixing, and then electrospun either as pure At-ECM, or a 1:10 At-ECM:PDO blend at 100mg/ml in HFP. The opaque solution was then loaded into a 5ml (Becton-Dickinson) plastic syringe with a blunt tipped 18.5ga needle and placed into a syringe pump (KD Scientific) set at 2.5ml/hr. A 0.3mm X 10mm X 2mm rectangular receiver mandrel was situated 12cm from the needle and set to spin at 650RPM with a 2cm/s translation speed over 7.2cm total travel. The anode from a Spellman CZE1000R high voltage power supply was clipped to the needle for generating a +25kV field, with the mandrel being charged at -5kV with a second amplifier. Pure At-ECM scaffolds were tested with and without cross-linking for 72h at RT in 30mM genipin (Sell et al., 2008) for stability and gelling in warm media for 7 days.

Scaffold Seeding and Tissue Culture

For static seeding, scaffold discs 10mm in diameter were formed with tissue biopsy punches from At-ECM and At-ECM:PDO sheet made at 80-100mg/ml concentrations and placed in 48-well plate. Scaffolds were disinfected with 80% ethanol for 30min, and then washed 3 times for 5min in PBS. Cells to be seeded upon the discs were concentrated to 25,000 cells/100µl, and a single 100µl drop of cells was careful placed on the center of the disc. Cells were allowed to adhere in the incubator for 15min and then 500µl of media was then added. Media was carefully aspirated every 3-4 days and replaced with fresh media. The discs were collected at days 1 and 14 for analysis.

Histological Scaffold Evaluation

Scaffolds were washed in PBS and fixed in 10% formalin, then paraffin embedded, cryosectioned, and mounted on slides for standard histological staining and immunohistochemistry (IHC) at the Anatomic Pathology Laboratory Research Services at VCU. Using a Dako Artisan Staining System X automated system, scaffolds were evaluated for Jones (basement membrane), Mason's (collagen), Gomori (connective tissue/collagen), Periodic Acid-Schiff (glycogen, proteoglycans and glycoproteins), Verhoeff-Von Gieson (elastic fibers/elastin) and H&E staining.

Paraffin embedded scaffold were also sectioned and mounted on slides for IHC using standard techniques. Immunohistochemistry (IHC) was performed on control placental, kidney or liver sections, as well as on an abdominoplasty section of human fat, or purified At-ECM, of electrospun At-ECM, and a 10% At-ECM 90% PDO blended electrospun scaffold. Deparafinized slides were blocked with PBS containing 1% BSA for 60 min at RT. A 300μg/ml aliquot of the collagen type IV monoclonal antibody (Abcam) was diluted in PBS with 1% BSA and one drop was applied to each section, with the slides placed in a humidified chamber overnight at 4°C. The slides were then washed 5X over 50 min in PBS with 1% BSA, followed by immersion in Peroxidase Suppressor (Pierce) for 30 min at RT, followed by 4 washes in PBS with 1% BSA. Next 1-2 drops of the secondary peroxidase-labeled antibody (diluted 1/1,000 in PBS with 1% BSA) was added for all experimental slides but omitted for controls (no primary antibody) which were only washed with 1% BSA. Slides were incubated for 1hr at RT then washed 5X over 50 min in PBS. Slides were dried and then 1/10 diluted 3'-Diaminobenzidine (DAB) metal concentrate (Pierce) in stable Peroxidase Substrate Buffer (Pierce) was added, with

the reaction allowed to occur for 10-15min, followed by a distilled water wash. The slides were dehydrated in 80%, 90% and 2x 100% ethanol for 1 min each, then immerse in 2 changes of xylene for 1 min each, and mounted with cover slips using Permount.

Fiber Diameter Measurement

SEM images of pore morphologies, fiber alignments, and fibers size of dry electrospun sheets were captured using a Zeiss Evo50 scanning electron microscope. ImageJ 64 (NIH shareware) was used to measure fiber diameter. A total of 50 separate fibers in total were used to determine the mean fiber size and to calculate the standard deviation from n=3 scaffolds per count, with calibration for each image made from the corresponding size scale bar on each SEM micrograph. The mean fiber diameter and error was determined using the Student's t-test.

.

RESULTS:

After significant testing and protocol modifications, it was determined that the crucial step in At-ECM extraction was to freeze-thaw the lipoaspirate using liquid nitrogen prior to chemical purification. Lipoaspirate was frozen in liquid nitrogen with subsequent pulverization of the frozen sample with a heavy blunt object or in a blender, followed by additional freeze-thaw cycles in liquid nitrogen or at -80C in order to lyse the resilient adipocytes, which must be removed for successful At-ECM harvesting. While only providing around 6.4% yield based on estimated dry weights (n=3), the At-ECM extracted using cryotreatment was amenable to electrospinning, producing nanofiber scaffolds **(Figure 6A and 6B)** with a fibrous structure similar to electrospun Matrigel **(Figure 6C)**.

The ability of the purified At-ECM to co-electrospin was also verified with a synthetic polymer, PDO, as shown **(Figure 6D)**. The average fiber diameter of the electrospun adipose tissue ECM with 80mg/ml and 100mg/ml starting concentration and the fiber size of the 100mg/ml adipose ECM:PDO blend were also calculated (**Table 6)**. At-ECM concentrated above 100mg/ml generally sputtered ECM material onto the collector, and less than an 80mg/ml concentration of At-ECM:HFP electrospun erratically and produced extremely thin fibers, prohibiting the calculation of any fiber properties. In purifying freeze-thawed At-ECM, we observed a well-dissolved mixture of connective tissue when mixed in acetic acid **(Figure 6E)**. After dialysis and mild lyophilization, we consistently found a light, fluffy material produced with a slight yellow hue **(Figure 6F)**.

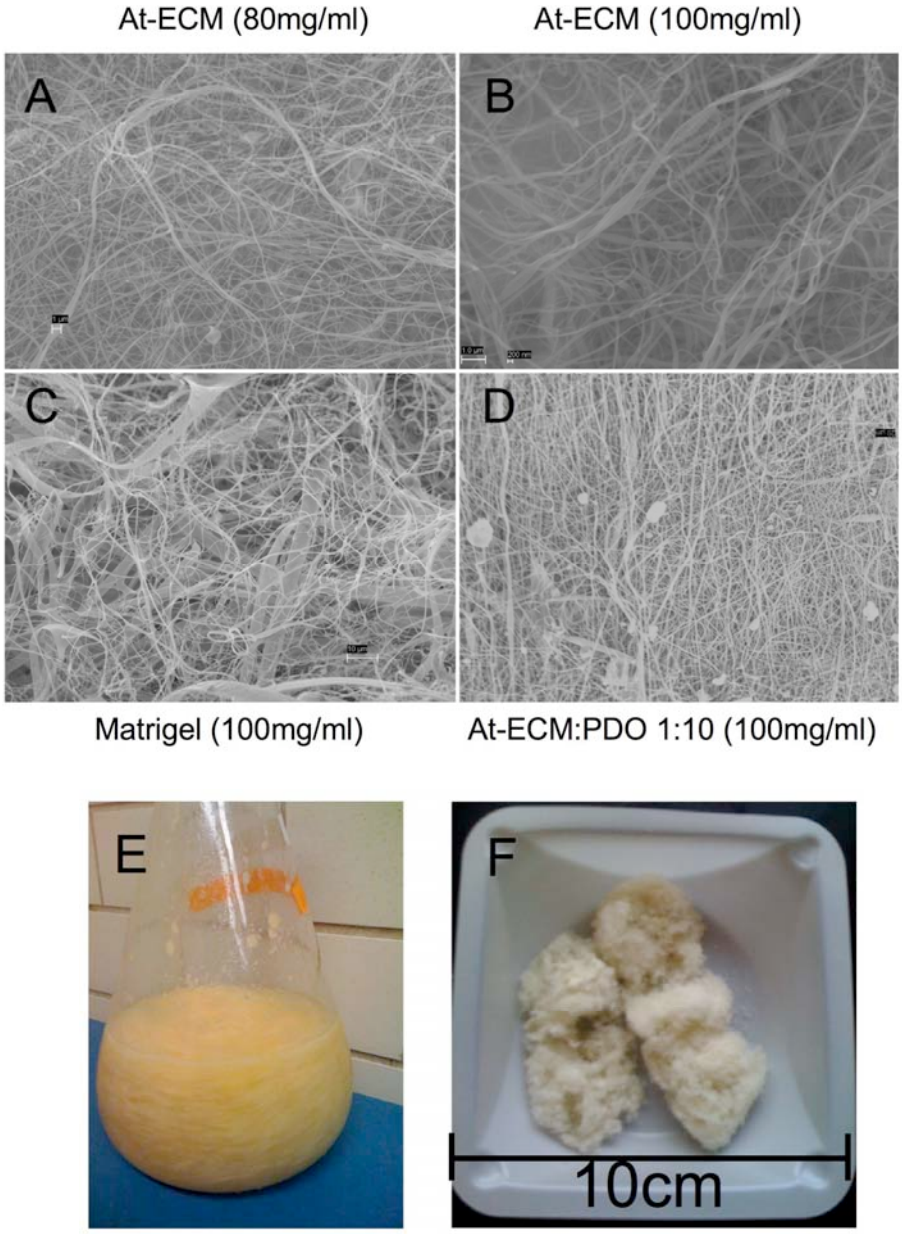

Figure 6. Adipose ECM Extraction and Electrospinning. At-ECM was electrospun at 80mg/ml (A) and 100mg/ml (B) produce a biomimetic tissue engineering substrate with fibers formed in the biologic ~20-400nm range (A-B), morphologically resembling a related electrospun basement membrane matrix of Matrigel (C). At-ECM also readily copolymerized when electrospun as blended at 10% At-ECM with 90% PDO (weight per volume) to form a nanofibrous mesh (D). The appearance of the freeze-thawed lipoaspirate processed for 24 hours in acetic acid is shown while vigorously stirring for reference, free of large floating clumps of adipose tissue typical of tissue that was not pre-treated to remove contaminating adipocytes and lipids (E). 0.5g of purified, dialyzed and mildly lyophilized At-ECM with a light and fluffy texture is shown for reference in a 10cm weighing dish (F).

Table 6: Average Fiber Sizes of Pure and PDO Blended Electrospun Adipose ECM

	Average Fiber Diameter (n=50)	Min-Max Fiber Size Range (n=50)
80mg/ml Adipose Tissue ECM	130 ± 123 nm	18 – 430 nm
100 mg/ml Adipose Tissue ECM	298 ± 266 nm	31 – 772 nm
10:90 Blend of 100 mg/ml Adipose ECM:PDO	251 ± 56 nm	66 – 348 nm

We also determined that briefly lyophilizing the matrix was crucial for successfully dissolving the adipose tissue in HFP. To ensure a rapid lyophilization process, the At-ECM was frozen in an ice cube tray then blended into small ice chips in a food processor with the chips adhering to the walls of the lyophilization containers, which enhances the available surface area for a rapid lyophilization process. Excessive lyophilization produced an excessively hard material that was resistant to HFP or TFA and thus not amenable to the electrospinning process. We also found that a thorough dialysis was required for producing pure ECM for electrospinning. By skipping the dialysis step and just collecting digested At-ECM by centrifugation with PBS washing and direct lyophylization, this unpurified At-ECM was soluble in organic solvent (HFP or TFA) and electrospun, yet the resulting spun matrix appears impure and disorganized under SEM (**Figure 7A-C**), with large particulate matter intertwined within the nanofiberous mesh (n=3).

We observed that standard salt/acid-based ECM purification methods alone fail to significantly dissolve At-ECM tissue, leaving adipocyte-dense spheres that persisted even after 2 weeks of acid digestion and making fat ECM purification yields extremely poor (0.9% yield of calculated starting dry tissue weight, or 3% yield with a 1:10 pepsin blend added, n=2). We have found that acetone can be used to efficiently lyse the adipocytes in the lipoaspirate, followed by isopropanol to wash the acetone, lipids, and cell debris out of the tissue. In two separate trials, the acetone/2-propanol processing produced a yellowish and fluffy matrix material **(Figure 7D)** with good yields (~11% starting dry tissue weight). The acetone/2-propanol treatment appeared to leave the resulting, partially purified scaffold largely insoluble in organic solvent **(Figure 7E)**, and hence unable to be efficiently electrospun. In characterizing this newly derived matrix, the

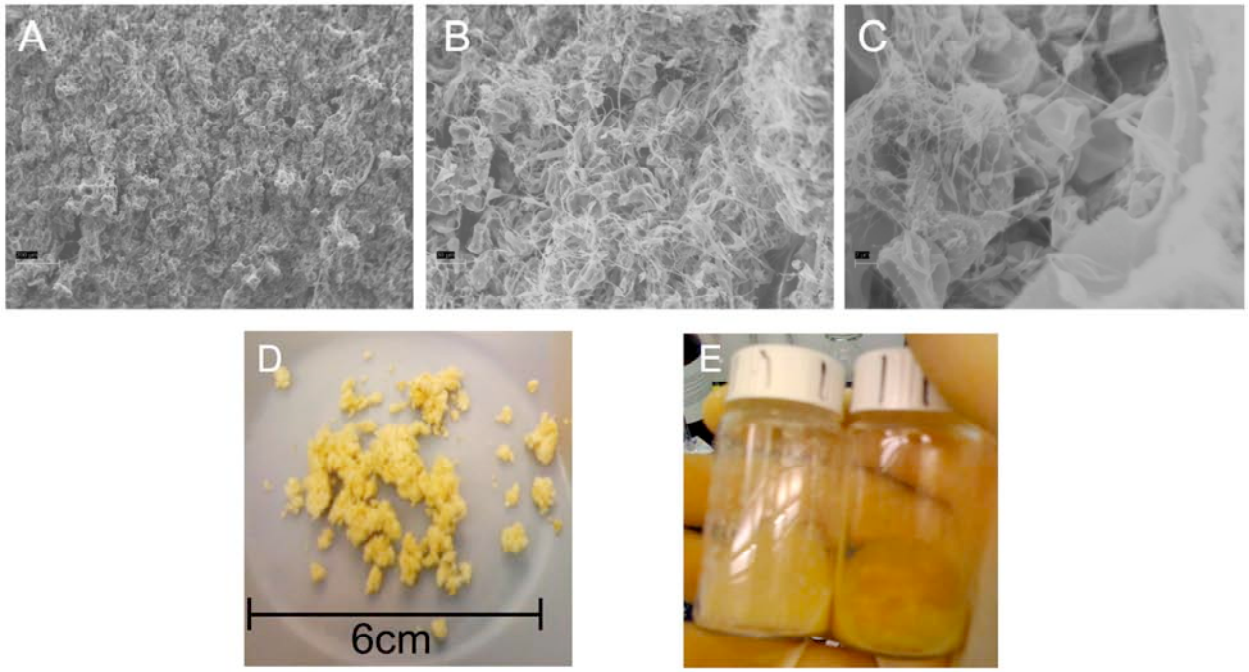

Figure 7. Partially Purified Adipose ECM Extraction and Electrospinning. Adipose matrix not dialyzed was electrospun at 60mg/ml to produce a particulate filled fibrous mesh as seen at 1000x (A), 4000x (B) and 8000x (C). Partially purified, un-dialyzed At-ECM, with its dense and strong yellow hue is shown for reference in a 10cm dish (D). Also shown are two batches of adipose ECM dissolved in HFP overnight, with one batch (F, left vial) of a freeze-thaw pre-treated tissue dissolving thoroughly in organic solvent, and the other batch (F, right vial) of acetone-isopropanol pre-treated lipoaspirate only partially dissolving in the organic solvent, leaving very large clumps of material behind.

At-ECM that has been salt extracted showed appropriately sized bands and patterning, similar to batches of purified bovine collagen type I **(Figure 8)**, suggesting the presence of type I collagen in the mixture.

Using histochemical analysis, we further determined the composition of our extracted adipose tissue ECM in its native, purified, electrospun, and co-electrospun forms. Our results strongly indicate the presence of basement membrane (Jones Stain, **Figure 9**), collagen (Mason's Trichrome stain, **Figure 10**), elastic fibers or elastin (Verhoeff-von Gieson stain, **Figure 11**), and connective tissue and collagens (Gomori's Trichrome Stain, **Figure 12**) in unprocessed and At-ECM, all of which were also present after electrospinning At-ECM, and to a lesser degree in a electrospun 10:90 At-ECM:PDO blend, as expected. Periodic acid-schiff (PAS, **Figure 13**) stains further suggested an abundance of glycogen, glycoprotein, and proteoglycans in adipose tissue, purified fat, and electrospun At-ECM, although PAS only moderately stained At-ECM:PDO scaffolds. Finally, immunohistochemistry confirmed the presence of collagen type IV in fat tissue, purified At-ECM, and in electrospun At-ECM **(Figures 14 and 15)**.

In order to better replicate the native cell niche using electrospun At-ECM instead of tissue culture plastic, we were able to produce an efficient and effective method for directly electrospinning natural and synthetic materials onto tissue culture plastic, illustrated in **Figure 16 A and B**. We were able to directly generate electrospun nanofiber-coated culture dishes as shown **(Figure 16C)**. Light microscopy analysis confirmed the formation of non-woven fibers deposited by electrospinning on the culture dish using At-ECM or PDO **(Figures 16D-F)** for the coating substrate.

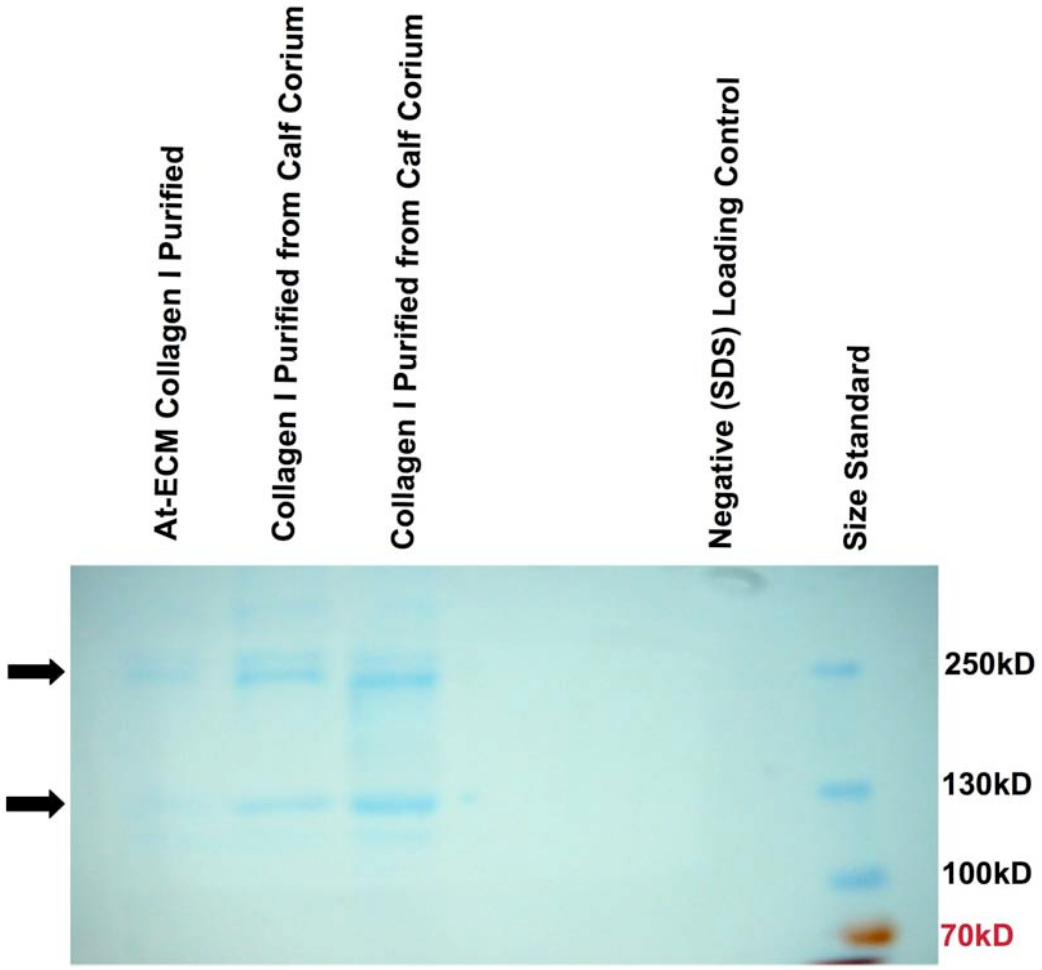

Figure 8. Adipose Tissue ECM Matrix Composition. At-ECM was extracted from human lipoaspirate and bovine skin with selective salt precipitation to isolate type I collagen, with purity assayed via SDS-PAGE gel and stained with biosafe Coomassie Blue. In 2 separate extractions of calf corium (positive control), were observed two prominent bands at 130 and 260KD, typical of type I collagen (lanes 1 & 2). The purified human At-ECM that was salt/acid extracted for type I collagen produced a similar banding pattern (lane 4) as purified and suggests that type I collagen is present in the purified At-ECM. Additional proteins were apparent in the crude, non-salt/acid extracted At-ECM (lane 5).

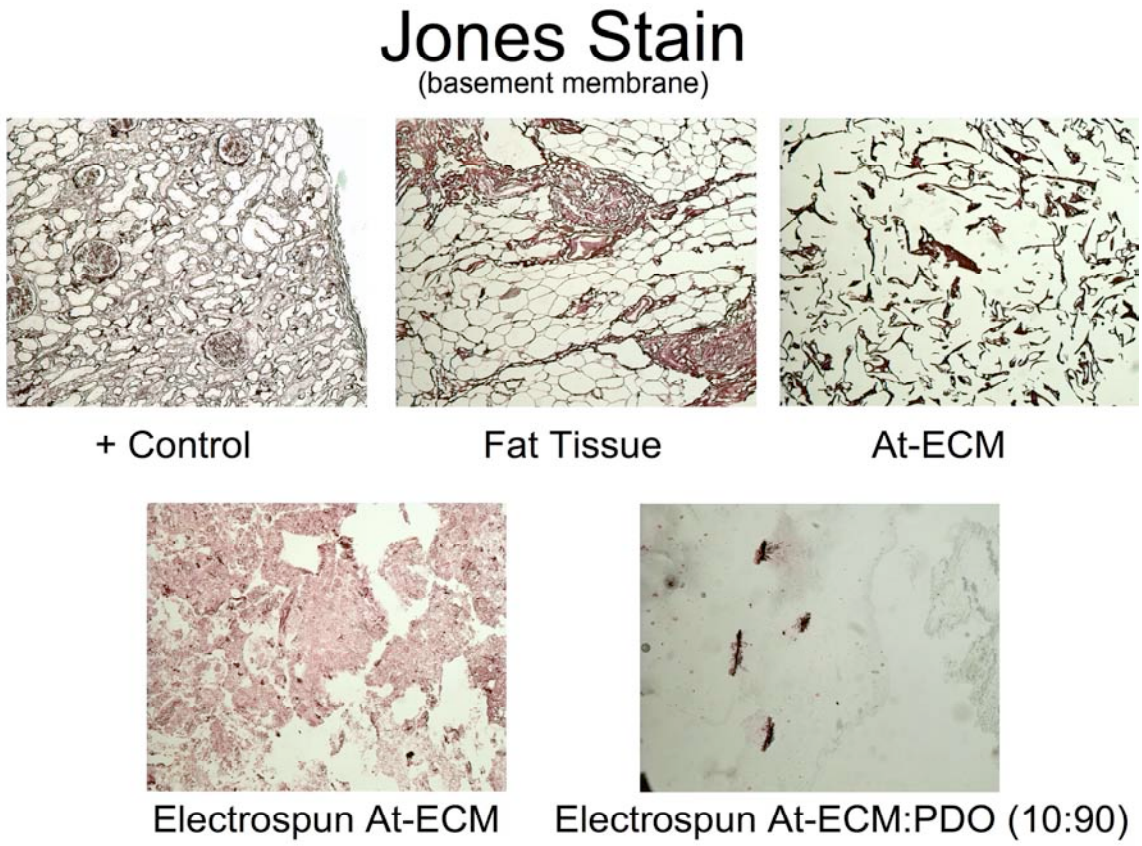

Figure 9. Jones Staining for Basement Membrane. Jones stains indicated an abundance of basement membrane present in the placenta positive control, fat tissue, purified At-ECM and electrospun At-ECM as seen by the red fiber coloration, while lightly staining the electrospun At-ECM:PDO scaffold, suggesting the trace presence of basement membrane persisting in this blended electrospun processed scaffold (20x).

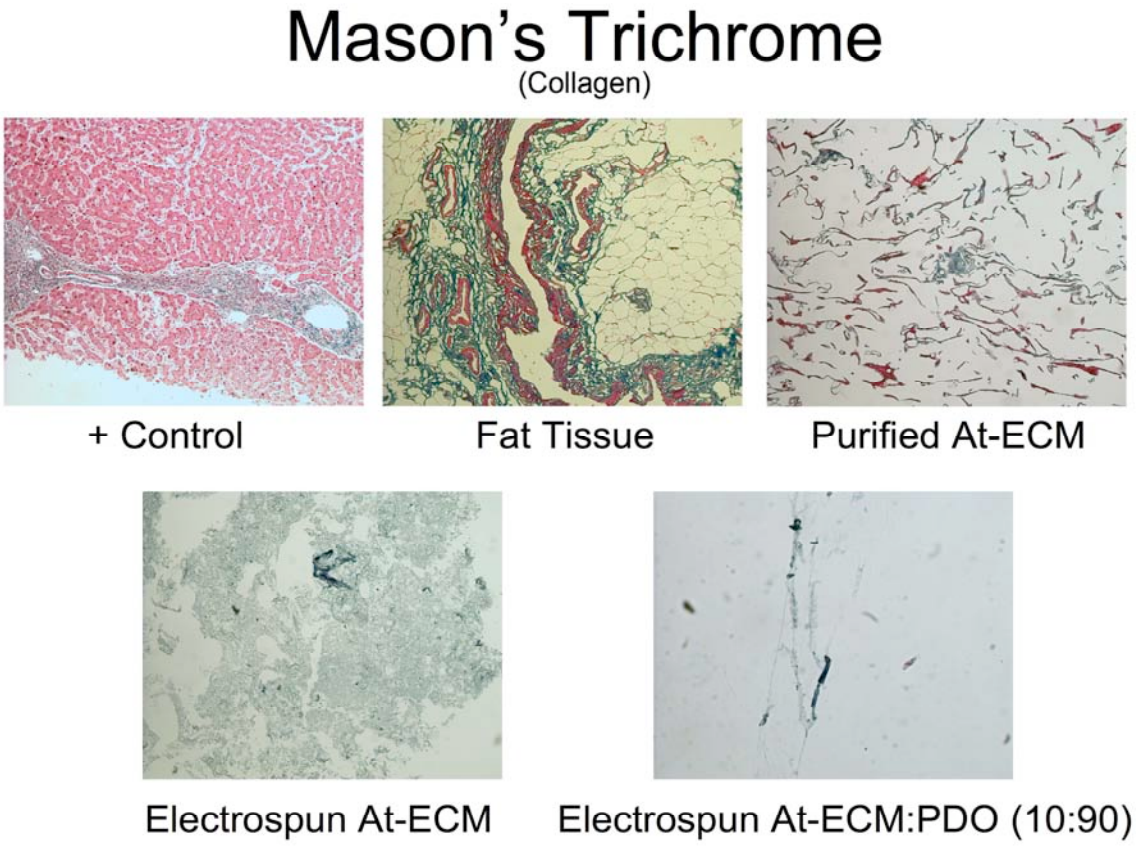

Figure 10. Mason's Trichrome Staining for Collagen. Mason's Trichrome strongly stained the placenta positive control, fat tissue, purified At-ECM and electrospun At-ECM blue, and also moderately stained the electrospun At-ECM:PDO scaffold, suggesting the presence of collagen in each sample (20x).

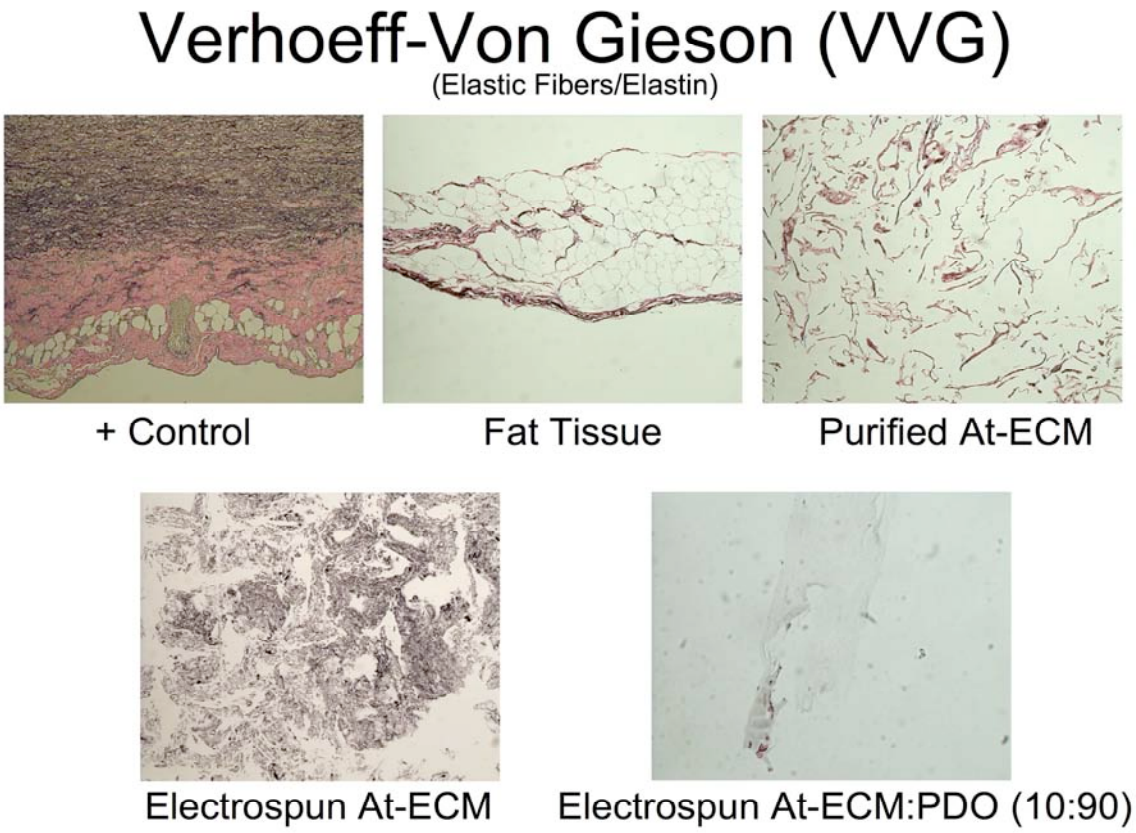

Figure 11. Verhoeff-Von Gieson (VVG) Staining for Elastic Fibers/Elastin. VVG evenly stained the placenta positive control, fat tissue, purified At-ECM and electrospun At-ECM a magenta hue, with dense staining localized to the vasculature in the abdominoplasty fat tissue sample. VVG also moderately stained electrospun At-ECM:PDO, suggesting the presence of elastic fibers or elastin in all sample (20x).

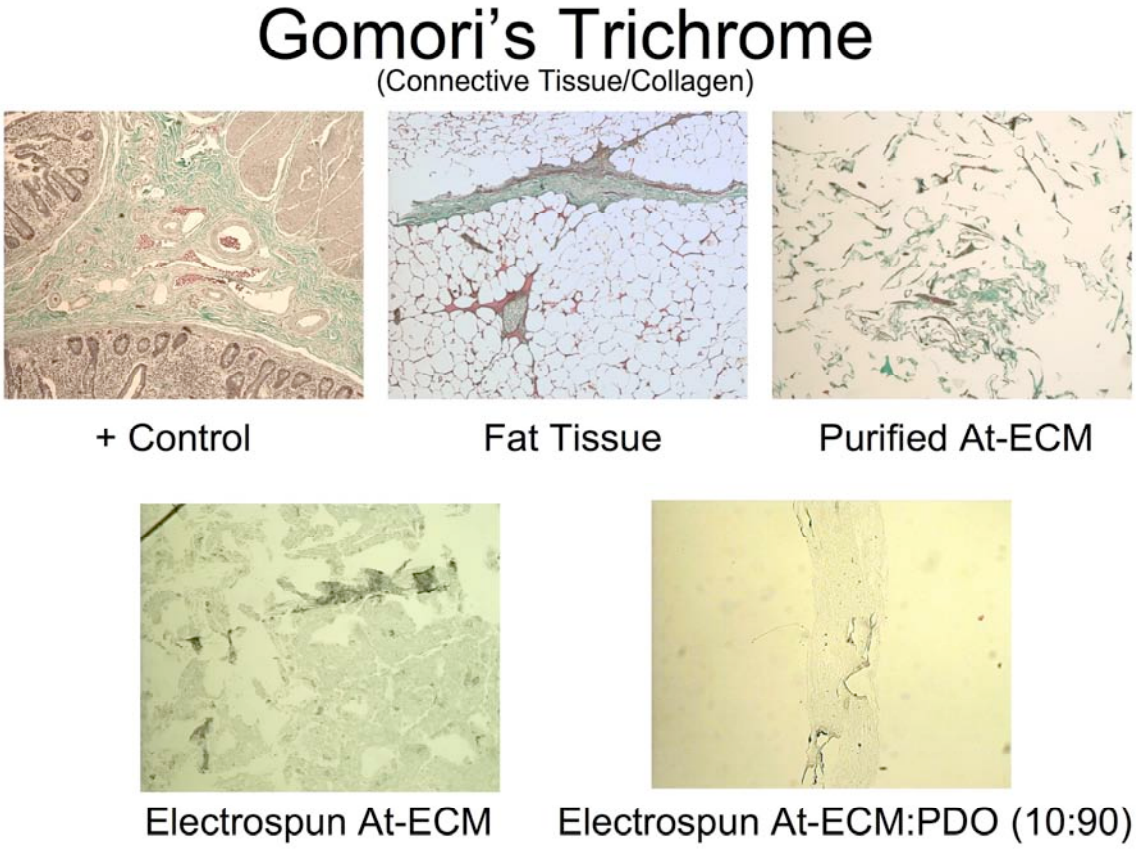

Figure 12. Gomori's Trichrome Staining for Connective Tissue/Collagens. Gomori's Trichrome evenly, strongly and positively stained the kidney positive control, fat tissue, purified At-ECM and electrospun At-ECM a light blue coloration, and also moderately stained electrospun At-ECM:PDO, suggesting the presence of connective tissue in each sample (20x).

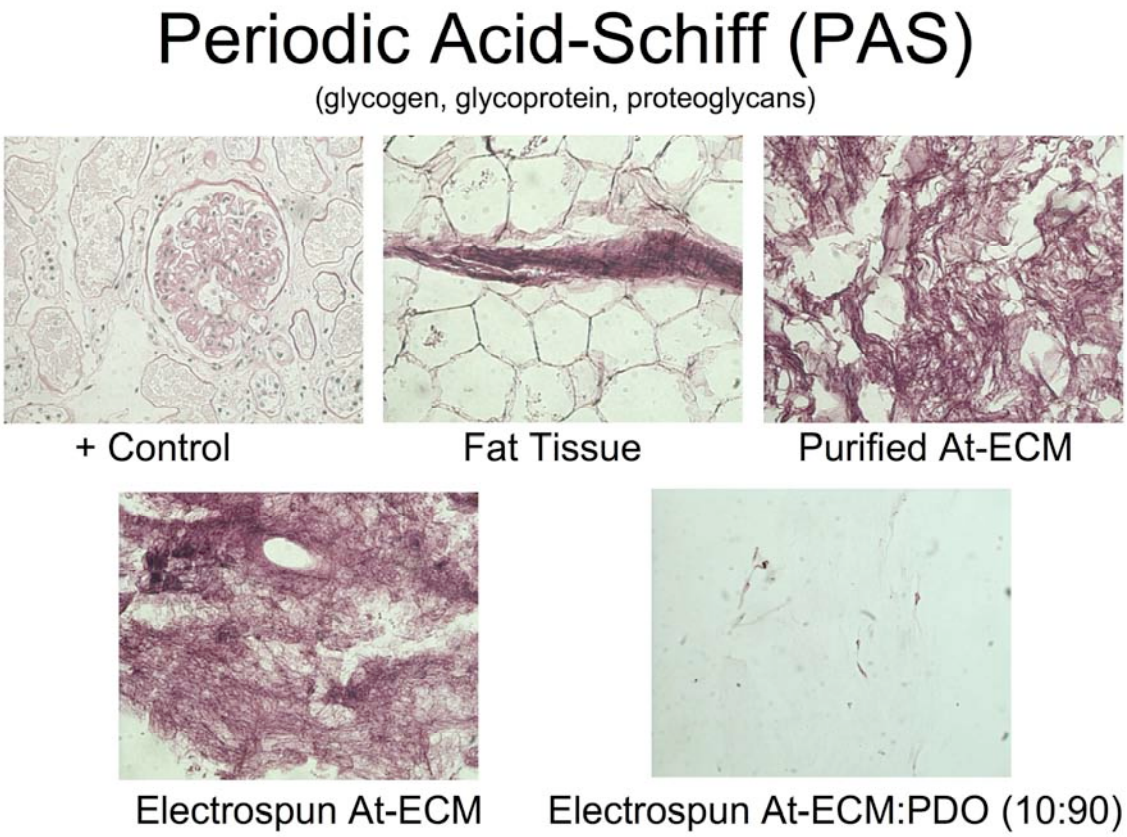

Figure 13. Periodic Acid-Schiff Staining for Glycogen, Glycoproteins and Proteoglycans. PAS staining indicated that *in vivo* and purified adipose tissue, as well as electrospun At-ECM contained a very large and orderly array of glycogen, glycoprotein, and proteoglycans, indicated by the reddish-pink coloration. Such high amount of staining was expected as glycoproteins and proteoglycans are covalently cross-linked to collagens *in vivo* and should remain tightly bound through the processing. Normal kidney served as a positive control (40x). An electrospun At-ECM:PDO blend showed trace PAS staining.

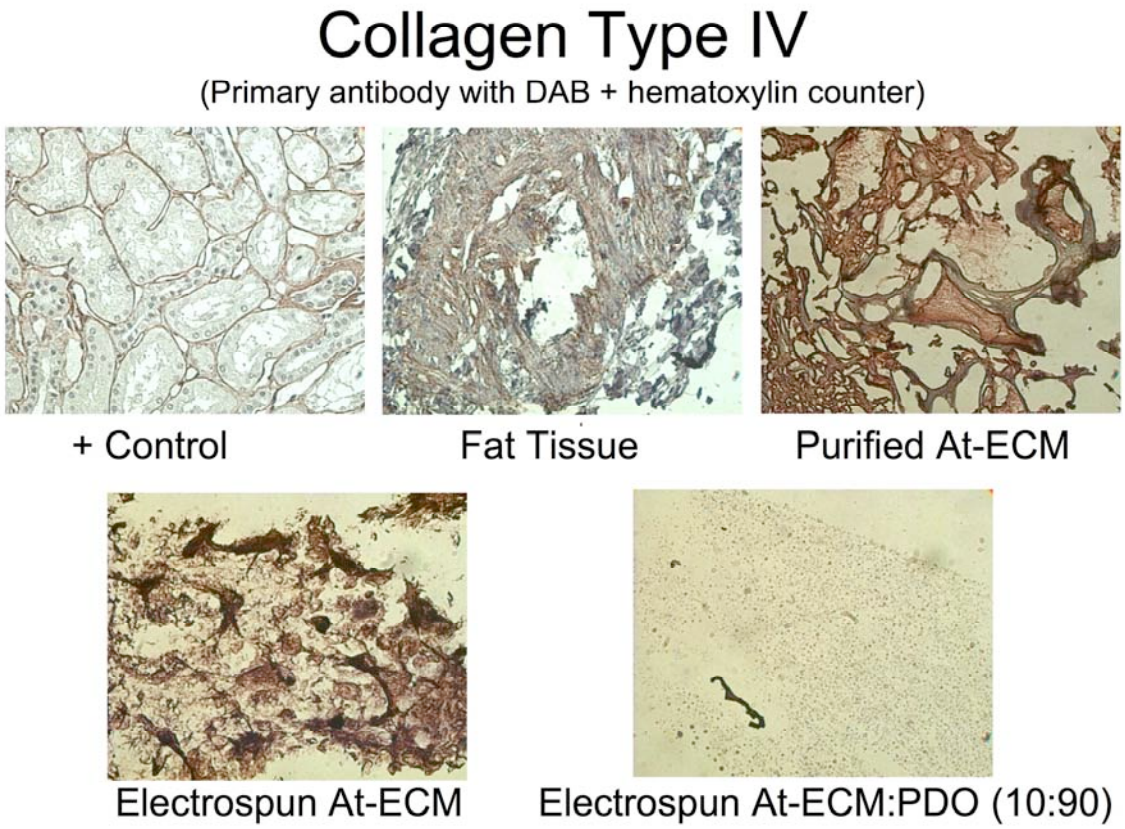

Figure 14. Collagen Type IV Protein in At-ECM. An antibody against type IV collagen was used to identify the protein in adipose tissue, purified At-ECM, electrospun At-ECM and At-ECM:PDO blend, as detected by DAB. The presence of collagen IV is indicated by the brown DAB staining against the blue hematoxylin counterstain and compared to placental tissue as a positive control (40X).

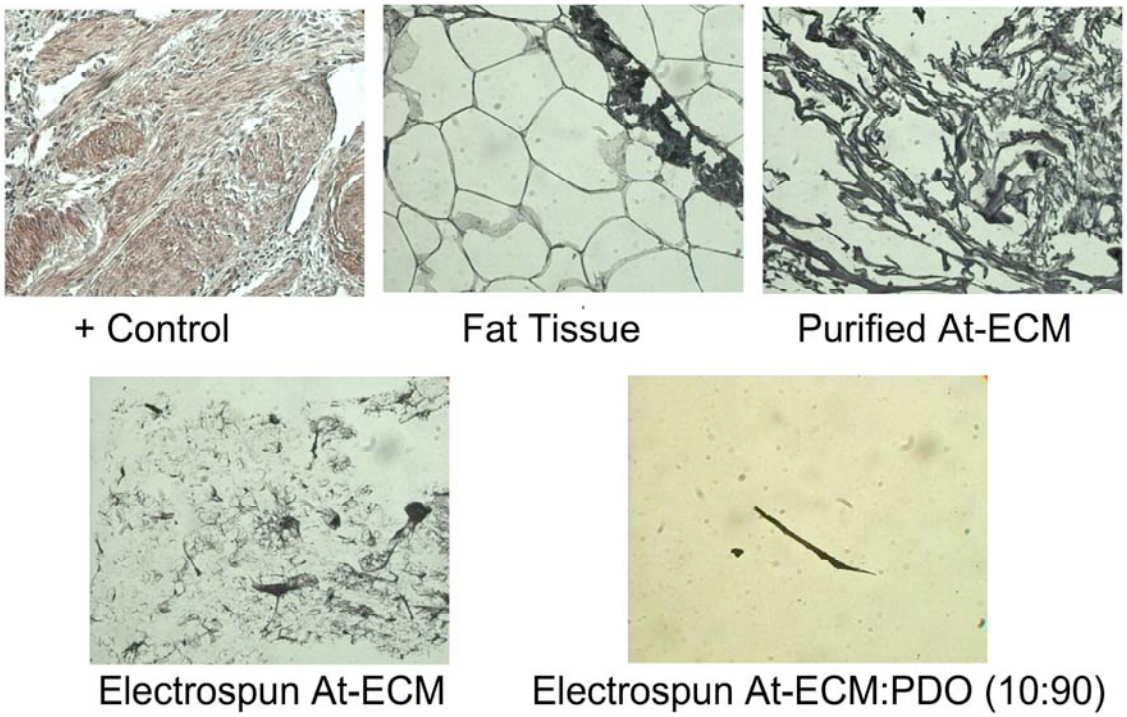

Figure 15. Antibody Control for Collagen Type IV in Adipose Tissue ECM. For validating antibody specificity, the antibody against type IV collagen was applied, per figure 9, but without the primary antibody, on fat tissue, purified At-ECM, electrospun At-ECM and At-ECM:PDO blend, with subsequent application of DAB. DAB was found absent on all experimental (no primary antibody) samples and present only on the positive placenta control to which the secondary antibody was applied. Images were captured by phase microscopy at 40X.

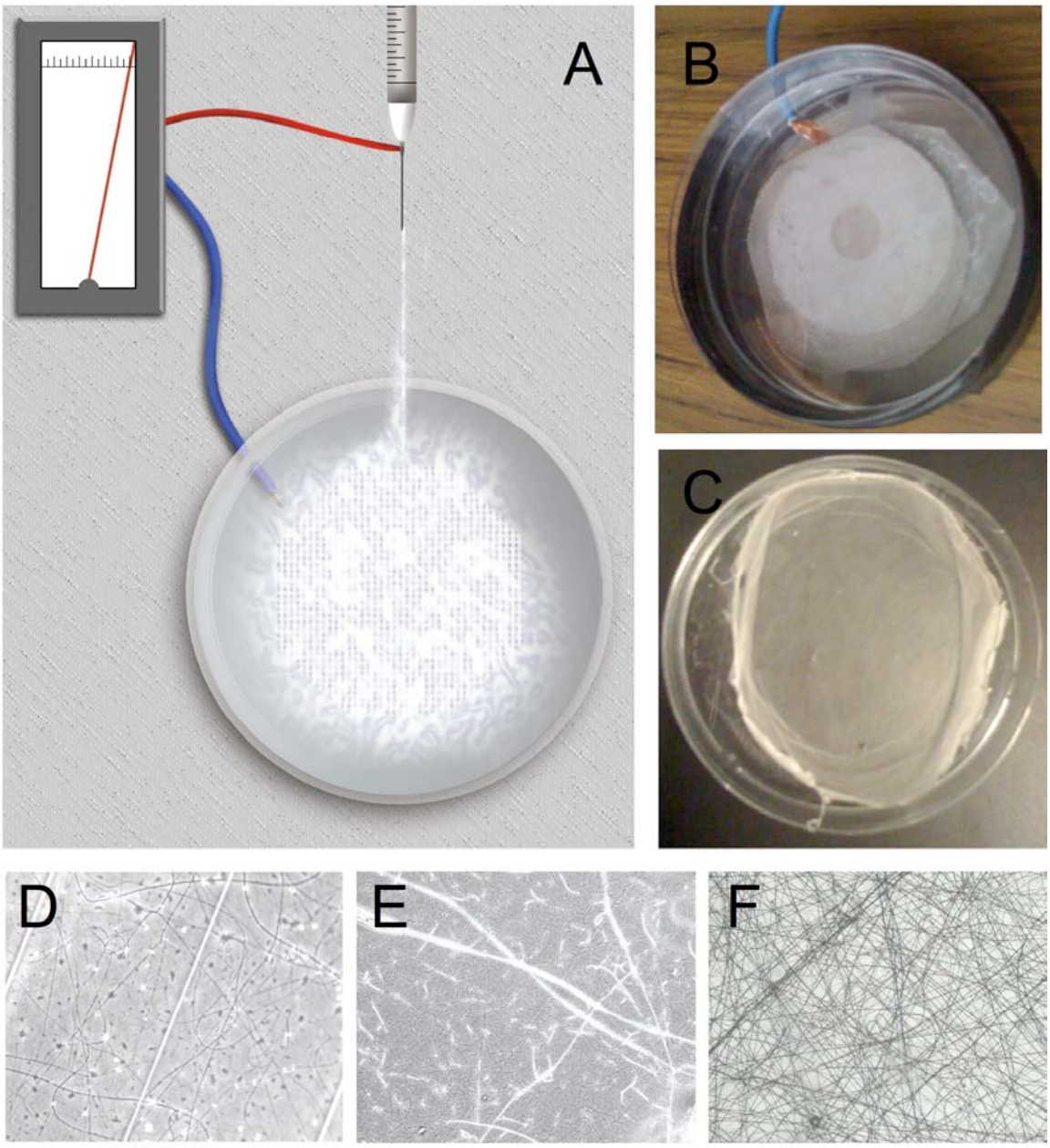

Figure 16. Direct Culture Dish Coating by Electrospinning. A cartoon representation shows the typical electrospinning apparatus modified to directly coat fibers by free hanging the dish backed with a metal mesh connected to the power supply cathode to attract the spinning fibers (A). The modified mesh and 100mm^2 dish used is also shown with attached 16ga wire (B), along with the appearance of a dish heavily coated with PDO fibers (C). A 40x magnification of coated dishes with adipose tissue ECM at 80mg/ml (D) and at 100mg/ml (E) and PDO (F) are shown to produce small, randomly arranged fibers of varying density and thickness as visualized by light microscopy.

Electrospun At-ECM proved stable in warm media, both genipin cross-linked and uncross-linked, so uncross-linked scaffolds were used for cell-based experiments. We next confirmed the ability of At-ECM matrix to support stem cells. Approximately 25,000 ASCs were seeded on At-ECM and a 10:90 At-ECM:PDO blend at day 0, and collected at 1 day and 14 days. The scaffolds were fixed and processed for H&E staining, which showed the presence of cells attached to the electrospun adipose ECM scaffolds at day 1 and 14 for the electrospun discs **(Fig. 17)**. After 7 days of culture, around 5% of the cells on the At-ECM-coated material accumulated many small lipid vacuoles, highly suggestive of adipogenesis induction just by being in contact with the fibers alone, in normal growth media. However, by day 14 these vacuoles were undetectable. We further confirmed the presence of cells growing on At-ECM and At-ECM:PDO using DAPI, a DNA intercalating agent, to identify cell nuclei. Using ECM samples from a different batch of electrospun At-ECM **(Fig. 18)**, DAPI positively indicated the presence of ASC growing on the electrospun scaffolds, with a slight increase in cell number noted from 1 day to 14 days of culture on electrospun At-ECM fibers **(Fig. 18 and Table 6)**.

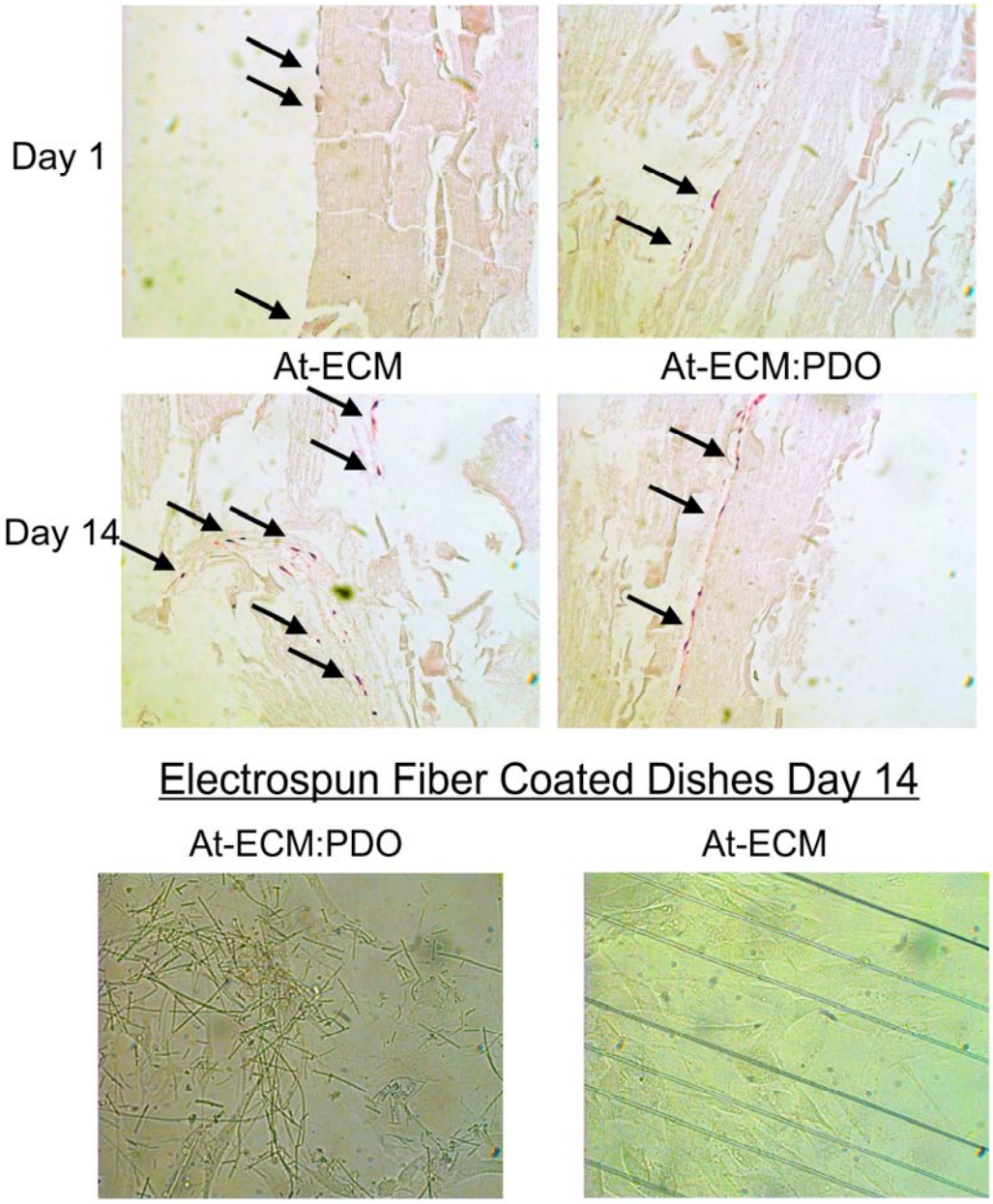

Figure 17. Electrospun At-ECM and At-ECM:PDO Blend Supports ASC Viability. ASCs were seeded for 1 or 14 days on 10mm punched discs of electrospun pure adipose or a 10:90 blend of adipose ECM:PDO then fixed for H&E staining as shown (Arrows indicate cells/stained nuclei and cytoplasm). ASCs were also maintained on At-ECM coated dishes and cultured for 14 days and imaged under DIC microscopy, with At-ECM;PDO scaffolds showing moderate cellularity and a highly fractured scaffold fibers. At-ECM coated dishes were highly cellularized, yet few of the original electrospun fibers remained visible with phase microscopy (parallel lines are a dish artifact from acid-etching).

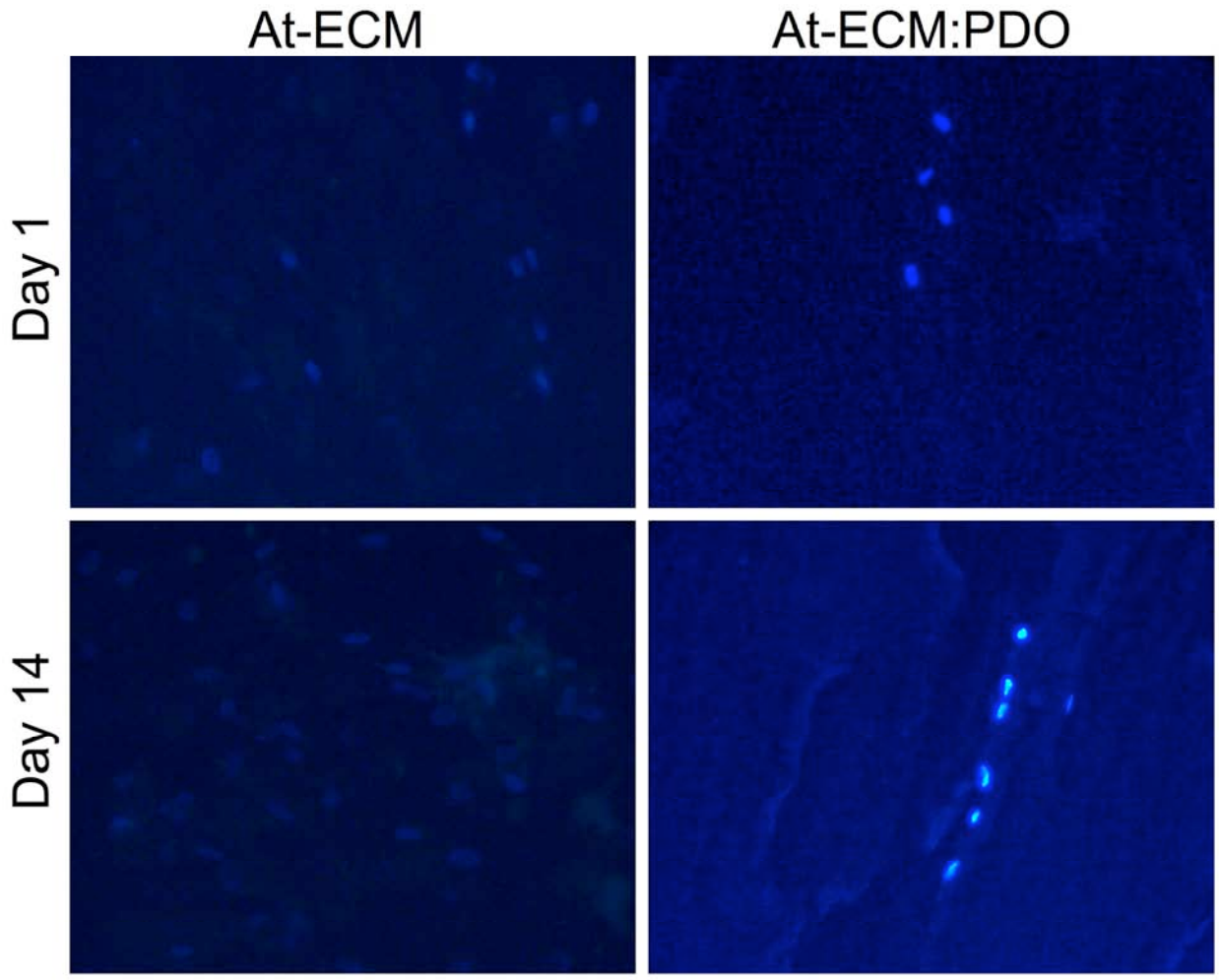

Figure 18. DAPI of ASCs Grow on Electrospun At-ECM and At-ECM:PDO. Around 25,000 cells/cm^2 ASCs were seeded and cultured for 1 to 14 days on 12mm punched discs of electrospun pure At- ECM and a 10:90 blend of At-ECM:PDO. The scaffolds were then stained with DAPI and imaged on a fluorescent microscope to verify cell attachment to the electrospun At-ECM matrices.

Table 7: Cell Seeding and Growth of ASCs on Electrospun At-ECM.

	AVG # CELLS DAY 1	AVG # CELLS DAY 14
Adipose ECM:PDO	**3 ± 2**	**7 ± 3**
Adipose ECM	**25 ± 14**	**53 ± 18**

DISCUSSION:

To our knowledge, this is the first report of the electrospinning of adipose extracellular matrix (At-ECM), producing a nanofibrous tissue engineering matrix composed of various collagens, basement membrane, and elastic matrix materials, potentially providing a scaffold suitable for stem cell cultivation and additional practical applications. While the use of At-ECM has just recently garnered attention as an excellent material for tissue engineering (Choi et al., 2009a; Choi et al., 2009b), previous methods for extracting and processing At-ECM produced very large macro-scale fibers and large sheet-like structures, which is atypical of native ECM components. In contrast, electrospun At-ECM fibers uniquely mimic the *in vivo* fibers. Along with fibrinogen, At-ECM may be the most abundant and readily accessible patient-derivable scaffolding for regenerative medicine and stem cell tissue culture applications. Other than harvesting of cadaverous tissue, skin- and At-ECM are among the rare sources of human ECM that could potentially be widely collected and banked for medicinal and research purposes. Further, plastic surgery clinics have no shortage of liposuction refuse for source materials.

Extracting purified At-ECM in suitable quantities for regenerative medicine and tissue engineering purposes has proven extremely challenging. The ECM literature, even classical ECM papers from the 1940's-1970's, sets no precedent (Haaralson et al, 1995). In fact, most all ECM extraction protocols from varied tissue sources have within their initial steps a careful removal of all fat from the target tissue for discard. The reason for this is that adipose tissue is notoriously resilient to chemical treatment, and adipocytes and At-ECM interfere with the standard collagen isolations steps. We report here that a rapid freeze-thaw cycling of the adipose tissue greatly aids in removing lipids from the dense connective tissue. This allows for

purification of the At-ECM without use of expensive chemicals and enzymes, such as pepsin and dispase (Choi et al., 2009a), which may damage the ECM and make it undesirable for further use.

While pre-treating the lipoaspirate or abdominoplasty sections with acetone proved more effective in removing adipocytes and lipids from the tissue than our freeze-thawing protocol, the resulting acetone-purified tissues unfortunately were unable to dissolve in HFP or TFA organic solvents. Given the constant reports of new solvents for electrospinning, it is possible that a unique solvent would allow the acetone-treated material to dissolve and electrospin, which would lead to a dramatic increase in material yield and simplified purification process. Given our extensive research experience with type I collagen and its strict requirement for a rapid lyophilization to produce workable purified material, it may also be possible that adjusting the lyophilization time of the acetone-treated ECM could alleviate its resistance to common organic solvents, which is worthy of further exploration. Alternatively, the acetone/isopropanol treatment may be acting in some unknown way to crosslink the connective tissue, thus keeping it from becoming soluble. The application of chemical or physical processing to break the cross-links may result in a material capable of dissolving in solvents appropriate for electrospinning.

We additionally discovered that the At-ECM co-electrospins with PDO, creating biologic electrospun fibers in the 250nm diameter range. The ability to blend At-ECM with a synthetic polymer reduces the amount of starting At-ECM needed for fabricating a sizeable construct, while still potentially having a scaffold with biologically relevant cell binding sites from the At-ECM. The blended scaffolds also have the advantage of added material strength and elastic properties being more actively tailored for the desired tissue type. It is worth noting that while

the histological stains for collagens, basement membrane, and elastin matrix components were positive for the At-ECM:PDO blend, the stains were light and highly scattered throughout the sectioned electrospun sheet. Such minimal amounts of material, however, may or may not ultimately be sufficient for cell growth, proliferation, migration, and cell-ECM functional activity. We are currently investigating various cell types and different PDO blend ratios with our electrospun At-ECM material.

Our protein and extensive histological analyses have given strong indications that the ECM types present in adipose tissue *in situ*, particularly collagen I and IV, basement membrane components, and elastic fibers are readily purified by our technique. Moreover we have demonstrated that these materials persist in an electrospun state. Given our findings, we believe electrospun At-ECM is a promising alternative for Matrigel **(Table 7)** in some situations. Being autologous in nature, the possible uses for research and clinical applications for At-ECM seems extensive, particularly when used in concert with autologously derived ASCs, cells already proven to have exceptional utility in regenerative medicine (Katz et al., 2006). Potential applications for electrospun At-ECM include the culture of embryonic and induced pluripotent stem cells, the culture of hepatic cells and stimulating ductal outgrowth of certain breast cells prone to branching morphogenesis in Matrigel, to name but a few. The *in vivo* potential of this novel electrospun scaffold material is still unknown, and it remains to be seen whether electrospun At-ECM will elicit an immune response if used autogeneically in animal models.

Finally, we have discovered a novel method for directly coating tissue culture plastic of a culture dish with electrospun fibers, with acid etching and deionizing of the plate coupled to a fine steel mesh to provide the cathode for targeting the electrospinning fibers to the plate. This

Table 8: At-ECM Fiber Characterization and Material Comparisons Summary

ECM proteins	Adipose Tissue[1]	Capillaries and Small arteries[1]	Matrigel[2]	Purified & Electrospun Adipose ECM
Type I Collagen	+	+	**low**	+
Type II Collagen	**low**	-	-	**nt**
Type III Collagen	+	**low**	-	**S**
Type IV Collagen	+	**low**	+	+
Type V Collagen	+	**low**	-	**S**
Type VI Collagen	+	+	-	**S**
Elastin	+	+	-	+
Fibronectin	+	+	-	**nt**
Laminin	+	+	+	**S**
Nidogen	+	+	+	**nt**
Proteoglycans, Glycosoaminoglycans & Glycoprotein	+	+	+	+

Adapted from Nakajima et al. 1998 (1) and BD Bioscience product sheet data (2).
(+)= Positive, (nt) = not tested, (S) = Suggested

produced a layer of random fibers on the scaffold that could be layered as a thin coating only a few fiber layers thick to a dense layer entirely opaque by light microscopy and measuring more than 0.2 microns thick, depending upon the amount of material deposited. This process proved useful for supporting the growth of mesenchymal stem cell cultures and may have many other applications, such as for use in migration assays, culturing feeder layers, or ECM-dependent cell types such as embryonic stem cells and hepatic cells. The prospect of large scale manufacturing of dishes or multi-well plates coated with electrospun nanofibers would further hold significant potential in medicine and research by replacing non-biologically relevant gel-coated plates as standard culture protocol for many cell types.

In summary, this study describes a novel tissue engineering scaffold of human adipose tissue origin. By electrospinning At-ECM, we are able to create a highly porous 3D scaffold of nanofibers with a high degree of interconnectivity. This engineered scaffold retains abundant amounts of collagen type I and basement membrane components (collagen type IV, elastin fibers, and glycosaminoglycan-based ECM) and supports the adhesion of human ASCs, appearing to mildly induce adipogenesis after a week of culture. These findings suggest human adipose tissue, from living or even cadaveric donors, could provide a readily harvested source of basement membrane biomaterials. Further development of this electrospun At-ECM scaffold will likely provide new opportunities in tissue engineering and significant therapeutic applications.

-CHAPTER 4-

RESULTS: RECAPITULATING OSTEOBLASTOGENESIS WITH ELECTROSPUN NANOFIBERS AND ADIPOSE STEM CELLS

ABSTRACT

Addressing a pressing need for generating new bone in the clinic and for research, we explored using electrospun fibrinogen (Fg) nanofibers in concert with adipose-derived stem cells (ASC) for stimulating osteoblastogenesis *in vitro*. Electrospun discs of Fg, polydioxanone (PDO), and a Fg:PDO blend were seeded with early passage ASCs, BJ fibroblasts, bone marrow mesenchymal stem cells (BM-MSCs), or osteosarcoma cells (MG63s) and grown for 7-21 days in osteogenic or regular growth media. These constructs were analyzed weekly both histologically and molecularly for evidence of osteoblastogenesis. The appearance of regular, porous, mineralized-appearing structures were found in osteogenic-induced ASC seeded scaffolds but only with those scaffolds containing Fg. We observe robust new collagen synthesis and matrix remodeling on all Fg and Fg:PDO scaffolds, the levels of which were elevated over time. There was pronounced mineralization throughout bone-induced ASC scaffolds while control scaffolds showed no mineral deposition despite excellent cellularity. Analysis of alkaline phosphatase and osteocalcin gene expression (qPCR) indicated that electrospun Fg supported osteoblastogenesis. To confirm our gene expression result, osteogenic-induced ASCs on Fg scaffolds also stained positive for osteocalcin protein, a key marker in osteoblastogenesis. Thus, we find that electrospun Fg and Fg:PDO are excellent materials for ASC viability, proliferation, and osteogenic differentiation, providing a high-quality biomimetic system to further bone model-based research and regenerative medicine advances.

INTRODUCTION

In the U.S. alone over 500,000 surgical procedures are performed annually requiring new bone tissue or bone analogues, with 2.2 million grafts annually performed worldwide (Giannoudis et al., 2005). While autologous and cadaveric bone grafts have proven effective clinically, bone tissue is not free from infection or immunological rejections, with extreme enduring pain and donor site morbidity associated with autologous grafts (De Long et al., 2007; Huffer et al., 2007; Ahlmann et al., 2002; Sasso et al., 1998). Further, donor bodies are rare, which has created a considerable black market for stolen cadaveric bone tissue (Powell et al., 2006). Failures of the bone organ can occur as the result of numerous clinical conditions, including cancers (osteosarcomas or as a target tissue of metastatic cancers), infections (commonly osteomyelitis), blunt traumas that may result in non-unions, and congenital defects (e.g. osteogenesis imperfecta). Many bone diseases will result in moderate to extreme pain and also partial or total loss of mobility. New bone tissues are clearly needed, both to model bone-related diseases in the lab, and for grafts clinically. New tissue engineering strategies for bony repair have developed a major research thrust in orthopaedics. Recent compelling scaffold biomaterials and stem cell technology advancements have energized regenerative medicine and the tissue engineering of bone, making their clinical acceptance imminent (Olvier et al., 2004).

With its simplicity, relative affordability, and excellent cellular response, electrospinning composite nanofibers is rapidly becoming the standard practice in the tissue engineering of bone. Electrospinning produces scaffolds highly amenable to cell adhesion, viability, and osteogenic differentiation (Li et al., 2006; Wutticharoenmongkol et al., 2007) using an array of template scaffold materials. Electrospinning involves the application of a 15-30kV DC electric potential

induced in a polymer solution, or melt, which whips the solution onto a metal collection target, leaving a dry polymer fiber in the electrostatic field to be collected as a non-woven fibrous mesh. Natural matrix materials, such as collagen, laminin, elastin and silk, with or without supporting synthetic blends (polydioxanone (PDO), PLGA, PCL, etc.), can be electrospun into scaffolds of nearly any size, shape, or microscopic properties (Venugopal et al., 2008; Barnes et al., 2007; Matthews et al., 2002; Bhattarai et al., 2005). Electrospun scaffolds can highly resemble native extracellular matrices in geometry, fiber size, and material composition, whereas conventional polymer processing techniques generally produce greater than 10μm diameter fibers.

Our chosen scaffold building material, fibrin(ogen) (Fg), is an integrin-spanning glycoprotein that binds collagen, fibrin, and heparan sulfate and has been clinically used for a variety of applications for more than 60 years (Giannini et al., 2004). Fg actively binds fibroblast growth factor-2 (bFGF), a crucial stem cell signaling molecule, and vascular endothelial growth factor (VEGF) (conveniently secreted by ASCs), both factors potentiate endothelial cell proliferation and may contribute to the healing response. Fg has another important advantage, being an autologous matrix that can be easily purified in as little as 20 minutes (Valbonesi et al., 2006). Our lab has further demonstrated that fibrinogen can be electrospun with great success (McManus et. al., 2006; 2007). As Fg is the primordial wound-healing matrix initially deposited in fractured bone, vast potential exists for engineering new bone with this biomimicry blueprint. As an alternative to pure Fg matrices, we propose the blending of PDO, a synthetic material commonly used in resorbable sutures (Boland et al., 2008) in order to reduce the amount of natural matrix required and improve mechanical properties and stability in culture as previously reported (Smit et al., 2005).

Cells as varied as amniotic and bone marrow-derived mesenchymal stem cells (BM-MSCs) have been used as a template for developing or repairing bone in recent electrospinning-based research (Steigman et al., 2009; Thibault et al., 2009). However these progenitor cell types are not without complications in their painful extraction, scarcity and often heterologous natures. While BM-MSC have been the most widely studied of the mesenchymal stem cell (MSC) types, the existence of an analogous adipose-derived stem cells (ASCs) in human fat have gained considerable interest (Zuk et al., 2002), in part due to sharing a nearly identical transcriptome, immunophenotype, and differentiation potential with BM-MSCs.

ASCs appear more advantageous than BMSCs, being up to 1,400 times more abundant and a more readily accessible tissue source relative to bone marrow (Izadpanah et al., 2006; Kern et al., 2006). Liposuction also offers greatly reduced patient morbidity relative to tapping into the bone marrow for BMSC extraction. ASCs furthermore are reported to secrete potent growth factors in high quantities, such bFGF, insulin like growth factor 1 (IGF-1), hepatocyte growth factor (HGF), and VEGF (Wang et al., 2006). These factors are crucial for tissue development and regeneration and are likely to prove essential for constructing many artificial tissues. Collectively, these advantages make ASCs an ideal stem cell for our studies.

In light of the increasing need for generating new bone, the primary purpose of this study is to determine the osteogenic potential of electrospun fibrinogen scaffolds seeded with ASCs. We hypothesize that electrospun fibers of fibrinogen and fibrinogen:PDO are able to support ASC attachment, proliferation and osteoblastogenic differentiation, providing the groundwork to using entirely autologous materials for various bone-related therapeutics.

MATERIALS AND METHODS

Adipose Stem Cell Primary Isolation and Culture

Lipoaspirate was obtained as surgical waste from patients undergoing elective surgery using standard techniques, in accordance with Virginia Commonwealth University's IRB. ASCs were isolated and characterized as described previously (Zuk et. al., 2002, Francis et al., 2010). ASCs were cultured in low glucose DMEM (Gibco) with 10% FBS (Hyclone), 10nM recombinant human EGF (Sigma), and 1% antibiotic-antimycotic (ABAM, Gibco), and incubated at 37°C with 5% CO_2. Cells were characterized as multipotent and were shown to exhibit a mesenchymal stem cell immunophenotype as we reported previously (Francis et al., 2010). To determine the immunophenotype of our ASCs, ~100,000 cells were flow sorted on a Beckman CoulterEpics XL-MCL for the presence or absence of CD14, CD29, CD31, CD34, CD45, CD73, and CD105 and compared to BMSCs.

BM-MSC, BJ and MG63 Cell Culture

Human foreskin fibroblasts (BJ) were obtained from ATCC (Manassas, VA) and expanded in D9C media (DMEM, 1X Medium 199, 10% CCS (Cosmic Calf Serum, Hyclone) and 1% ABAM. Cells were incubated at 37˚C and 5% CO_2 at 100% humidity. MG63 osteosarcoma cells were cultured in basic ASC growth and differentiation medias and incubation conditions. BMSCs were obtained from the iliac crest of healthy human patient donors in accordance with the IRB, using standard isolation procedures (Friedenstein et al., 1976). BMSCs were maintained in DMEM supplemented with 10% FBS, 15ng/mL bFGF, and 1% ABAM.

Osteogenic Differentiation

Osteoblastogenesis was induced by cultivating stem cells for 2-4 weeks in osteogenic media (OM) as previously described (Zuk et al., 2002), and compared to BMSCs and BJs as positive and negative controls, respectively. OM was made of high glucose DMEM with 10% FBS was supplemented with 2-ascorbate-2-phosphate, ß-glycerophosphate, and dexamethasone (Sigma-Aldrich). The control media (CM) was formulated as OM minus dexamethasone.

Adipogenic Differentiation

ASCs, BM-MSCs, and BJ cells were grown to around 80% confluence in normal ASC media, followed by the addition of adipogenic induction media (0.5mM isobutyl-methylxanthine, 1µM dexamethasone, 10µM insulin, 200 µM indomethacin, and 1% ABAM). Freshly prepared adipogenic induction media was changed every 2 days for 14-21 days. The respective cell lines were maintained in basic ASC media at confluency as negative controls. Differentiation-induced and control cultures were then fixed in 4% paraformaldehyde for 30min, followed by staining with Oil Red O for 40min at RT for detection of lipid droplets.

Chondrogenic Differentiation

Cells were harvested when around 75% confluency, during mid-log phase growth, and concentrated at 400 cells/µl in chondrogenic media. Around 250,000 cells in 500µl of media were centrifuged for 10min at 450 x g in a 15ml conical tube. The tube was then placed in the incubator, humidified at 37ºC with 5% CO_2, with a loose cap and allowed to incubate overnight. The visible pellet was then transferred to a 12-well plate the next day, with the chondrogenic

media changed every 3-4 days for 4 weeks for each pellet. The chondrogenic media consisted of high glucose DMEM base, 10ng/ml TGF-ß3 (R&D systems), $1x10^{-7}$M dexamethasone (Sigma), 50µg/ml L-ascorbic-2-phosphate (Sigma), 10µl ITS+/1ml media (B&D Biosciences), 10% FBS, 1% ABAM. At 21-28 days, the pellet was fixed in 4% neutral buffered formalin (NBF). Successful chondrogenesis was verified by Safranin O histochemical staining. Briefly, pellets fixed in NBF were first washed in PBS, followed by a brief wash with 1% glacial acetic acid. The monolayer culture was then stained with 0.5% Safranin O for 5min until a pink/orange stain was observed, then washed, and stored in tap water. As with most cartilage histological stains, Safranin O stains proteoglycans and glycosaminoglycans.

Electrospinning Fibrinogen, Polydioxanone and Fibrinogen:PDO

Solutions of lyophilized bovine fibrinogen (Fraction 1, Type 1-S from bovine plasma, Sigma Aldrich) were made with a 10% (by volume) minimal essential medium (MEM, Sigma Aldrich) and 90% weight/volume 1,1,1,3,3,3 hexafluoro-2-propanol solution (HFP, TCI America, Portland, OR) at concentrations of 100mg/ml. Polymers were allowed to enter solution overnight with shaking at RT. Solutions of polydioxanone (PDO) (Ethicon, Somerville, NJ) were made at 100mg/ml concentrations, dissolved in HFP overnight with shaking at RT. Fibrinogen:PDO blended scaffolds were combined in one vial after mixing overnight with an additional 10% MEM to allow the polymers to remain in solution and effectively electrospin.

A syringe pump (KD Scientific), high voltage power supply (Spellman CZE1000R, Spellman High Voltage Electronics Corp.), 1-to-10ml plastic syringes (BD Bioscience) with a 18.5-gauge blunt-end needle, and a 303 stainless steel mandrel (10.2 cm length x 2.5 cm width x

0.3 cm thick) were used for a collection target. Electrospinning parameters were typically constant at 30kV applied voltage, 125mm distance between the needle and grounded mandrel, 2.5mL/hr solution dispensing rate, 2cm/s translational speed over 7cm, and approximately 500 RPM rotational speed.

Static Scaffold Seeding and Tissue Culture

Scaffold discs 12mm in diameter were formed with tissue biopsy punches from electrospun fibrinogen, PDO and Fg:PDO sheets, with the punches tightly placed in 48-well plate. Scaffolds were disinfected in 80% ethanol for 30min, then washed 3 times for 10min in PBS. Cells were concentrated to 50,000 cells/100µl, and a single 100µl drop of cells was careful placed on the center of the disc. Cells were allowed to adhere in the incubator for 15min and then 500µl of control or differentiation media was added. Media was carefully changed every 2-4 days.

Quantitative Real Time RT-PCR

Total cellular RNA was extracted from electrospun tissues-analogues using Trizol Reagent (Gibco) according to the manufacturer's protocol. For good RNA yield, a set of 5 cell-seed scaffolds (12mm) were homogenized for each sample condition, being pulverized together with a tissue grinder in 1ml of Trizol. RNA concentrations and purity were estimated on a Nanodrop spectrophotometer (Thermo Scientific, DE). RNA was reverse transcribed using a random hexamer and the SuperScript First Strand Synthesis System (Gibco). A Stratagene Mx300P QPCR System (Stratagene, La Jolla, CA) was used for gene expression analysis in the

VCU Nucleic Acid Research Facilities core. Taqman primers for 18S, osteocalcin and alkaline phosphatase were used. Relative expression levels for the lineage specific genes were calculated using standard curves generated from the triplicate dilution series of the cDNA, with normalization to the 18S housekeeping gene. Comparative statistical analysis was performed using a one-way ANOVA followed by a Tukey test, with the α level set at 0.05.

Histology

Scaffolds were fixed in 10% formalin, paraffin embedded, cryosectioned and mounted for hematoxylin and eosin (H&E), Ki67, and Masons Trichrome staining using a Dako Artisan Staining System X automated system at the VCU Anatomical Pathology Research Laboratory. For Alizarin Red S (ARS) staining, discs were fixed in ice cold ethanol, then paraffin embedded, sectioned then rehydrated for staining. The transverse scaffold sections were incubated at room temperature for 30 min in ARS stain with gentle shaking. The staining solution was removed and discs washed 4x with water. The stained constructs were mounted on slides and then visualized by phase microscopy.

Microscopy

For SEM evaluation of the structural morphology of seeded and unseeded electrospun scaffolds, constructs were fixed in gluteraldehyde and processed by standard methods with gold sputter coating prior to analysis by a Zeiss EVO 50 XVP (Nano Technology System Division, Carl Zeiss). For confocal fluorescence microscopy scaffolds were washed with PBS and fixed with 3.7% paraformaldehyde for 30min, then permeabilized with 0.5% Triton X-100 for 10min.

Following PBS washing, cells were blocked with 4% goat serum in PBS for 1hr, then incubated in 4% goat serum in PBS with a polyclonal antibody for osteocalcin (100μg/ml) overnight at 4^{o}C in a humidified chamber. After rewashing with PBS, cells were incubated in a 4% goat serum solution in PBS with AlexaFluor 488 goat anti-rabbit IgG (Invitrogen A21245) for 1h at RT. Cells were stained with 4',6-diamidino-2-phenylindole (DAPI) upon mounting in Vectashield (Vector Lab H-1000). A Leica TCS-SP2 AOBS confocal laser scanning microscope was used to capture images, using Leica LCSLite imaging software. Phase and fluorescent microscopy images were captured on an Olympus BX51 using Q-Capture Pro software (QImaging).

RESULTS

Using common histological stains, we initially verified that our ASC strains on tissue culture plastic were capable of adipogenic differentiation (Oil Red O), chondrogenesis (Safranin O), and osteogenesis (Alizarin Red S) **(Fig. 19-21)**. Late-stage osteogenesis was confirmed by the expression of osteocalcin secreted by differentiated cells **(Fig. 22)**. Young ASCs (PD4-6) analyzed by flow cytometry exhibit an immunophenotype of CD14-, CD29+, CD31-, CD34low/+, CD45-, CD73+ and CD105+, which was identical to BM-MSCs for all markers except CD34 (absent for CD34) **(Fig. 23 and Table 8)**. BJ fibroblasts and HL60 cells served as useful controls, where HL60s were positive for CD14, CD31, and CD45 to confirm antibody function.

With the stem cell attributes of our ASC strains confirmed, their ability to attach and remain viable on electrospun sheets of Fg and PDO was assessed using SEM. ASCs seeded on Fg scaffolds for 1 day and 7 days showed strong attachment and apparent scaffold surface migration and proliferation over time. No cells were detected on pure PDO scaffolds (**Fig. 24**). Unexpectedly, it was found that early passage ASC (<PD 10) exhibited strikingly distinct morphology compared to later passage ASCs (>PD 20) as shown **(Fig. 24e-f),** with the later passage ASCs morphologically resembling fibroblasts. Based on these observations, early passage ASCs were used for all subsequent experiments.

To determine the long term viability and proliferative and migratory potential of ASC into the scaffold interior for each matrix type, around 50,000 cells were grown on discs and collected every 7 days for H&E and Ki67 staining. Since cross-linking Fg leaves the scaffold impermeable to ASCs and fibroblasts (Sell et al., 2008), scaffolds were left in their native,

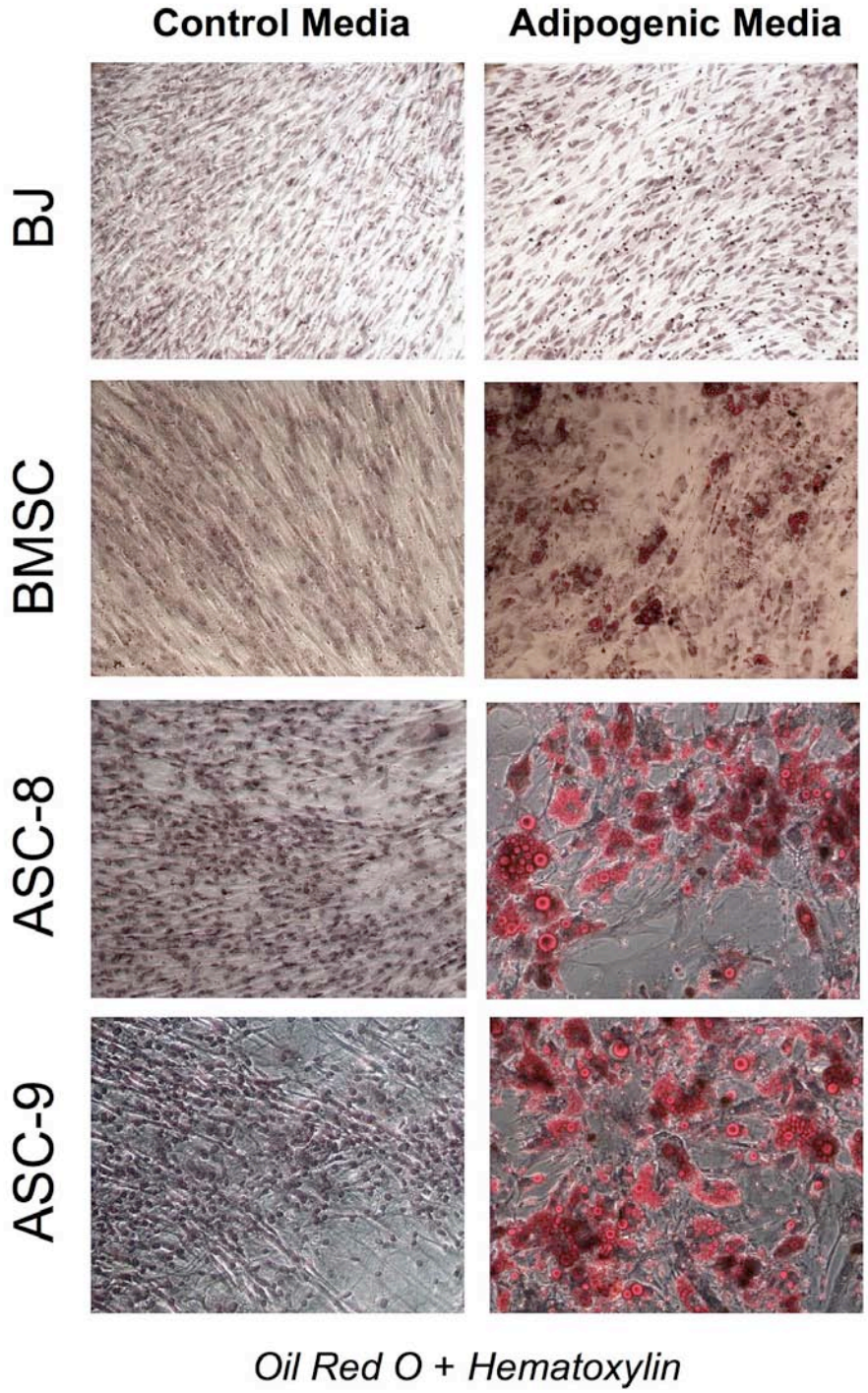

Figure 19. Adipogenic Differentiation. ASC cells strains 8 and 9, BM-MSCs and BJs were cultured for 2 weeks in adipogenic induction media or regular growth media, fixed and stained for hematoxylin and Oil Red O for lipid detection. ASCs and BM-MSCs showed positive staining in induction media only, where BJ's did not indicate any apparent staining (20x).

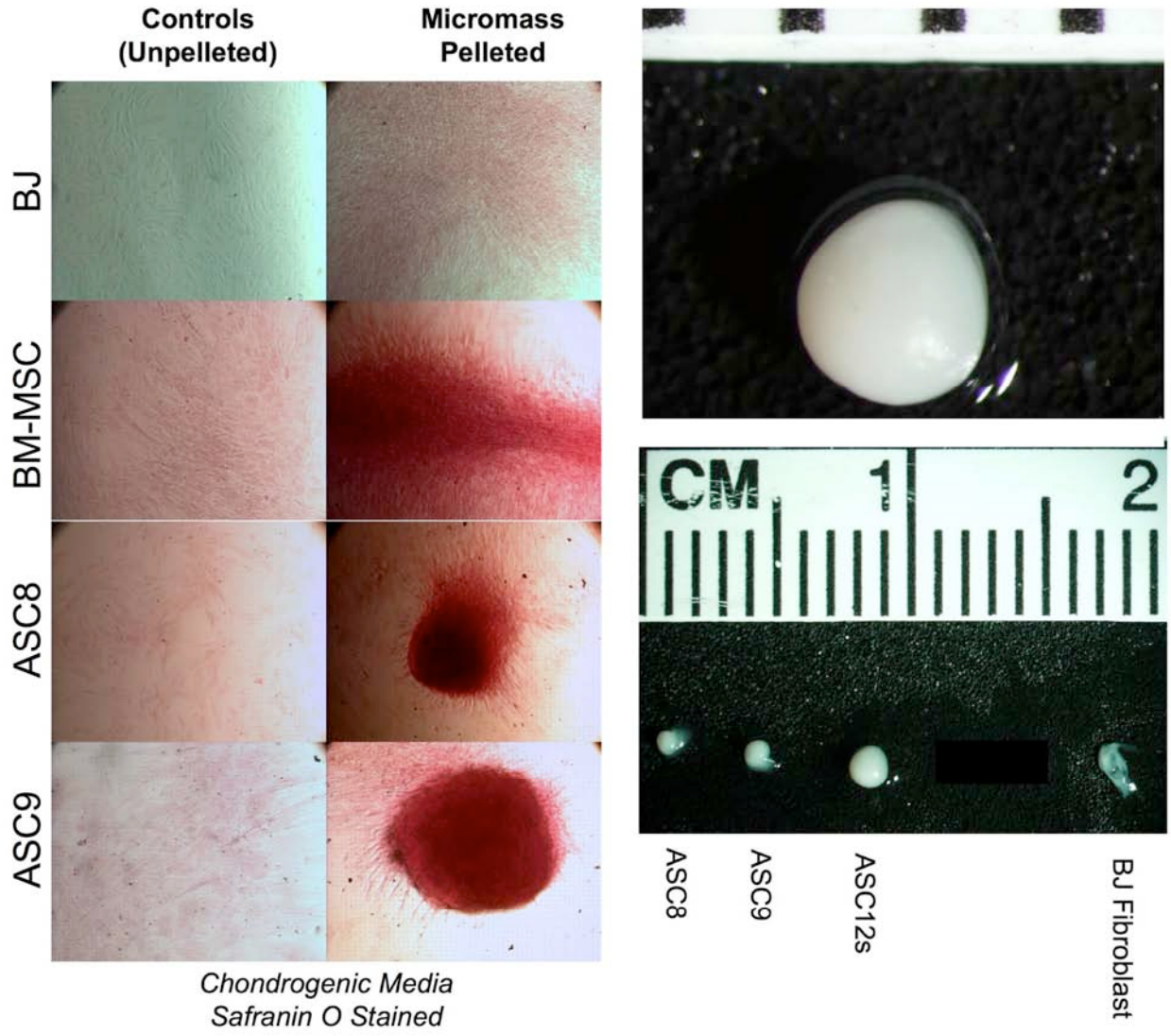

Figure 20. Chondrogenic Differentiation. Two ASC cell strains (#8 and #9), control BM-MSCs and BJs were cultured for 4 weeks in chondrogenic induction media as micromass cell pellets or as unpelleted cells, fixed and stained with Safranin O to detect proteoglycans. Unstained and uncut micromass pellets are shown for reference for relative size, morphology and texture from each line. ASCs and BM-MSCs showed positive staining in induction media only and formed solid, spherical pellets, where BJ's did not indicate any apparent staining and did not form a distinct micromass pellet (10x).

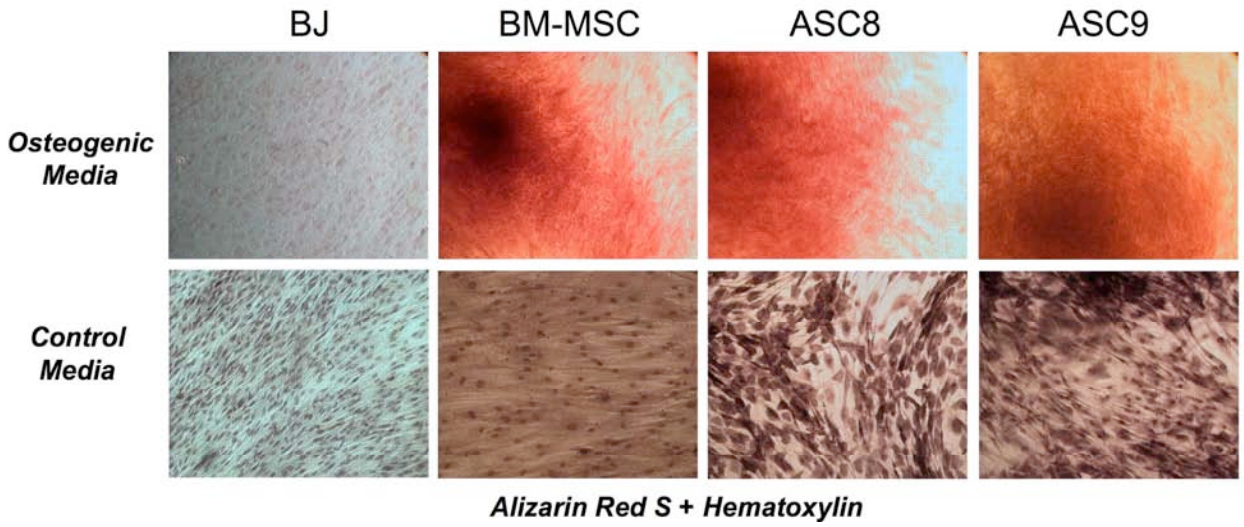

Figure 21. Osteogenic Differentiation. ASC cells strains -8 and -9, control BM-MSCs and BJs were cultured for 3 weeks in osteogenic induction media or regular growth media (Osteogenic media minus Dexamethasone), fixed and stained for hematoxylin and Alizarin Red S for calcium deposition. ASCs and BM-MSCs showed positive staining in osteogenic induction media only, where BJ's did not indicate any apparent staining (20x).

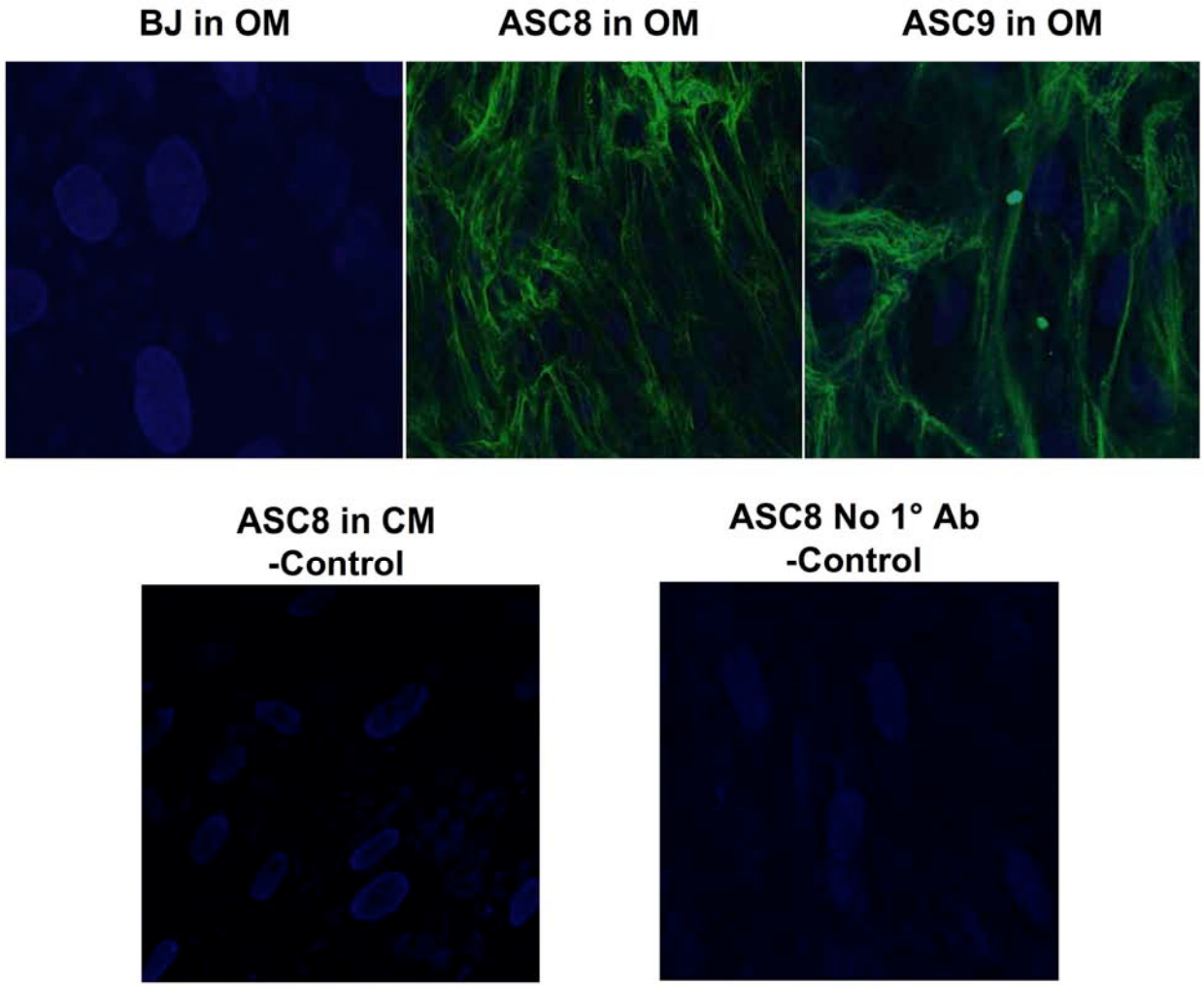

Figure 22. Osteocalcin Expression in Differentiated ASCs. BJ fibroblasts, ASC8 and ASC9 cells strains cultured 21 days in osteogenic media on tissue culture plastic were stained for osteocalcin (green) and DAPI (blue), and imaged under fluorescence microscopy, as grown in coltron media (CM) or osteogenic media (OM). Only the ASC strains showed the expression of the secreted osteocalcin protein. ASCs grown in normal growth media and stained with DAPI and osteocalcin and ASCs grown in osteogenic media but not stained with the primary antibody are shown for negative controls.

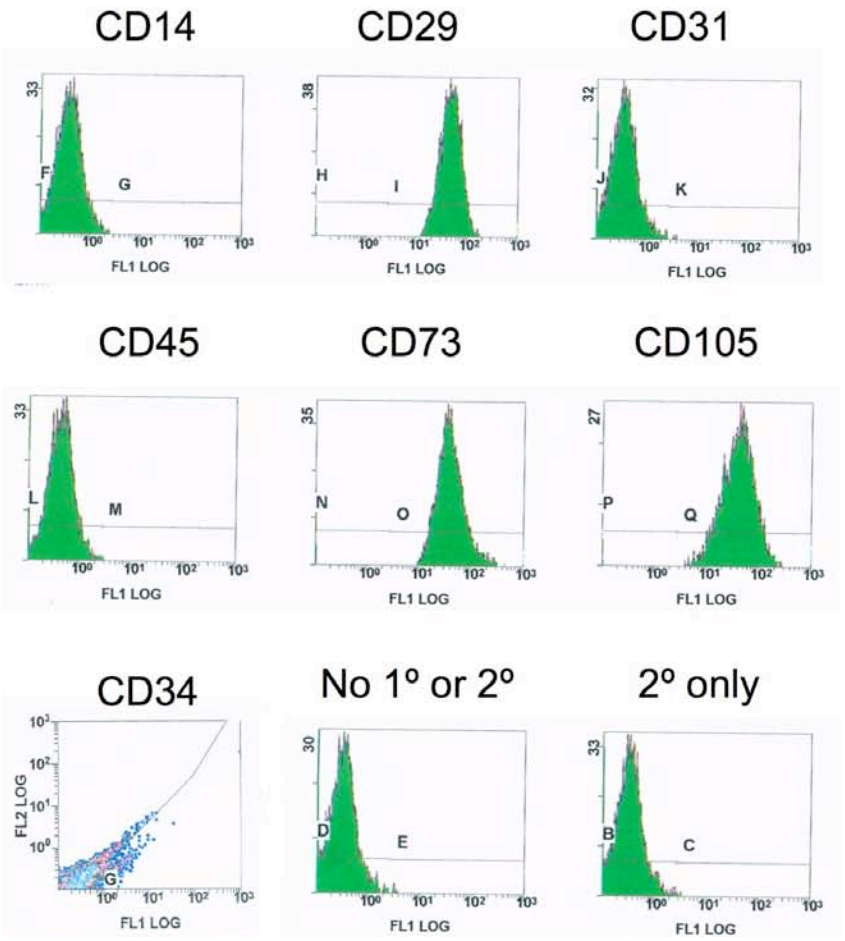

Figure 23. ASC Immunophenotype. Representative flow cytometry results of our ASC cell strains show a typical MSC immunophenotype of CD14-, CD29+, CD31-, CD 45-, CD73+, CD105+ and CD34 low/+ (dot plot for CD34 shown for better elucidation of positive sub-population present).

Table 9: Comparisons of ASC, BMSC and BJ Fibroblast Immunophenotypes.

	CD14	CD29	CD31	CD34	CD45	CD73	CD105
ASCs	-	+	-	+/low	-	+	+
BM-MSCs	-	+	-	-	-	+	+
BJ Fibroblasts	-	+	-	-	-	+	+
HL60	+	n.t.	+	n.t.	+	n.t.	n.t.

n.t = not tested.

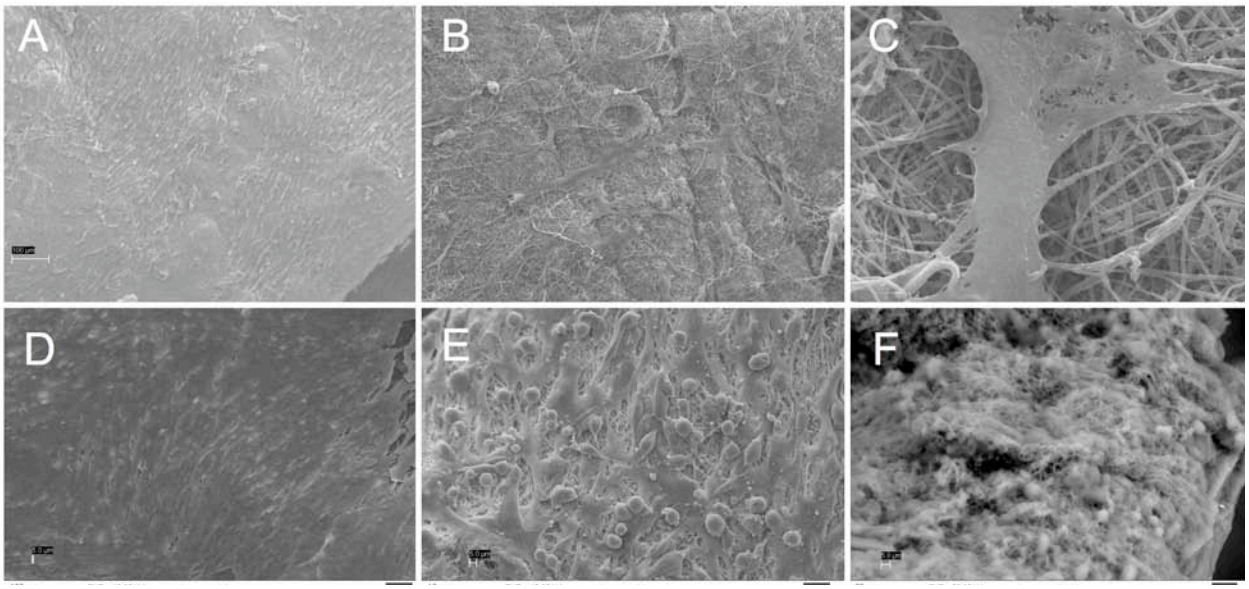

Figure 24. SEMs of Electrospun Fibrinogen Supporting Adipose Stem Cells. SEM images of ASCs on electrospun fibrinogen at 1 week growth at 500x (A) and at 1000x (B) shows cells with extensive cell-cell and cell matrix interactions. A 4000x view of panel "B" of a single ASC suggests *de novo* matrix deposition though visible fibers present that are much smaller (40-80nm range) then typically formed by the Fg electrospinning process (~300nm) (C). SEM of a confluent sheet of late passage (PD 15+) ASCs covering the matrix at 14 days (D) with a flat sheet of non-distinct cells is distinct from young, early passage ASCs upon the fibrinogen matrix at 14 days in culture (E) that show a unique blebbing morphology. The irregular and 3D morphology of young ASCs on fibrinogen is a feature further suggested by a live/wet mount SEM of the construct (F).

un-crosslinked state after electrospinning. In our initial studies on PDO, few cells attached and no cells penetrated the scaffold surface, yet, on pure Fg and Fg:PDO scaffolds, high cellularity at 14 and 21 days of culture was observed with apparent scaffold penetration **(Fig. 25A-D)**. These results were further confirmed though DAPI staining of the nuclei of ASCs that have incorporated into the matrix of 50:50 and pure Fg scaffolds grown for 14 days in control media **(Fig. 25E-F).**

There was an overall significant increase ($p<0.05$) in cell number in 50:50 Fg:PDO and Fg scaffolds as compared to pure PDO scaffolds, comparing ASCs growing in osteogenic or growth media to BJs and MG63s as controls, from 7, 14 and/or 21 days **(Fig. 26)**, with representative images shown for comparison **(Fig. 27-32)**. Interestingly, we maintained ASCs on electrospun fibrinogen for 75 days in culture, with sections of H&E stained scaffolds from 3 different punches showing cells persisting after 2.5 months of culture **(Fig. 33)**. At day 75, the fibrinogen discs still remained solid and associated, macroscopically appearing to have a rougher texture relative to day 1 discs.

By assessing mitotically active cells using Ki67 staining **(Fig. 34),** we calculated the average number of proliferative cells to be highest ($p<0.05$) in pure Fg containing scaffolds at week 1 in osteogenic media (14.8%), decreasing weekly to 11.7% after 2 weeks and 8.0% of cells at 3 weeks of differentiation. Cells in growth media at week 3 showed a comparable percentage of proliferative cells (8.8%) **(Table 9 and Fig. 35).** The average percent of proliferative cells found on Fg:PDO scaffolds was less than that seen on pure Fg scaffolds at all time points. The number of cell layers formed in PDO, Fg:PDO, and pure Fg scaffolds was also quantified. A singe-cell layer of ASCs was found to circumscribe the periphery of pure PDO

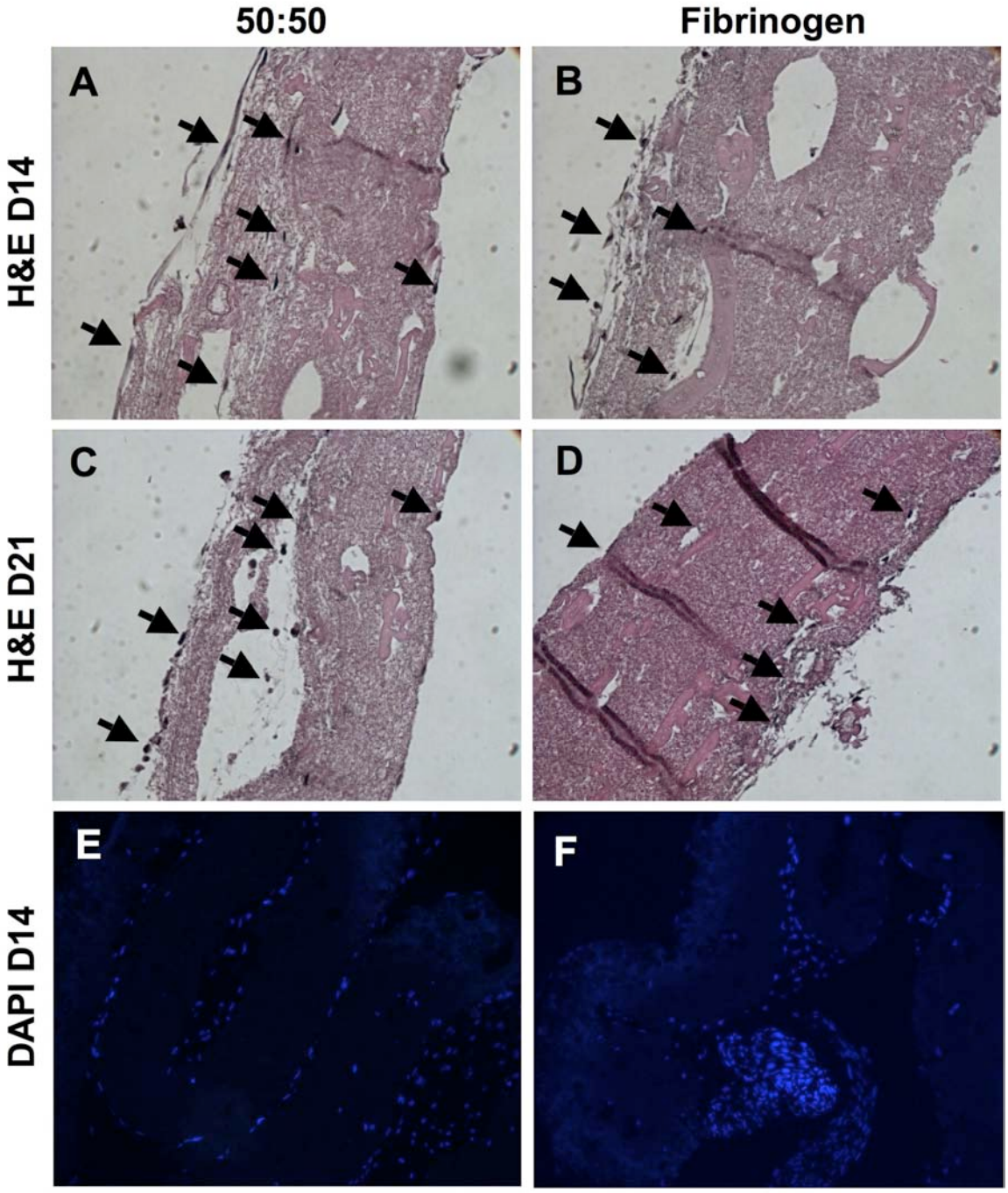

Figure 25. ASC Cellularity and Penetration of Electrospun Scaffolds. ASCs seeded on 50:50 blended fibrinogen:PDO (A, C, E) and pure fibrinogen (B, D ,F) showed a thick layering of cells of the scaffold surface with cells seen throughout the constructs at 2-3 weeks of culture as assayed by H&E (a-d) or DAPI staining (e and f). Arrows indicate areas containing one or more cells (nuclei) in H&E sections.

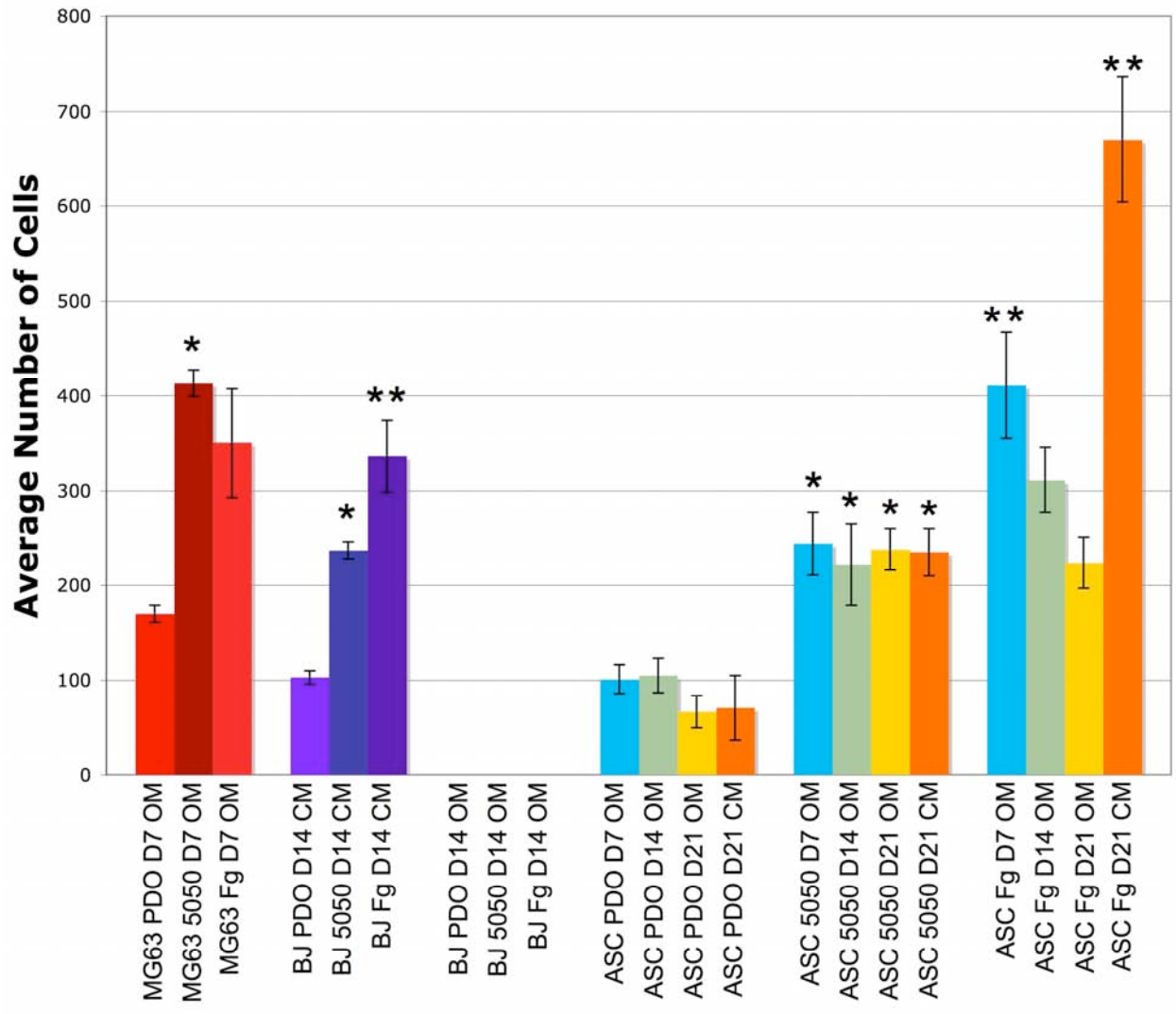

Figure 26. Electrospun Scaffold Cellularity. The average number of cells (ASCs, BJ's or MG63's) growing on PDO, Fibrinogen or Fibrinogen:PDO was determined over 1, 2 or 3 weeks in culture with osteogenic media (OM) or control/growth media (CM) by averaging the number of cells seen in 10 random fields at 40x scored in triplicate. A trend of increasing cellularity with increasing Fg content seen with ASCs, while ASCs grown in CM for 3 weeks appeared most proliferative in this experiment. BJ fibroblasts were not apparently viable in OM on any electrospun scaffold type tested, though were viable in normal ASC CM (osteogenic media minus dexamethasone). (Statistical analysis performed by One Way ANOVA with $p<0.05$. *=significant increase in cell number over PDO scaffolds, **=significant increase in cells over both PDO and 50:50 scaffolds, as compared at the respective time point).

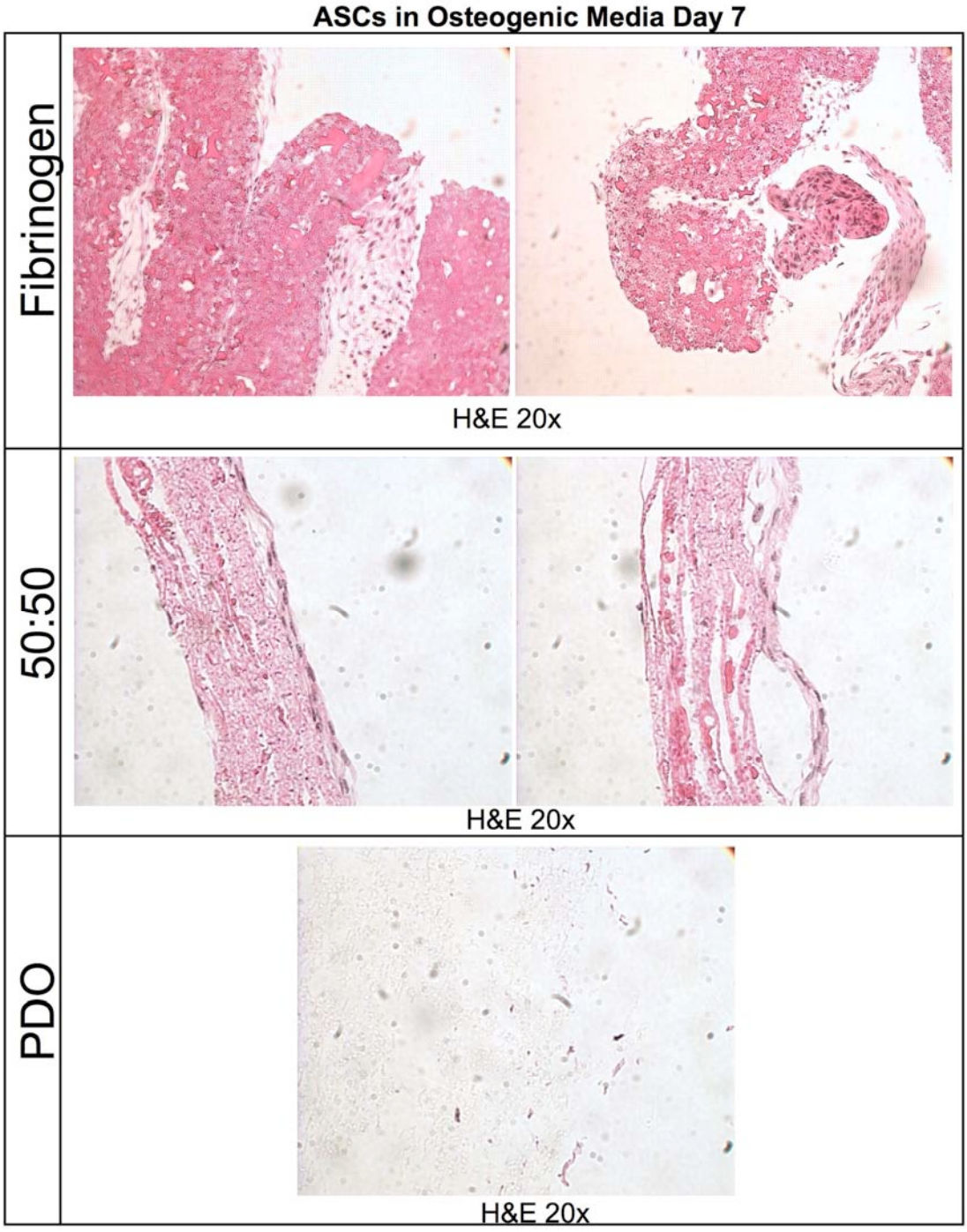

Figure 27. H&E Histology of Osteo-Induced ASCs on Fibrinogen, Fibrinogen:PDO, and PDO at Day 7. H&E stained sections of electrospun fibrinogen revealed excellent ASC cellularity at 7 days of culture in osteogenic differentiation media with cells found throughout the construct. The 50:50 fibrinogen:PDO scaffolds supported a thick layer of cells on the surface, and pure PDO scaffolds appeared largely acellular apart from a thin encapsulating cell layer.

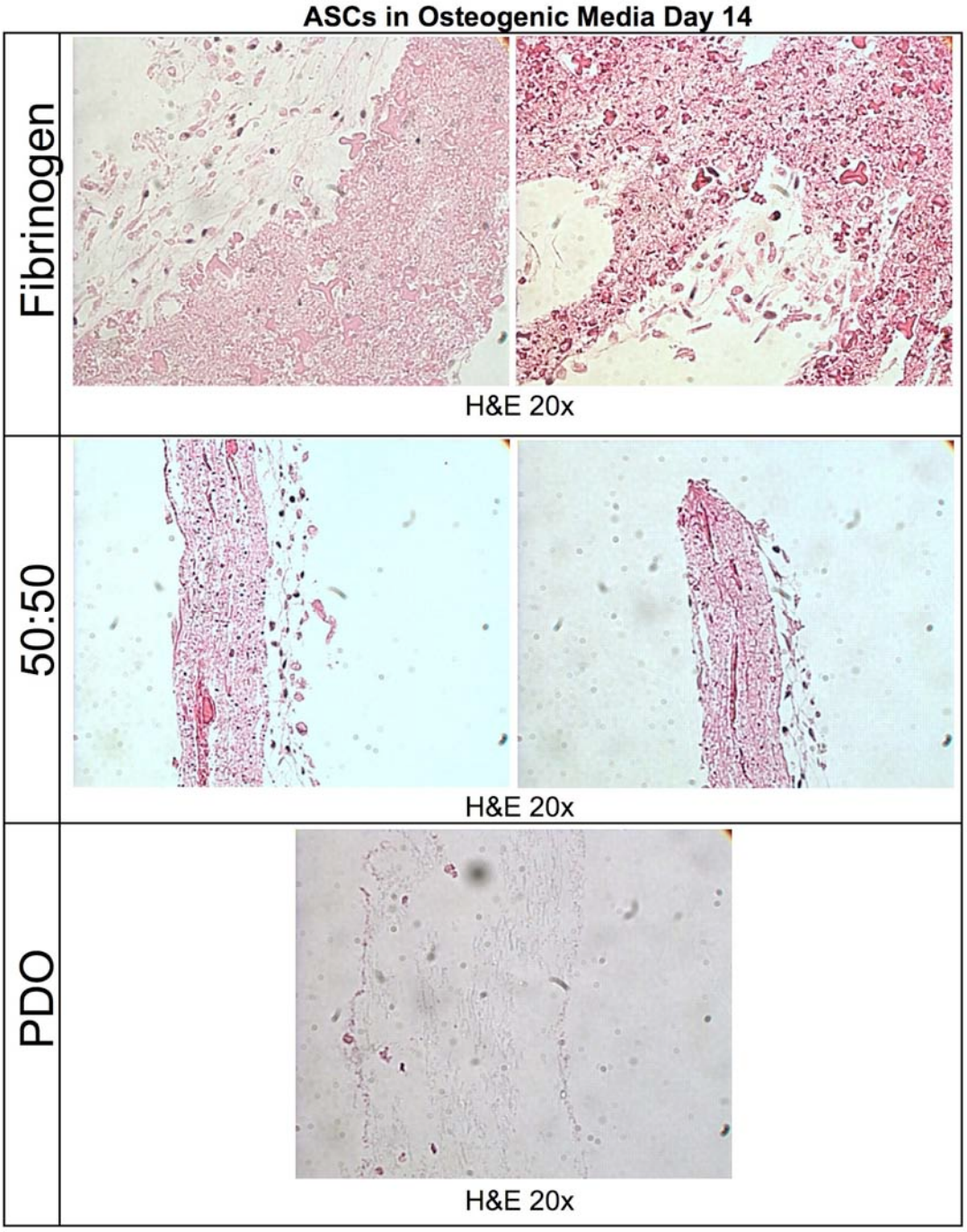

Figure 28. H&E Histology of Osteo-Induced ASCs on Fibrinogen, Fibrinogen:PDO, and PDO at Day 14. H&E stained sections of electrospun fibrinogen reveal excellent ASC cellularity maintained at 2 weeks of culture in osteogenic differentiation media with cells found throughout the construct. The 50:50 blended fibrinogen:PDO scaffolds maintained a 4-5 layers of cells on the surface with some cells seen inside the construct, and pure PDO scaffolds appeared acellular apart from a few cells seen on the periphery.

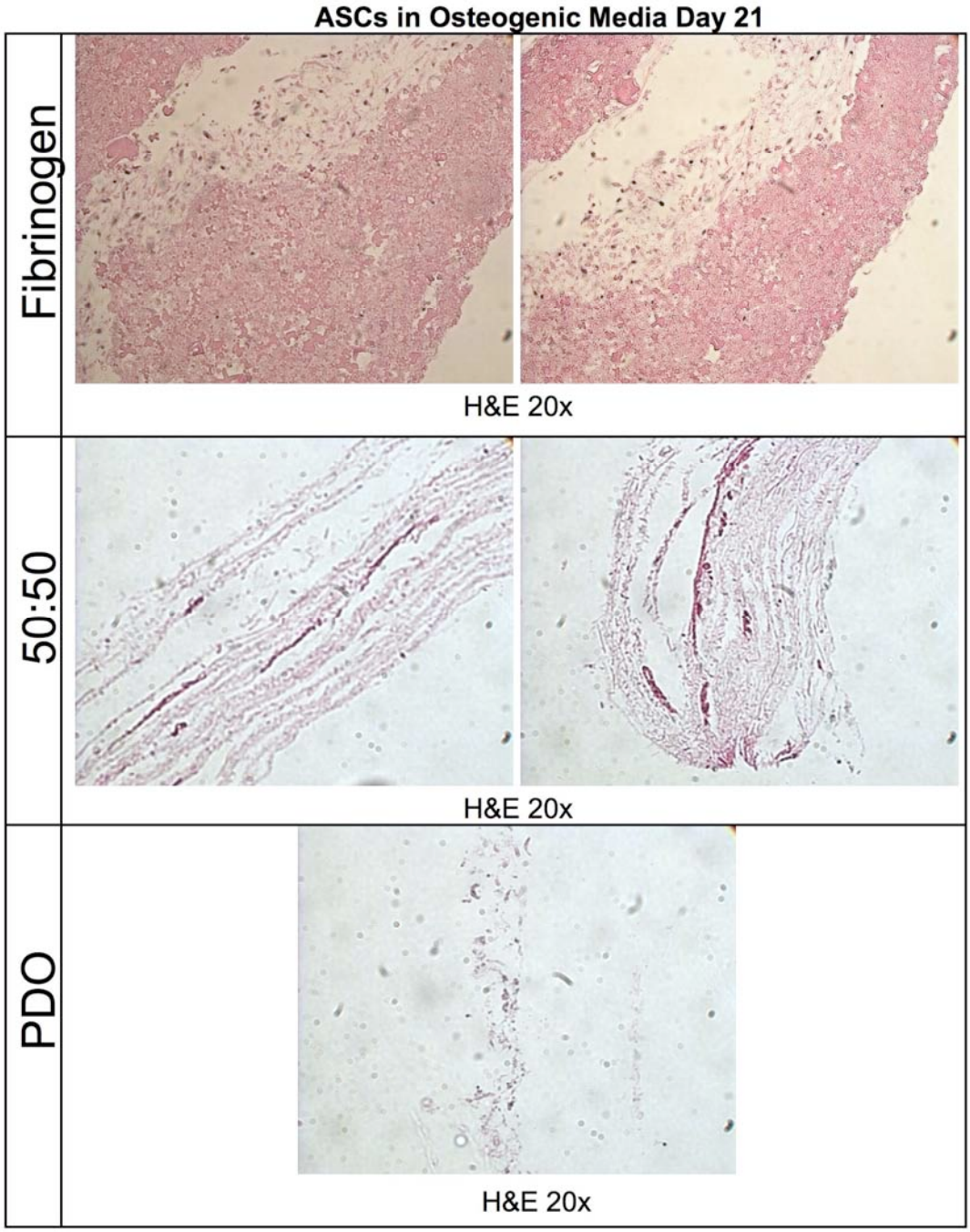

Figure 29. H&E Histology of Osteo-Induced ASCs on Fibrinogen, Fibrinogen:PDO, and PDO at Day 21. H&E stained sections of electrospun fibrinogen reveal excellent ASC cellularity at 21 days of culture in osteogenic differentiation media with cells seen throughout the construct. The 50:50 fibrinogen:PDO scaffolds were still seen supporting separate outer layer of cells on the surface with many cells found inside, and pure PDO scaffolds appear again acellular in the scaffold interior with a few cells found surrounding the construct.

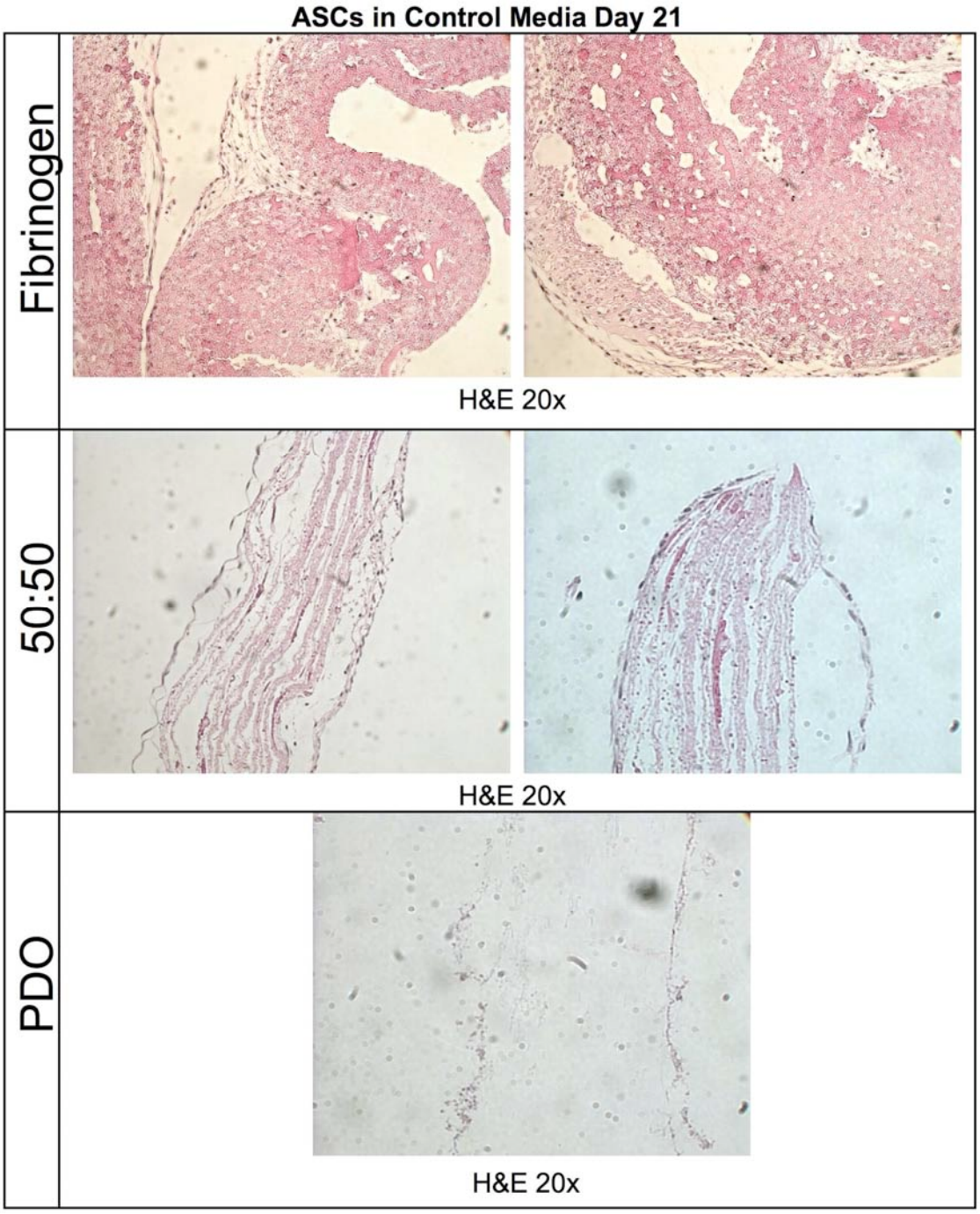

Figure 30. H&E Histology of ASCs on Fibrinogen, Fibrinogen:PDO, and PDO at Day 21 in Control Media. H&E stained sections of electrospun fibrinogen reveal excellent ASC cellularity at 21 days of culture in ASC control media, with cells found throughout the construct. The 50:50 fibrinogen:PDO scaffolds supported an apparently confluent layer of cells encasing the surface of the scaffold, and pure PDO scaffolds appeared scarcely cellular apart from a thin layer of cells around the construct.

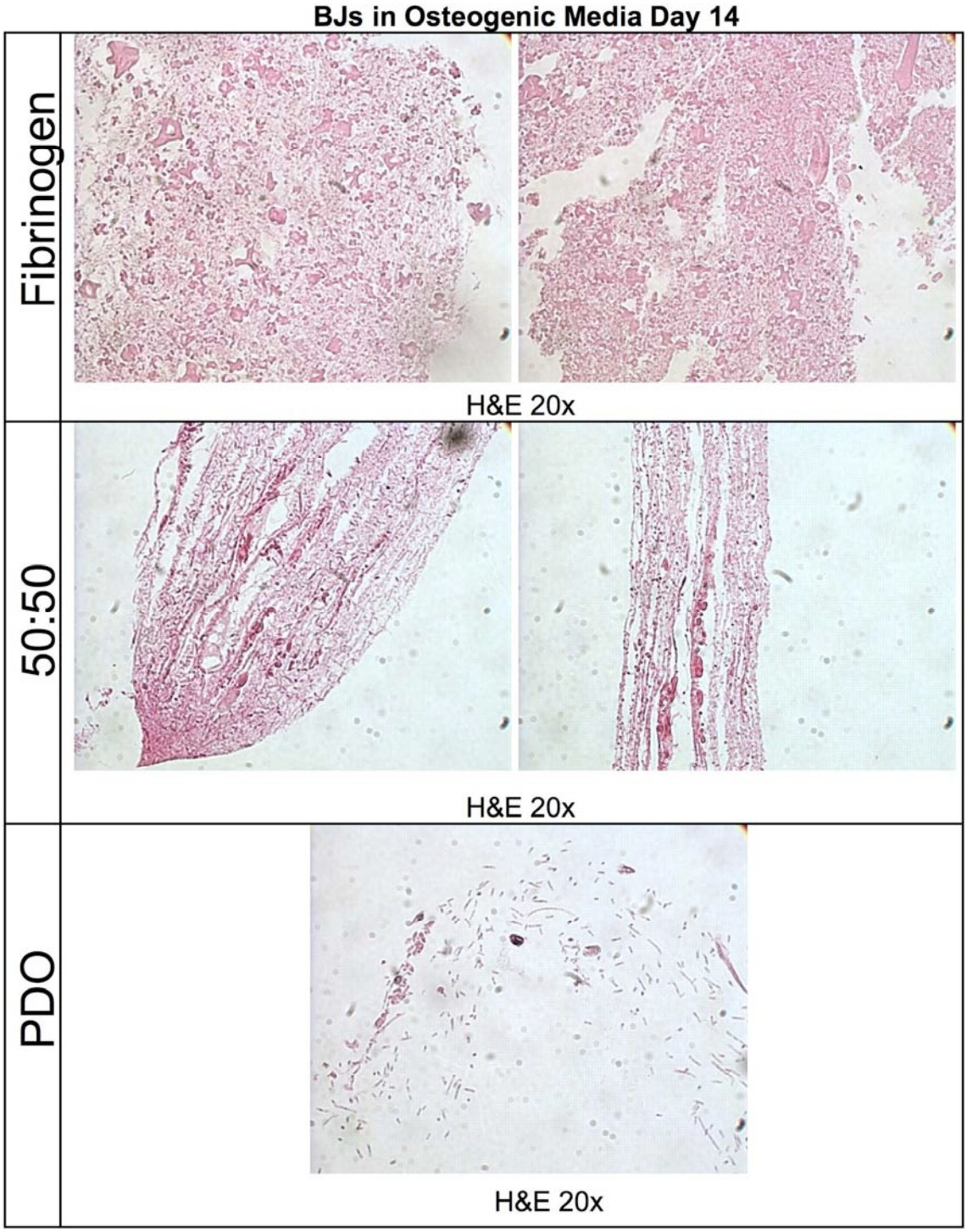

Figure 31. H&E Histology of BJ Fibroblasts on Fibrinogen, Fibrinogen:PDO, and PDO at Day 14 in Osteogenic Media. H&E stained sections of BJs on electrospun scaffolds reveal an absence of fibroblasts at 14 days of culture in osteogenic differentiation media in fibrinogen, 50:50 fibrinogen:PDO, and pure PDO scaffolds.

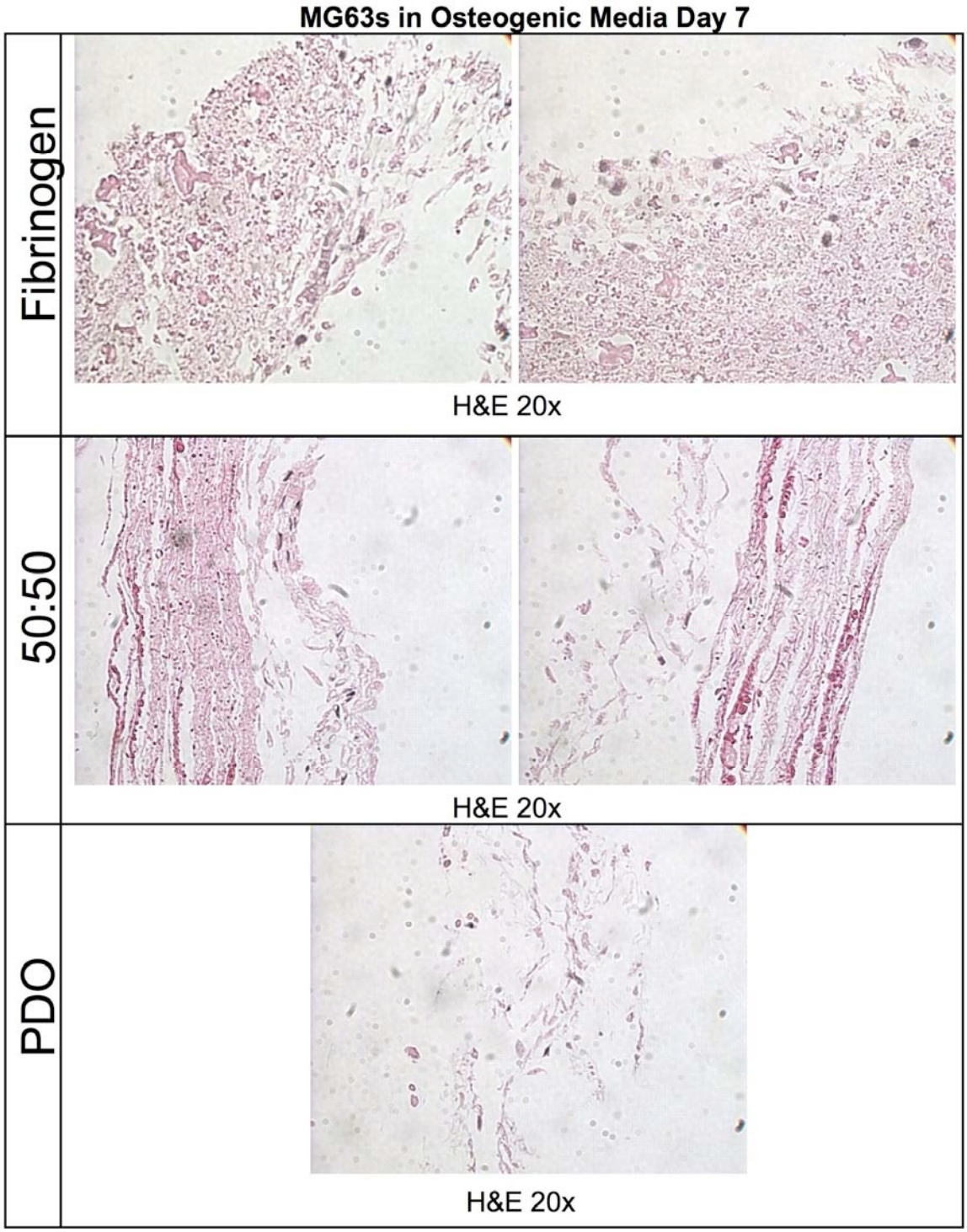

Figure 32. H&E Histology of MG63 Osteosarcoma cells on Fibrinogen, Fibrinogen:PDO, and PDO at Day 7. H&E stained sections of electrospun fibrinogen revealed high MG63 cellularity at 7 days of culture. MG63s also penetrated and layered efficiently into fibrinogen:PDO scaffolds, while pure PDO scaffolds appeared to support very few cells.

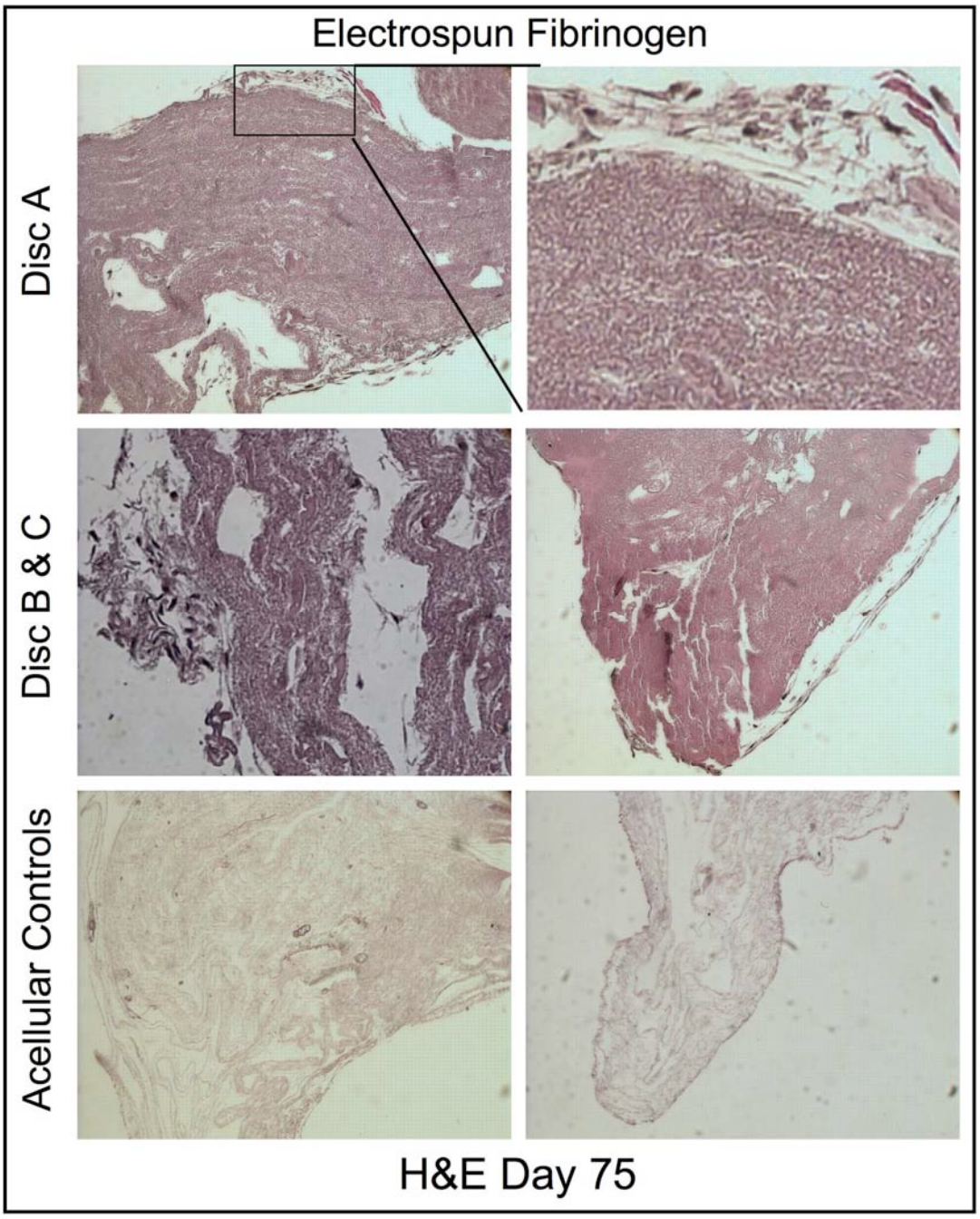

Figure 33. Day 75 in Culture on Electrospun Fibrinogen. ASCs grown in culture for 75 days on electrospun fibrinogen in control media and stained with H&E, with fields 3 of cellularized scaffolds shown for comparison (disc A and A with magnification, disc B & disc C). Ethanol cross-linked acellular fibrinogen scaffolds left in media for 75 days and H&E stained and are shown for reference as a control.

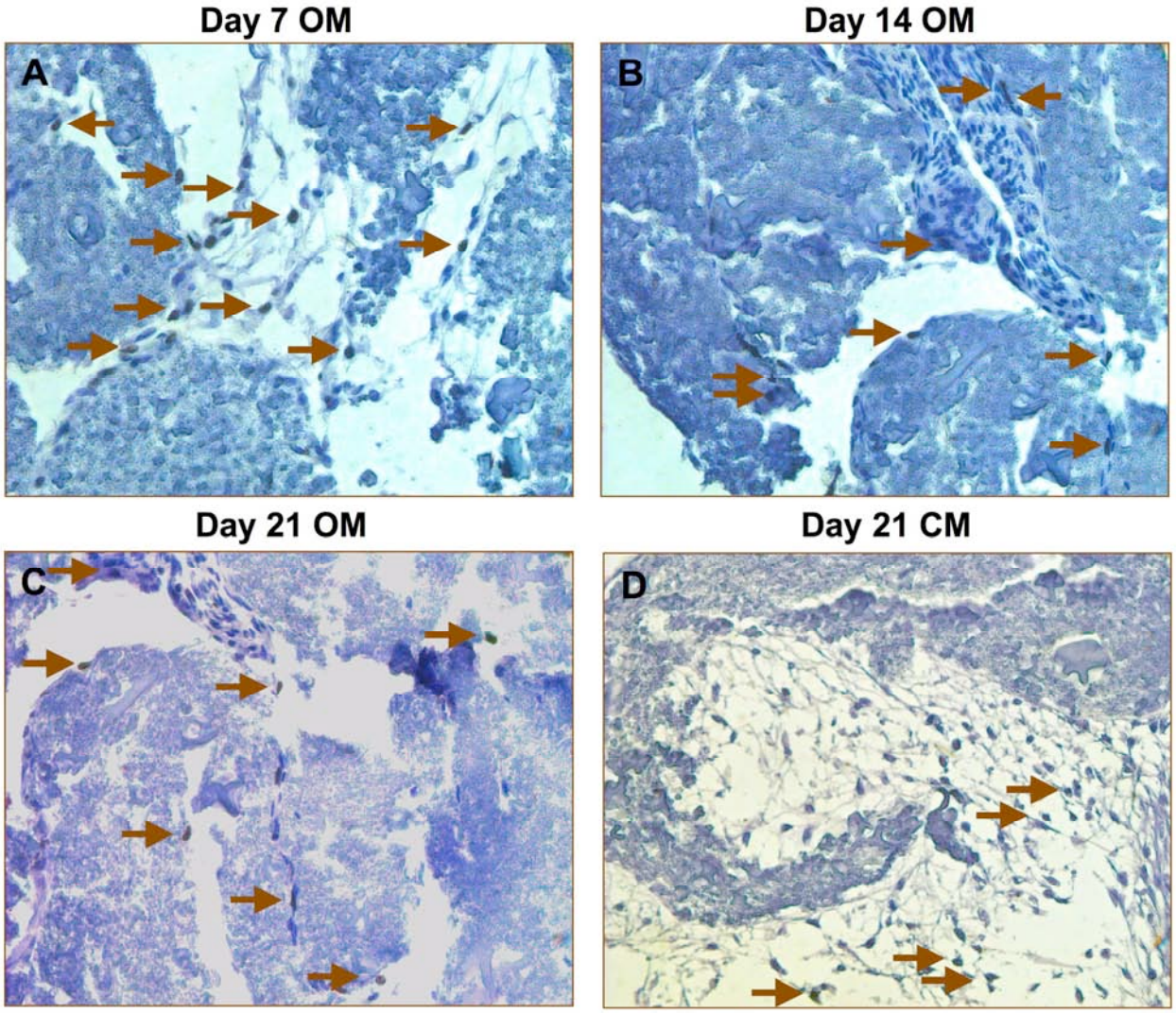

Figure 34. Ki67 Staining of ASCs Proliferation in Electrospun Fibrinogen. In either osteogenic (OM) or control media (CM) on pure fibrinogen, ASCs were found to retain a small population of mitotically active cells from 7-21 days of culture, as seen through positive Ki67 staining as the black/brown stained nuclei, which are demarked by arrows in the figures.

Table 10: Percentage of Ki67 Positive cells.

Samples	Average # of Cells (n=5)	% Ki67+ (n=5)
Fg:PDO OM D7	**244±66**	**4.5±1.2**
Fg:PDO OM D14	**222±83**	**5.4±1.7**
Fg:PDO OM D21	**238±56**	**1.7±0.8**
Fg:PDO CM D21	**235±69**	**6.0±0.7**
Fibrinogen OM D7	**411±103**	**14.8±2.1**
Fibrinogen OM D14	**311±77**	**11.7±1.4**
Fibrinogen OM D21	**224±60**	**8.0±0.6**
Fibrinogen CM D21	**670±141**	**8.8±3.2**

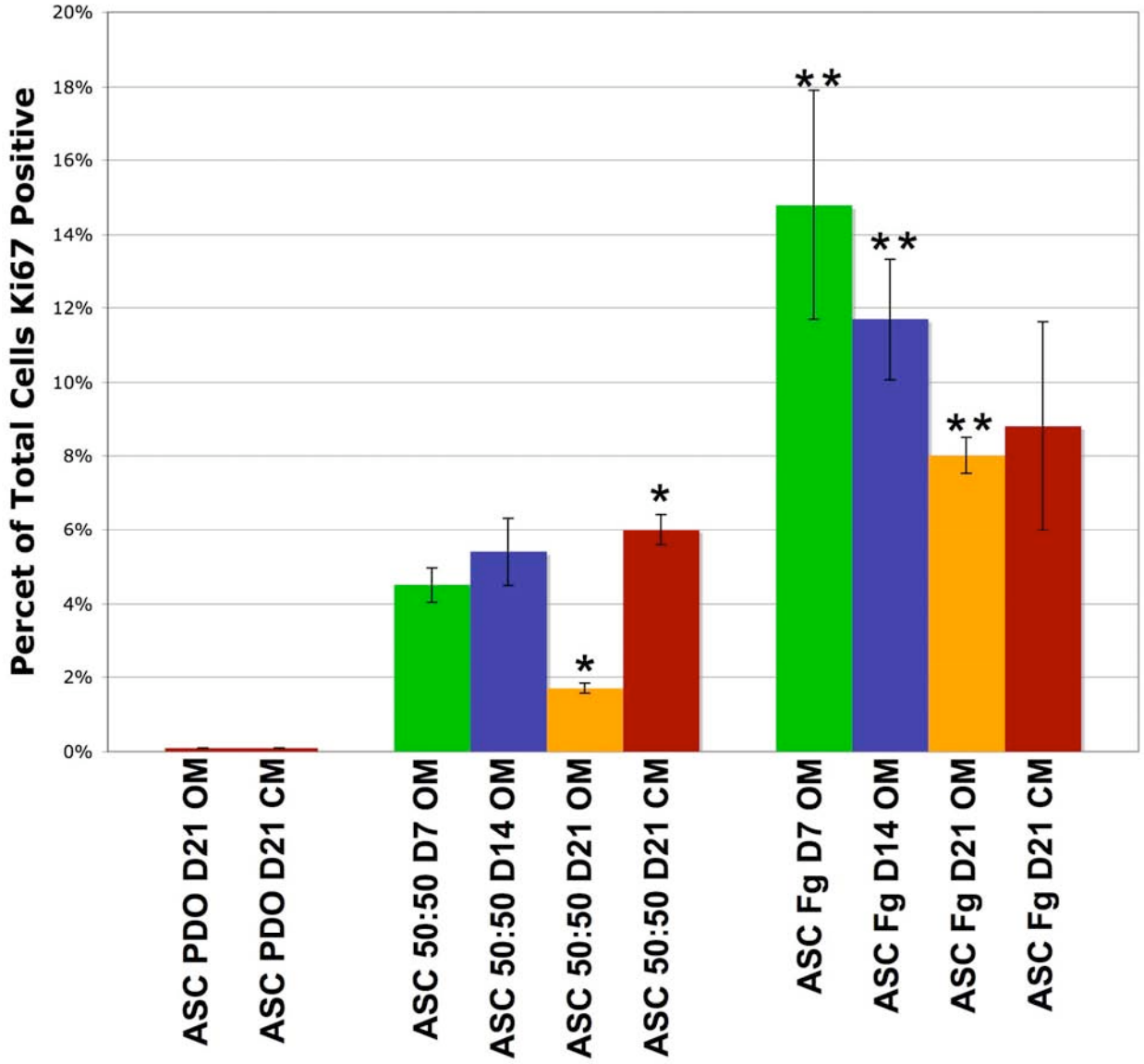

Figure 35. Percentage of Ki67 Positive cells. The average number of Ki67+ cells are shown along with the average number of total cells seen in the averaged fields for ASCs grown in either osteogenic (Osteo) media or control/growth media (Growth) from 1-3 weeks, on pure fibrinogen and on fibrinogen:PDO (Fg:PDO). (Statistical analysis performed by One Way ANOVA with $p<0.05$. *=significant increase in Ki67 cells over PDO scaffolds, **=significant increase in Ki67 cells over both PDO and 50:50 scaffolds, as compared at the respective time point).

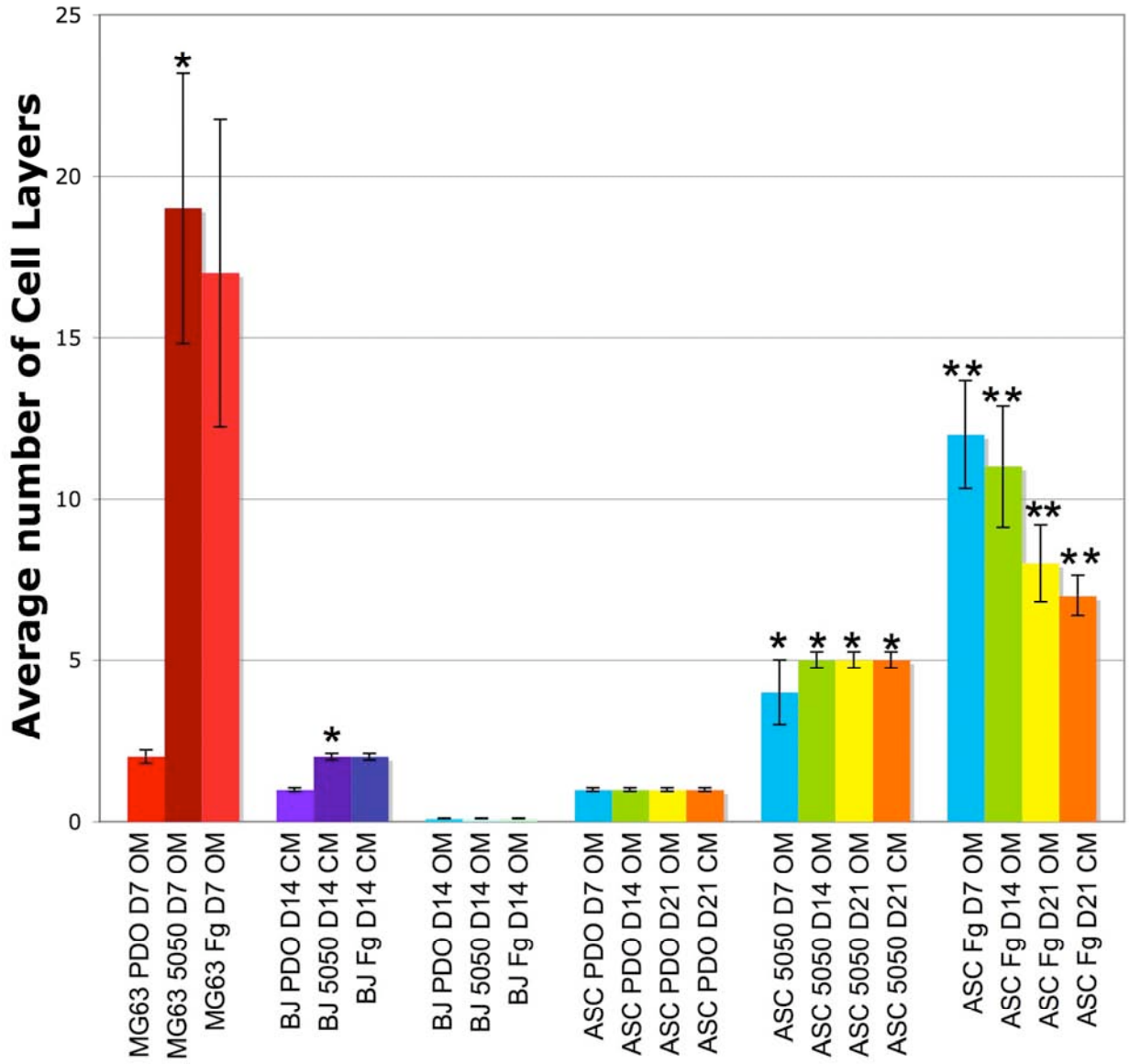

Figure 36. Cell Layers Formed with Electrospun Scaffolds. Electrospun PDO, Fg and Fg:PDO scaffolds were observed to form a clearly structured cell layer towards their surface when seeded with ASCs, BJs or MG63 cells, with clear difference seen in the thickness of the apparent tissue formed. Cells were grown in osteogenic media (OM) or control media (CM) and scored on representative fields at 40x. Cells on PDO formed a uniform single-layer thick barrier on the scaffold exterior, while ASCs on Fg:PDO formed an extremely even 4-5 cell layer thick barrier, with ASCs of pure fibrinogen creating a thick cell wall from 7-12 cells thick. This is in contrast to BJ fibroblast that formed no more then a 1-2 cell layer thick barrier on the periphery of the scaffold on all material types. (Statistical analysis performed by One Way ANOVA with $p<0.05$. *=significant increase in cell layers over PDO scaffolds, **=significant increase in cell layers over both PDO and 50:50 scaffolds, as compared at the respective time point).

scaffolds with no cells penetrating the interior (**Fig. 36**). The Fg:PDO scaffolds had 4-5 cell layer thick envelope around the scaffold with some cells within the scaffold, while pure Fg had many cells within the interior of the scaffold and the thickest number of cell layers formed, averaging 8-12 **(Fig. 36)**, suggesting ASCs had lost their contact inhibition on electrospun Fg.

To complete the characterization of ASCs on Fg- and PDO-containing scaffolds, we wanted to determine if the ASCs were able to remodel the spun matrix and lay down their own native extracellular matrix (ECM). Using Mason's Trichrome stain, which detects newly synthesized collagen, ASCs were able to dramatically remodel their new environment, laying down new collagen in place of existing Fg from 1 week to as many as 10 weeks of culture in both pure electrospun Fg **(Fig. 37)** and on electrospun Fg:PDO **(Fig. 38)**.

To evaluate the potential of ASCs seeded on electrospun Fg to form mature bone-like material, we assayed for calcification of Fg, Fg:PDO, and pure PDO scaffolds with bone-induced ASCs at 21 days in culture using Alizarin Red S (ARS) staining to detect calcified matrix (**Fig. 39**). While pure PDO scaffolds showed a marked absence of staining, matrix mineralization was clearly detected under light and fluorescent microscopy for Fg:PDO and particularly with pure Fg scaffolds at day 21, with staining appearing to become more intense with time on ASCs grown on pure Fg scaffolds (**Fig. 40)**. Fg scaffolds seeded with ASCs in osteogenic media (OM) without dexamethasone (control media, CM) for 21 days showed little if any ARS staining at 21 days of culture (**Fig. 40D**).

We further observed that bone-induced samples with Fg and Fg:PDO became hard and brittle phenotypically. In order to further define the changes in scaffold surface topology, we performed SEM of the bone-induced samples at 21 days. Only the ASC-containing scaffolds (not

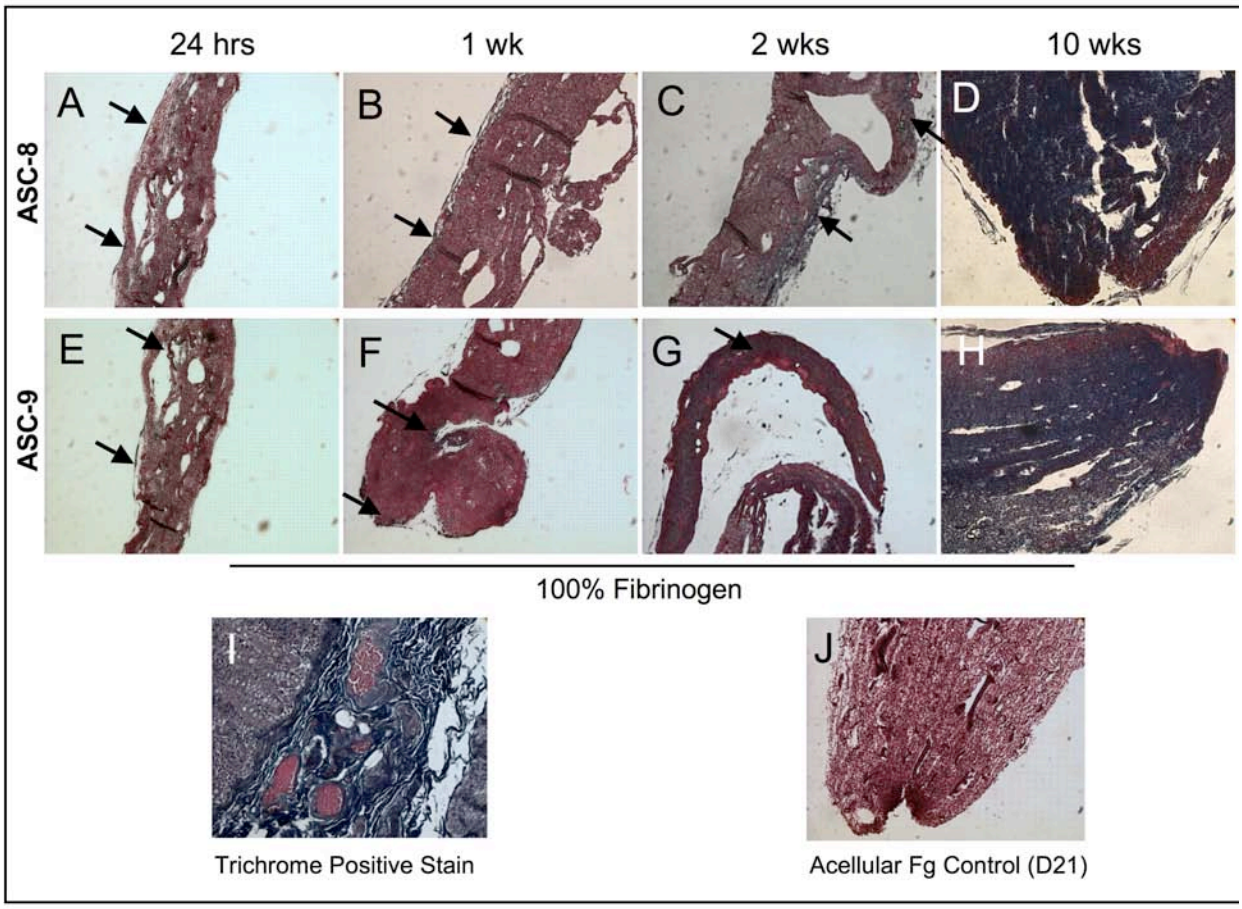

Figure 37. Mason's Trichrome of ASCs on Electrospun Fibrinogen. Masons Trichrome stain of two ASC cell strains (ASC-8 and ASC-9) grown on electrospun fibrinogen for 1 day (A,E), 1 wk (B,F), 2 weeks (C,G) and 10 weeks (D,H) along with an acellular control grown in osteogenic media for 21 days (J) and a positive trichrome stain of the human kidney (I), indicating increasing ASC collagen deposition with time.

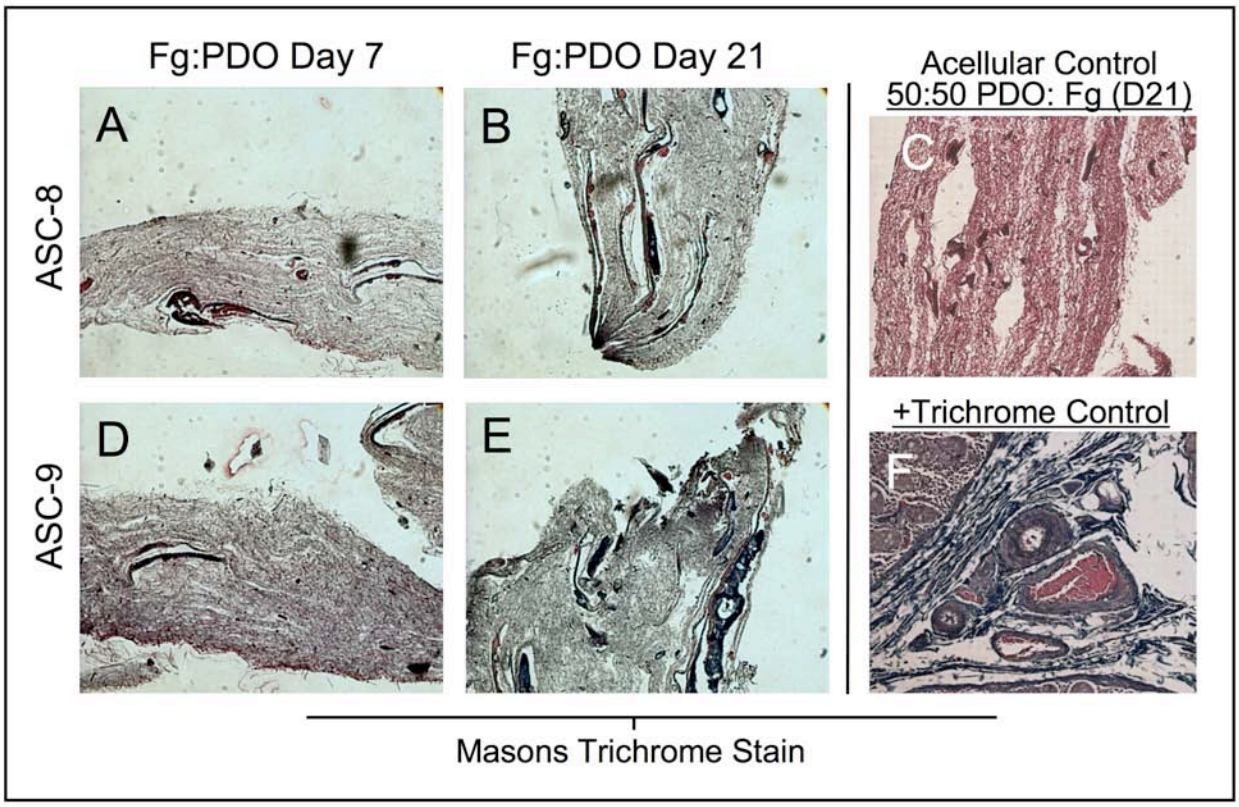

Figure 38. Mason's Trichrome of ASCs on Electrospun Fibrinogen:PDO. Masons Trichrome stain of ASCs (strains -8 and -9) grown on electrospun fibrinogen:PDO 50:50 blend for 7 (A,D) and 21 days (B,E) in culture show vast new collagen deposition seen though 3 weeks of culture with ASCs of 2 representative strains, along with an acellular electrospun Fg:PDO (C) and positive trichrome of kidney (F) shown as controls .

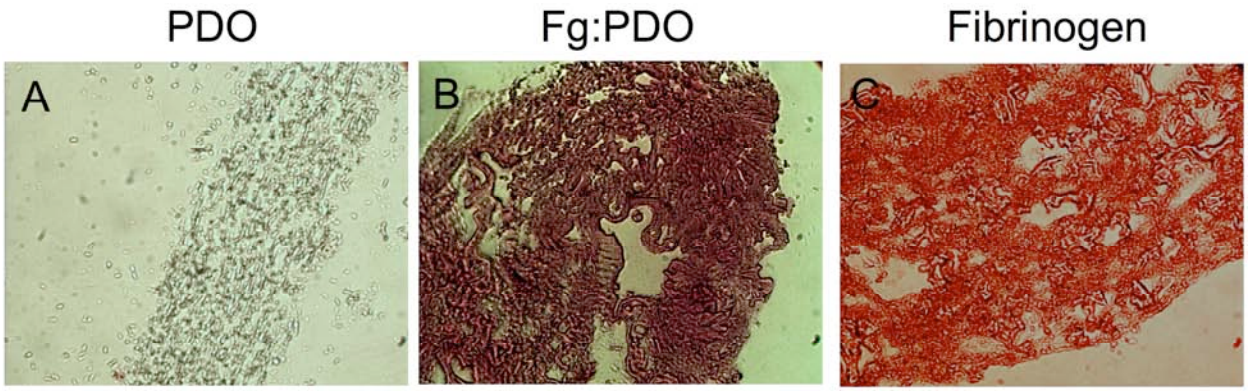

Figure 39. Mineralization of Electrospun Fg, PDO and Fg:PDO at Day 21. Phase microscopy images of ASCs grown in osteogenic media upon electrospun PDO (A), Fg:PDO (B) and pure fibrinogen (C) scaffolds for 21 days and stained with Alizarin Red S are shown under phase and fluorescent microscopy.

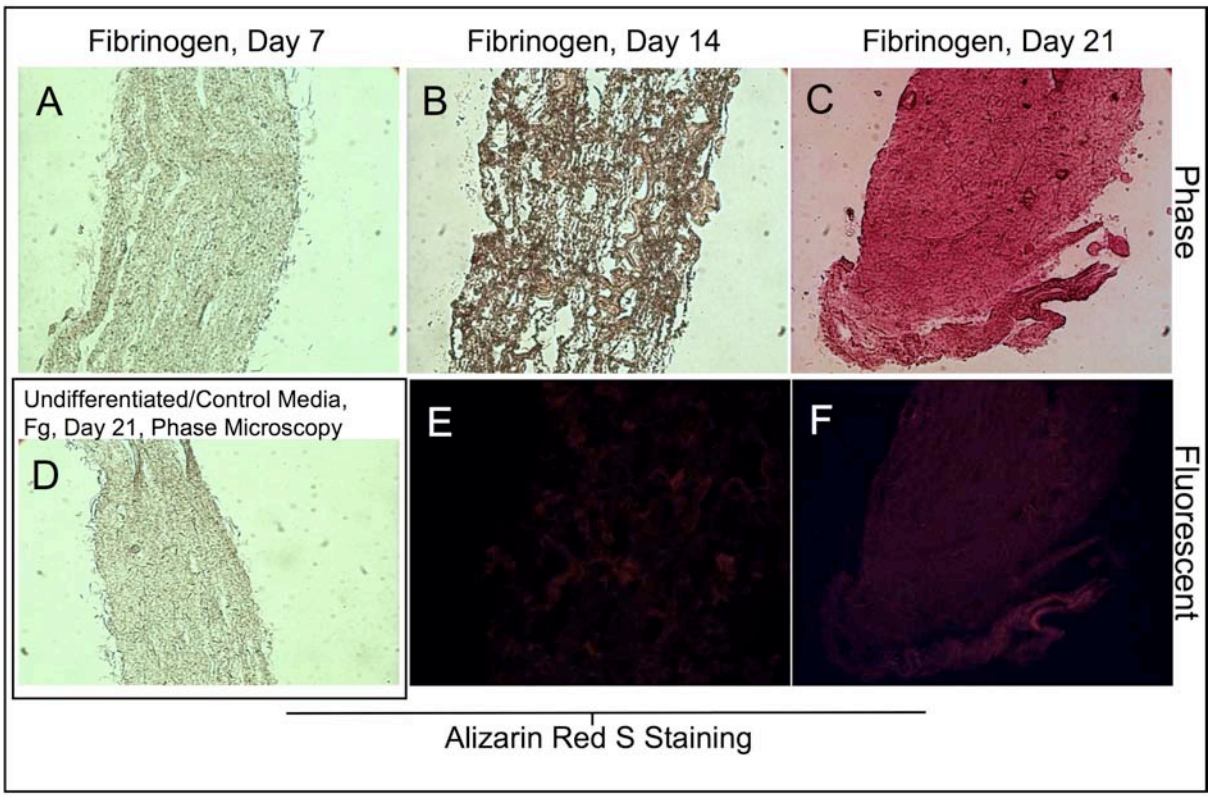

Figure 40. Mineralization on Electrospun Fibrinogen Time Course. Phase and fluorescent microscopy images of ASCs grown in osteogenic media upon electrospun fibrinogen for 7 days (A), 14 days (B,E) and 21 days (C,D,F) and stained with Alizarin Red S, along with a control scaffold grown in control media for 21 days that lacked apparent mineralization (D). Fluorescent images are shown for contrast and to indicate specific staining of the Alizarin Red fluorochrome on and between the scaffold fibers.

acellular, MG63-, or BJ-seeded scaffolds) exhibited a remarkable change in morphology to the structured topology shown **(Fig. 41**), having features suggestive of scaffold mineralization, which is consistent with our previous findings using a chemical mineralization protocol (Madurantakam et al., 2009). This is in stark contrast to the fibrous scaffolds found in **Figure 24** with ASCs grown in control/growth media on the same matrix, which essentially left the scaffold unchanged.

To determine if mature bone proteins were being synthesized and incorporated into the electrospun Fg matrix, osteocalcin expression of osteo-induced ASCs on electrospun Fg was assessed using immunofluorescence and confocal microscopy. No antibody controls showed a mild fiber auto-fluorescence in each panel, slightly obscuring the signal **(Fig. 42)**. However, the presence of osteocalcin protein is clearly observed in the area surrounding the cells in osteo-induced scaffolds on pure Fg and Fg/PDO blended scaffolds, with the intense signal absent on control media scaffolds **(Fig. 42)**. MG63 cells grown on electrospun Fg and Fg:PDO also showed strong osteocalcin expression in the ECM.

To further assess ASC osteoblastogenesis in electrospun Fg scaffolds, quantitative RT-PCR was performed revealing relatively higher level of Runx2 expression at 1 week of culture in both osteogenic and control media (osteogenic media without dexamethasone) at day 7 relative to day 21 for ASCs and BM-MSCs on pure Fg scaffolds **(Fig. 43)**. MG63 cells on electrospun Fg showed minimal Runx2 expression, as expected. A significant increase in alkaline phosphatase (ALP) gene expression was found at 3 weeks of differentiation as compared to 1 week of differentiation and also as compared to ASCs seeded on Fg for 1 and 3 weeks in control media (osteogenic media minus dexamethasone) **(Fig. 44)**. BM-MSCs and MG63 controls did not

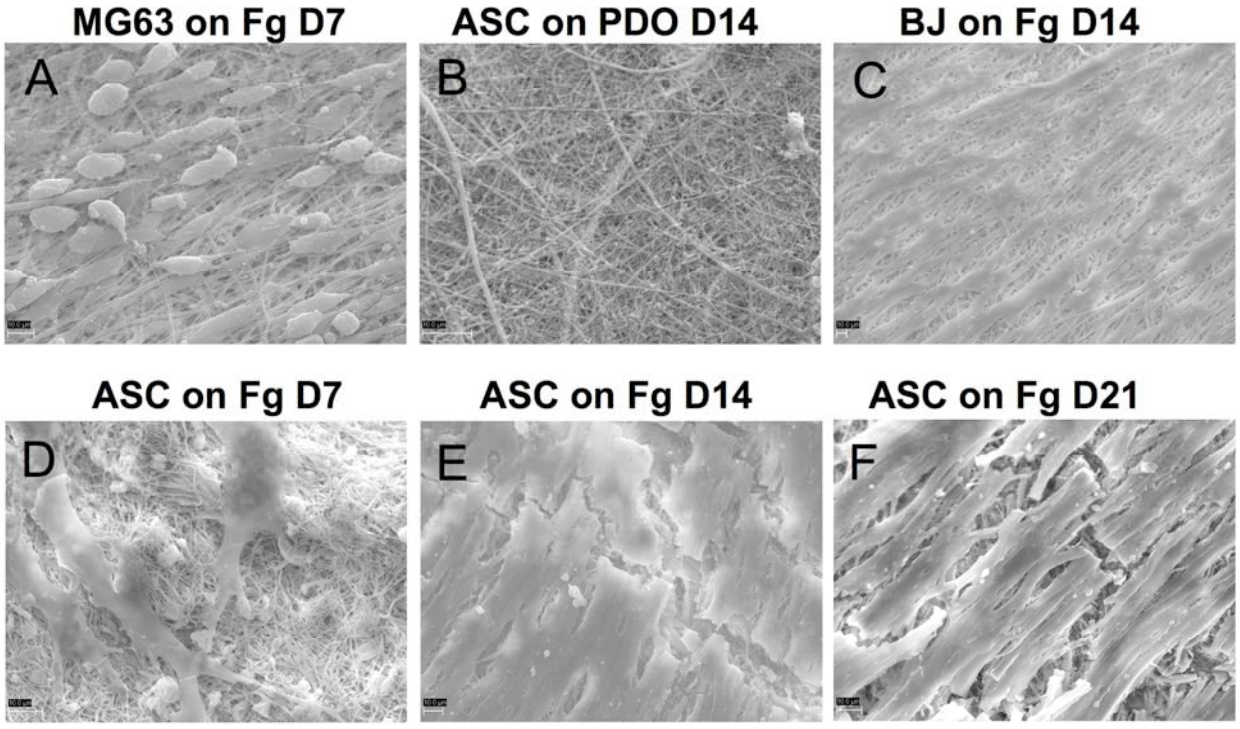

Figure 41. Topography of Bone-Induced ASCs on Electrospun Fibrinogen. ASCs maintained in osteogenic differentiation media are shown at 7-21 days of differentiation (D-F) via SEM (5000x) showed a unique, apparent calcified morphology on the surface. BJ fibroblasts were also grown in osteogenic media for 21 days on fibrinogen for a negative control (C) and these cells lacked the topographical changes seen with ASCs in osteogenic media. ASCs grown on PDO at day 14 and beyond showed limited cellularity on the scaffold surface (B), and MG63 osteosarcoma cells shown at day 7 on fibrinogen for reference appeared unchanged at the scaffold level (A).

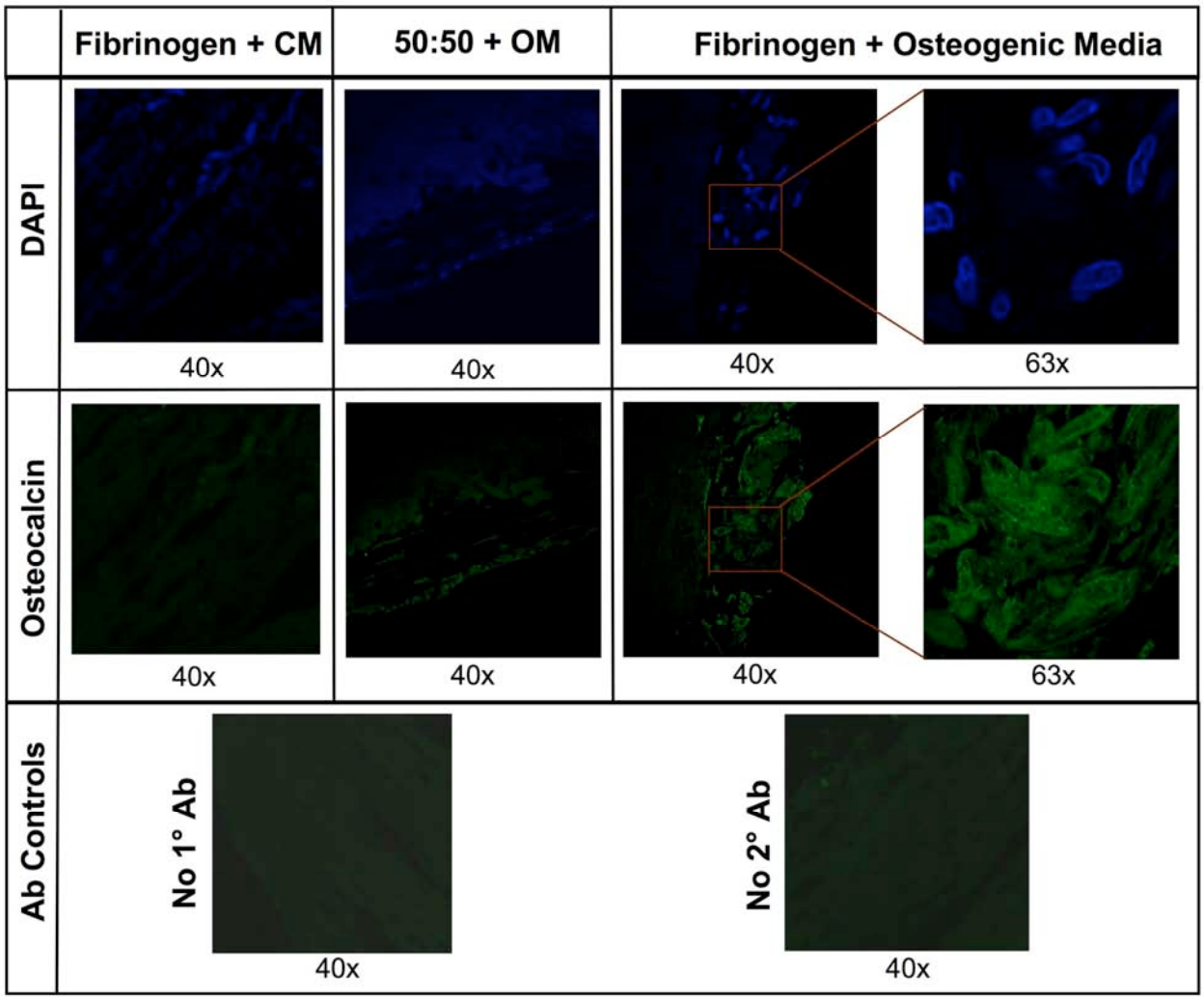

Figure 42. Osteocalcin Expression of Osteo-induced ASCs on Electrospun Fibrinogen. ASCs were seeded upon electrospun fibrinogen or fibrinogen:PDO and cultured for 21 days in osteogenic media, then labeled with DAPI and immunolabeled for osteocalcin. ASCs grown on spun fibrinogen without osteogenic differentiation were used as a negative control. A no primary osteocalcin antibody negative control is also shown for reference on the bottom panel, with very faint fiber auto-fluorescence seen at the 488nm detection wavelength. Mild fiber auto-fluorescence in seen in the each panel, yet osteocalcin expression is seen strongly in samples grown in osteogenic media yet nearly absent in growth media.

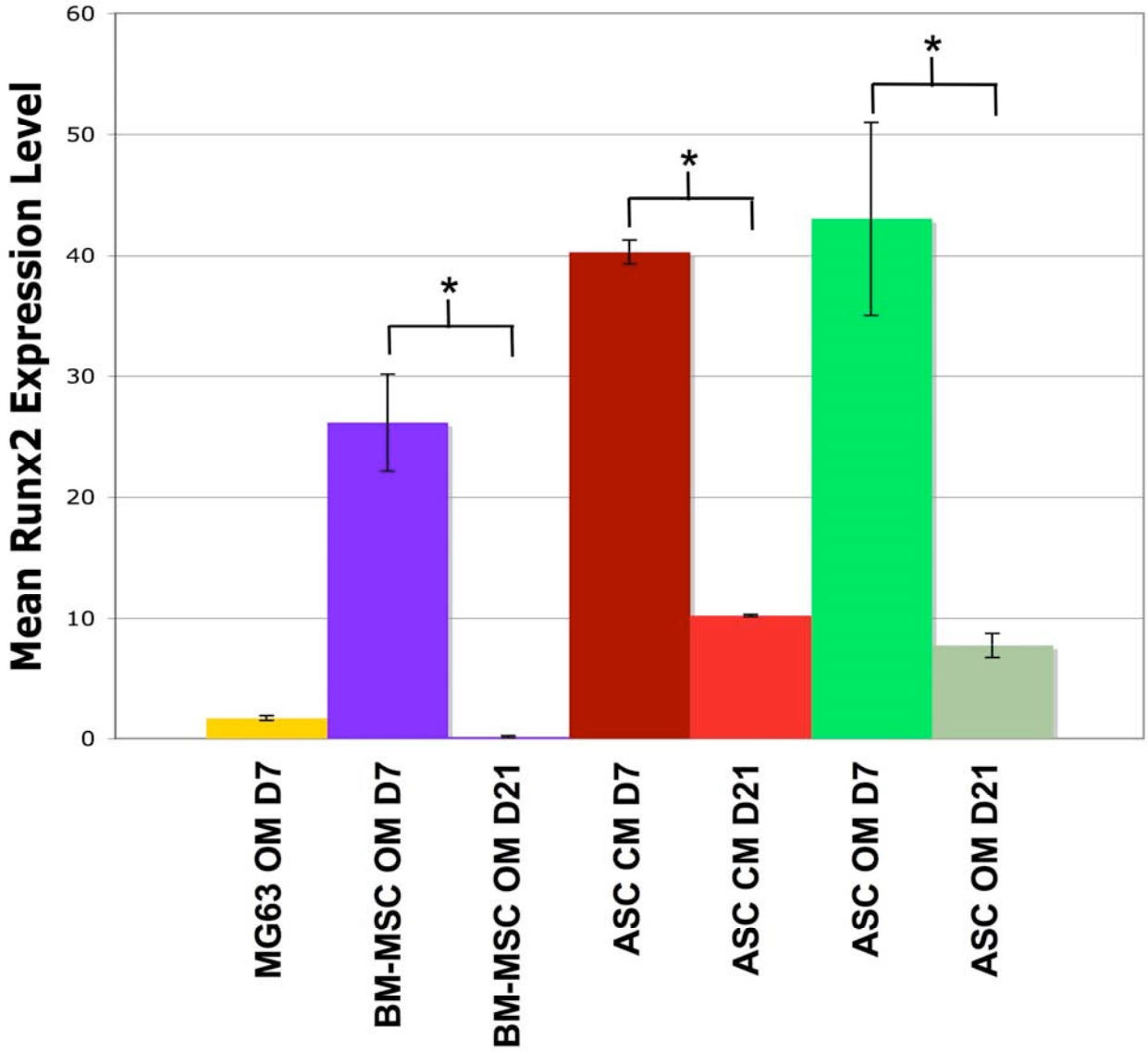

Figure 43. qRT-PCR Analysis of Runx2 Expression in Osteo-induced Cells on Electrospun Fg and Fg:PDO. Quantitative RT-PCR showed a significantly higher level of Runx2 expression at 1 week of culture in both osteogenic media (OM) and control media (CM, which is osteogenic media without dexamethasone) for ASCs and BM-MSCs grown on fibrinogen scaffolds. This effect is lost by the 3 week point in each case. (Analysis by One Way ANOVA followed by a Tukey's test for pairwise comparison, with *$p<0.05$ and considered significant).

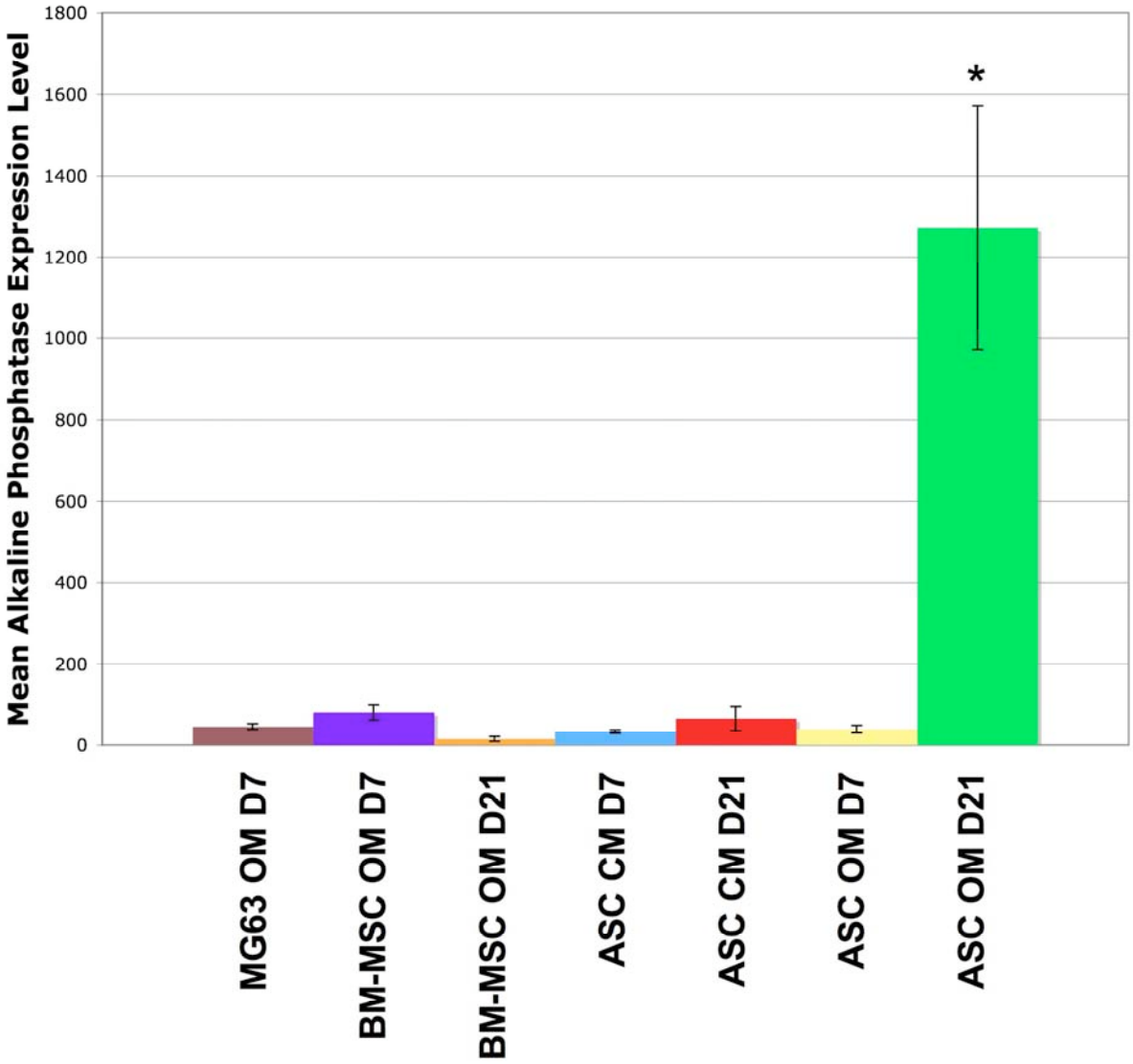

Figure 44. qRT-PCR Analysis of Alkaline Phosphatase (ALP) Expression in Osteo-induced Cells on Electrospun Fg and Fg:PDO. Alkaline phosphatase (ALP) gene expression was seen to increase markedly in ASCs at 3 weeks of differentiation in osteogenic media (OM), as compared to 1 week of differentiation and also as compared to ASCs seeded on fibrinogen for 1 and 3 weeks in control media (CM, or osteogenic media minus dexamethasone). Fg:PDO scaffolds appeared to have a potential osteo-inductive effect on ASCs, with high levels of ALP seen at 1 week of culture of ASCs in both CM and OM. BM-MSCs and MG63 cells were not shown to express significant levels of ALP on any scaffold type or time point as grown in OM (Analysis by One Way ANOVA followed by a Tukey's test for pairwise comparison, with *$p<0.05$ and considered significant).

express significant levels of ALP at any time point grown in osteogenic media. In terms of osteocalcin gene expression, only ASCs in osteogenic media seeded on pure electrospun Fg scaffolds showed significant upregulation of osteocalcin relative to 1 week of differentiation, and compared to 1 and 3 weeks of growth in control media on electrospun fibrinogen **(Fig. 45)**. The positive control, MG63 cells, showed high osteocalcin expression on Fg, while BM-MSCs expressed little osteocalcin at day 7 or 21.

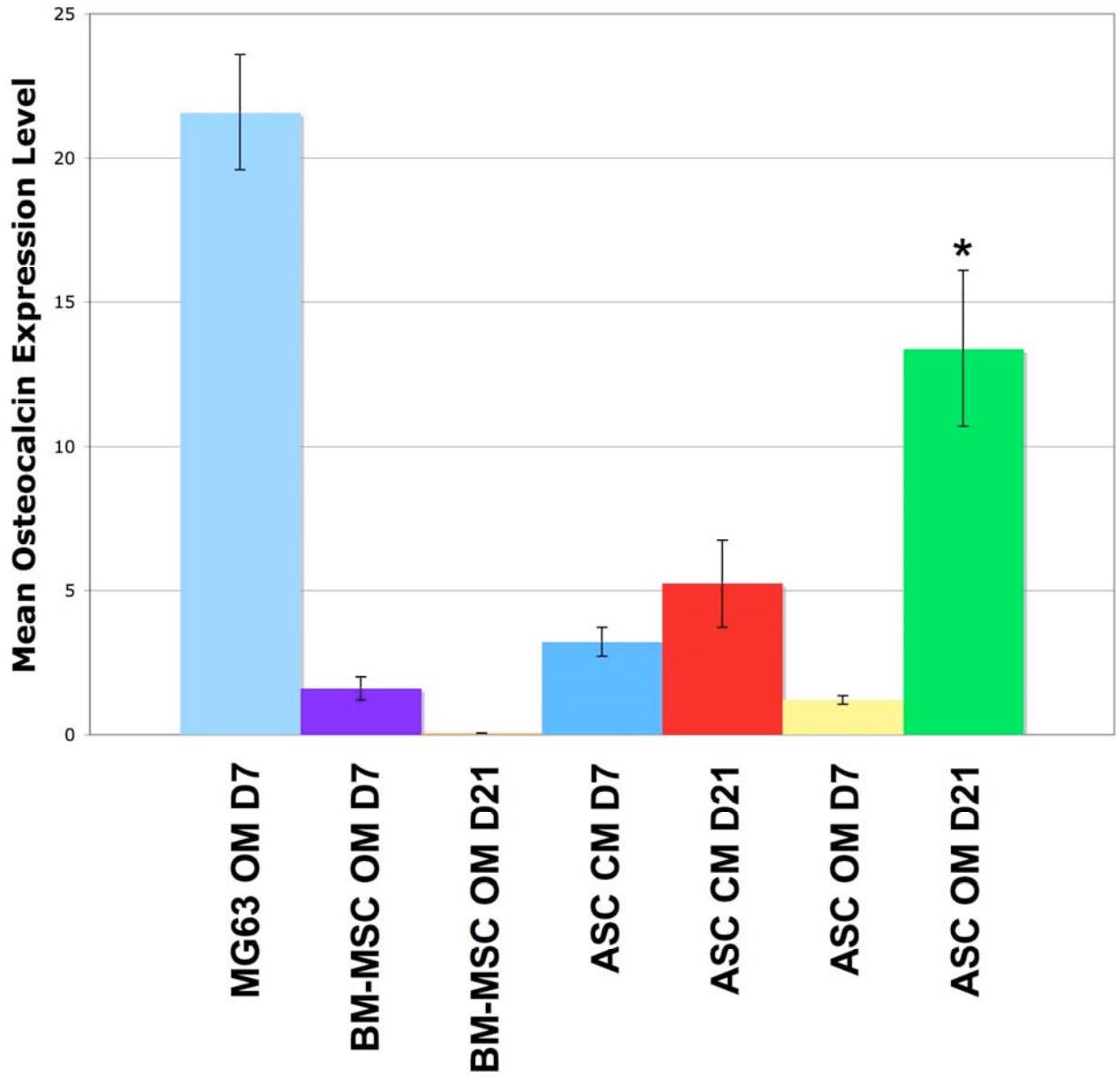

Figure 45. qRT-PCR Analysis of Osteocalcin Expression in Osteo-induced Cells on Electrospun Fg and Fg:PDO. ASCs in osteogenic media (OM) and seeded on pure electrospun fibrinogen scaffolds showed significant upregulation of osteocalcin expression relative to 1 week of differentiation and to 1 and 3 weeks of ASC growth in control media (CM, or OM -Dex) on either scaffold type. MG63 cells showed moderate expression on Fg and high expression on Fg:PDO (Analysis by One Way ANOVA followed by a Tukey's test for pairwise comparisons, with *$p<0.05$ and considered significant).

DISCUSSION

We show that electrospun nanofibers of Fg and a 50/50 Fg:PDO blend, but not electrospun pure PDO, are viable support materials for adipose-derived mesenchymal stem cell proliferation and osteoblastogenic differentiation. Electrospun Fg, in pure form or blended with PDO, can support osteoblastogenesis of ASCs in producing an engineered material that is similar to bone in its topography, gene expression, phenotype, and protein composition. While many approaches for generating artificial bone *ex vivo* have been developed with varying success, using autologous and biomimetic Fg nanofibers seeded with patient-derived ASCs as osteoblast precursors is a natural approach, important for basic science research and potentially clinical uses. As Fg is the primordial wound-healing matrix initially deposited after a bone fracture, there is tremendous potential for developing new bone with a biomimicry blueprint using electrospinning with Fg and ASCs.

Our results show that electrospun Fg and Fg:PDO are fully capable of supporting the proliferation of ASCs *in vitro*. Interestingly, with ASC grown in osteogenic differentiation media, we noted a general increase in cell number for up to two weeks of growth in electrospun Fg-containing scaffolds with a decrease in the total cell number at the third week, which corresponded to a decrease in mitotic activity from the first to third week of culture in osteogenic media. Conversely, ASCs grown in basic growth media on electrospun fibrinogen scaffolds exhibited a dramatic increase in cell number at the 3-week time points relative to ASCs grown in osteogenic media at any point. This data suggests that more ASCs in OM are exiting the cell cycle with time, perhaps either becoming quiescent, senescent, or more likely committing to differentiate into a mature bone cell type. Despite higher total numbers of ASCs at 3 weeks on

electrospun Fg with cells grown in growth vs. differentiation media, Ki67 staining was similarly high at 3 weeks for cells grown in both media types, with only around 8% of the cells showing mitotic activity.

Another interesting note on scaffold cellularity was the clear thin layer of ASCs found forming around PDO scaffolds. As ASCs contact inhibit in culture on tissue culture plastic, this response might be expected of ASCs on electrospun PDO or other materials. However, it appeared that ASCs either lost their contact inhibition on electrospun Fg, becoming capable of forming very thick 8-15 cell layer thickness across the top of this material. Additionally, ASCs were able to migrate into the scaffold in a controlled, layering manner, while still layering atop the scaffold. The nature of the H&E histology sections blurred the distinction between cells layering on top of the scaffold and penetrating into the scaffold to form layers, yet the appearance of large sheets of organized cells reminiscent of actual tissue was striking, and such order is rarely observed with other cells type on any electrospun material.

Synthetic materials are valued in tissue engineering due to their mechanical strength, elastic properties, and their general affordability and abundance relative to naturally derived materials. Yet synthetic materials tend to have poor cell-matrix interactions and can cause undesirable responses to the host immune system. It has been shown that the typically poor cellular response for many synthetic polymers can be substantially improved by the addition of natural materials (Kim et al., 2007). We show the typical poor cell response and poor osteoblastogenic potential of a synthetic material, PDO, can be enhanced by the addition of a natural ECM, Fg, with improved cellularity and osteoblastogenic differentiation potential. Determining the ideal ratio of Fg:PDO to obtain the maximal amount osteoblastogenesis, thereby

increasing mechanical strength and reducing the amount of Fg required therapeutically, is an exciting future direction of our work.

With its simplicity, relative affordability, and excellent cellular response, electrospinning composite nanofibers is rapidly becoming the standard practice in the tissue engineering of bone. Electrospinning produces scaffolds highly amenable to cell adhesion, viability, and osteogenic differentiation (Vepari et al., 2006, Wutticharoenmongkol et al., 2007, Venugopal et al., 2008) using an array of template scaffold materials. The electrospinning of Fg nanofibers, first published by Wnek et al. (2003), has provided a tissue engineering scaffold with significant research and therapeutic potential. The preliminary neonatal rat cardiac fibroblast (McManus et al., 2007a) and human bladder smooth muscle cell (SMC) (McManus et al., 2007b) culture experiments validated the high bioactivity of electrospun Fg scaffolds, with fibroblasts migrating and depositing new collagen, and SMCs placing new collagen almost completely throughout the scaffold within 2 weeks. Prior publications with electrospun Fg scaffolds ultimately lacked the requisite mechanical integrity to serve as tissue engineering scaffolds without crosslinking, a problem shared with electrospun collagen (McManus et al., 2006).

In contrast to previous studies, we show that ASCs inherently possess a unique ability to remodel a sustainable scaffold in extremely long term culture. For up to 75 days of maintenance culture, ASCs produced a highly cellularized Fg scaffold composed of new collagen and other ECM materials, making this an excellent and highly symbiotic combination of cells and materials for regenerative medicine purposes. The mechanical properties of electrospun Fg may be augmented by chemical crosslinking (Sell et al., 2008) or by adding synthetic polymers such as PDO to the fibrinogen scaffold (McManus et al., 2008) to produce a more stable scaffold in

culture. Unfortunately, our results showed that these approaches inhibit the cellular response for ASCs. Using a cell type (ASC) capable of rapidly synthesizing its own stable ECM may be the ideal approach for minimizing adverse cell-matrix responses and for enhancing cellularity, an important feature of a scaffold intended for therapeutic ends.

qRT-PCR revealed higher level of Runx2 expression at 1 week of culture in both osteogenic and control media at day 7 relative to day 21 for ASCs and BM-MSCs on pure Fg scaffolds. This unexpected data suggests a number of plausible explanations, including the optimal expression window for Runx expression may have been missed or that the matrix itself induced a mild osteogenic phenotype. One other the possibility is that the absence of dexamethasone only prevents full osteoblastogenesis, and ASCs can begin the differentiation process with Runx2 being an early marker only. Alternatively, Runx2 levels may be elevated in ASCs and a high baseline may have skewed the results. A finer analysis of Runx2 expression over more early time points would be required to better explain these results.

ASCs have recently been shown to exhibit enhanced proliferation and osteoblast induction by seeding the cells on tricalcium phosphate coated electrospun PCL nanofibers (McCullen et al., 2009). The ability of a scaffold to maintain and induce differentiation is a critical parameter of an ideal scaffold for therapeutic use (Khan et al., 2008**)**. The data presented here indicates that the blending of Fg and PDO appears to have an early osteoblastogenic inductive effect in our studies, as shown by qRT-PCR results. Determining the full extent of this induction with a finer time course following the upregulation of early differentiation marker genes is part of our future work.

Cells as varied as amniotic mesenchymal stem cells and BM-MSCs have been used as a template for developing or repairing bone in very recent electrospinning-based research with great results (Steigman et al., 2009, Thibault et al., 2009). These progenitor cell types are not without complications however in their painful extraction, scarcity, or heterologous nature. Here, we report the novel findings that ASCs, an abundant, autologous, and readily accessible progenitor cell, are a practical cell type for modeling osteoblastogenesis in tissue engineering with electrospun scaffolds, using a potentially autologous scaffold material, Fg, as well. In furthering the autologous cell and scaffold research, future studies using Fg and ASC-derived from the same patient would be a natural next step.

Surprisingly, little work has been done with adipose-derived or other adult stem cells seeded within any type of electrospun matrices, leaving much uncharted territory for discovery in many systems. Overall, our model presents an attractive template for future clinical and regenerative medicine research studies, for repairing bone and other tissues with abundant, affordable, and easily accessible and workable materials.

-Chapter 5-

Discussion and Future Directions

Adipose Stem Cell Characterization and Rapid Isolation

We have shown in chapters 3 and 4 a thorough characterization of newly derived adipose stem cell strains, as well as an improved technique for isolating viable population of mesenchymal stem cells from lipoaspirate saline using minimal reagents and a half hour of effort. We show these cells to share multipotent differentiation potential and immunophenotype with BMSCs.

In establishing our ASCs as a mesenchymal lineage with properties typical of MSCs, we assessed the immunophenotype of ASCs using markers typically associated with the MSC cell surface fingerprints as before (Izadpanah et al., 2006; Katz et al.; 2005, Kern et al., 2006; Lorenz et al., 2008; Lin et al., 2008; Noël et al., 2008; Rebelatto et al., 2008; Wagner et al., 2005; Yoshimura et al., 2006; Zuk et al., 2001; Zuk et al. 2002). Cell surface molecules CD14, CD29, CD31, CD34, CD45, CD73 and CD105 were determined to be markers commonly used for selecting a pure population of mesenchymal stem cells from the stem cell niches of bone marrow (BM-MSC), adipose tissue (ASC), umbilical cord stem cells (Rebelatto et al., 2008), and even stem cells found in menstrual blood (Meng et al., 2007).

As anticipated, flow cytometry analysis of early passage (PD 4-6) ASC-8, ASC-9, and BM-MSCs all show a typical MSC immunophenotype of CD14-, CD29+, CD31-, CD34 low/+, CD45-, CD73+, CD105+. These cells were not pre-sorted prior to flow cytometric analysis.

These cell lines were all selected by density gradient separation for mononuclear cells during their primary isolations, and only further selected on the basis of adherence to plastic and growth as adherent cells in ASC media after their initial isolation, and alternative methods may produce differing results. Interestingly, BJ fibroblasts, a mature, fully differentiated somatic cell type, express an immunophenotype of CD14-, CD29+, CD31-, CD45-, CD73+, CD105+, virtually indistinguishable from ASCs or BM-MSCs.

The shared immunophenotype between ASCs, BM-MSCs, and BJ fibroblasts strongly argues that other markers for somatic stem cells must be used or other methodologies employed, such as differentiation potential or perhaps gene expression profile to distinguish a true progenitor cell. These results argue against the use of costly and time-consuming flow cytometry for characterizing MSCs as requisite for confirming the identity of MSCs as MSCs, at least until better cell surface markers for characterization can be found, if such unique markers or combination of markers even exists. Large immunophenotype screens have been done in many laboratories in an attempt to find a unique ASCs fingerprint without success, suggesting that uncovering such a marker seems unlikely.

Comparing ASCs strains we derived using the established isolation method (Zuk et al., 2002), our ASCs also exhibited the expected multipotent differentiation potential and the typical lack of telomerase activity (not shown, pending publication, Francis and Sachs et al., 2010). We were also successful in rapidly isolating ASC in a streamlined 30-minute extraction process with characteristics indistinguishable from traditionally isolated ASCs and other MSC lines tested, presenting a modified technique that could lead to considerable time and cost savings (Francis et al., 2010). A method for rapidly deriving ASCs from lipoaspirate saline/blood in a minimally

equipped lab or hospital setting may even speed the realization of patient-derived stem cell therapies becoming common practice.

While ASCs were selected as an ideal progenitor cell type for previously mentioned reasons, embryonic or induced pluripotent stem cells (iPS) may prove superior still in generating the complexities of mature tissue, such as bone, in the laboratory and in the body. However, ASCs have not yet been shown to contribute to tissue resembling a wound blastema, such as that arising from the marrow of fractured bone and in the leading edge of all regenerating tissue. True pluripotent cells can form such blastema-like tissue and may prove (perhaps in concert with MSCs) to be important cells for generating complex tissues *in vitro* and *in vivo*, and this should be explored further.

Electrospun Fibrinogen, Osteoblastogenesis, and ASCs

Our results of chapter 5 show that electrospun Fg and Fg:PDO are excellent materials for ASC proliferation and osteogenic differentiation, and present a solid biomimetic system to further bone model-based research.

The initial experiments with ASCs seeded on cross-linked electrospun fibrinogen produced a largely impenetrable scaffold with a thin confluent layer of cells on the scaffold surface. While cross-linking may prove advantageous in some regards for enhancing mechanical integrity of the scaffold as it exists *in vitro* (Sell et al., 2008, McManus et al., 2006, 2007), the results presented here argue against cross-linking for creating a highly cellularized artificial scaffold, as a scaffold that has only a thin confluent layers of cells on the exterior is likely of limited utility clinically.

We have recently discovered that the shrinkage of pure fibrinogen observed can be largely prevented through weighing down the scaffold when it is hydrated to retain its original macroscopic size and shape, and logically generating larger pores and a more open architecture promoting cell infiltration. Though porosity measurements have not been made on unshrunken fibrinogen, it stands to reason that, without macroscopic shrinkage, little or at least less microscopic shrinkage is to be expected, removing another of the benefits of rigid chemical (rather then natural or biological) cross-linking.

Using unfixed scaffolds, ASC cellularity in fibrinogen was excellent, with a dense layer of cells found in the exterior of the scaffold and many cells throughout the scaffold by only 7 days of culture in either regular ASC growth media and also in osteogenic induction media. Fg:PDO blended scaffolds had high cellularity, with significantly more cells than found on PDO, yet reduced levels of cell proliferation over time from quantitated Ki67 data. Fg:PDO scaffolds with ASCs show extensive new collagen being deposited by the cells through trichrome staining. Pure PDO scaffolds were bereft of ASCs inside the scaffold and overall proved a poor substrate for ASCs in these studies. Further research is required to determine why PDO blended scaffolds had reduced bioactivity relative to pure fibrinogen scaffolds, and blending electrospun fibrinogen with other synthetic materials, such as PEG and PLGA, and even with other natural materials, such as collagen and silk, could prove highly informative.

Unexpectedly, MG63 osteosarcoma cells, used as a control to approximate osteoblasts, appeared highly active upon fibrinogen scaffolds, consuming the scaffold in a matter of days via an unknown mechanism, yet unlike ASCs or fibroblasts, MG63 cells did so without depositing a new support matrix in the process. This scaffold breakdown may be linked to protease secretion,

a common feature of many cancerous cells, which may be significant in modeling the stages of fracture healing. As the fibrinogen-containing hematoma forms early during fracture healing, it is quickly consumed by osteoblasts, and other precursor cells infiltrate the primordial healing matrix. Closer examination of this phenomenon is highly warranted, perhaps using normal osteoblast strains or fully differentiated osteoblasts derived from BM-MSCs or ASCs seeded directly onto the fibrinogen scaffold. In this type of system, we could then observe scaffold disintegration, assay for new collagen production, and also test mechanical strength. In other cancer-based studies with possible links to our research, using artificial bone generated from electrospun fibrinogen and MSCs may provide an excellent culture model system for studying the mechanism of breast or pancreatic cancer metastasis to bone.

Regarding material selection for modeling osteogenesis on electrospun scaffolding, it is arguable that collagen type I may be a superior material for modeling and stimulating osteogenesis, with type I collagen being the native and predominant ECM of mature bone. In fact, many studies have already shown electrospun collagen fibers to be a suitable template for bone differentiation and for potentially engineering bone *in vitro* (Ekaputra et al., 2009; Prabhakaran et al., 2009; Chan et al., 2009; Venugopal et al., 2008; Shih et al., 2006; Sefcik et al., 2006.). Though using collagen as a substrate for growing bone has clear advantages, collagen is typically only available from rat tails or bovine sources, which are problematic therapeutically. Human collagen, which would likely be far less immunoreactive than the xenogenic collagens, is not readily available or cost effective. Autologous collagen I is not currently harvested in large quantities without extreme patient morbidity associated with removing skin grafts.

Fibrinogen, however, can be readily harvested from the patient though simple blood collection. Fibrinogen is also potentially available in immense quantities though blood/plasma clinics, as fibrinogen is removed from donated blood and plasma prior to use and is generally discarded. Future studies may include isolating fibrinogen from the blood/saline phase of lipoaspirate for subsequent electrospinning and seeding with syngeneic ASCs. Additionally, a staggering amount of liposuction material, rich with basement membrane extracellular matrix and type I collagen, is discarded in the U.S. and therefore could potentially be used as a source of human collagen.

In these experiments, differentiating ASCs to bone while seeded upon electrospun fibrinogen provided an encouraging topological change by producing what appears to be a calcification on pure fibrinogen constructs. This feature was absent on acellular control scaffolds, on BJs seeded on fibrinogen, and on pure PDO-containing scaffolds with ASCs, even when grown in osteogenic media, which eliminates any possible interaction with the salts present in the differentiation media as being the causative factor responsible for these changes. Supporting the apparent matrix calcification found by SEM, the intense Alizarin Red S staining observed on Fg:PDO and particularly on pure fibrinogen scaffolds further asserts progression towards mature bone formation though presence of a highly calcified ECM. However, quantitation of the mineralization with time and as compared to acellular, and BJ, and BM-MSC seeded scaffold controls, is still required to determine the relative rate and extent of mineralization on electrospun fibrinogen, Fg:PDO, and PDO scaffolds.

While our qPCR results from pure fibrinogen scaffold were highly informative and support our findings that electrospun fibrinogen supports osteoblastogenesis from ASCs, future

studies could further this work. Our qPCR studies, as originally designed, included a comparison of Fg to Fg:PDO scaffolds for all genes tested yet, for assorted technical reasons, the results proved less informative then as originally designed. These studies could be replicated to directly compare the Fg and Fg:PDO scaffolds' ability to support osteoblastogenesis at the molecular level. For future studies, qRT-PCR could be performed on pure Fg and Fg:PDO scaffolds seeded with ASCs with collection of specimens over a finer time course (days 1, 3, 5, 7, 10, 15, 20 and 30) from cells in control and osteogenic media. This would permit a better assessment of the expression levels of genes typified of early to late osteoblastogenesis. Changes in gene expression with time could be followed with the genes products of Runx2, alkaline phosphatase, osteopontin, osterix, osteonectin, and osteocalcin to assess the rate and extent of osteoblastogenesis, to determine any difference as compared to the different scaffold material types, and to compare with other stem cell types, such as BM-MSCs or iPS cells. Lastly, while our studies focused on osteoblastogenesis, the ability of electrospun fibrinogen to support the differentiation of ASCs to adipocytes, chondrocytes, myocytes, and neurons would be another worthwhile avenue of exploration.

Electrospun Adipose Tissue Extracellular Matrix

The derivation of an ECM from adipose tissue (At-ECM) that can be electrospun may hold immense promise for future development. It is conceivable that such ECM would be an excellent substrate for the culture of ESC or induced pluripotent (iPS) stem cells, which currently require either mouse feeder cells or Matrigel® to successfully sustain an undifferentiated state in

culture. Should adipose tissue be able to support pluripotency of stem cell, it would be a significant breakthrough for 1) removing possible xenogenic contamination from mouse-derived feeder or ECM contributions, and 2) possibly leading to an autologous matrix material for one day deriving autologous iPS cells that will speed clinical development and translation for iPS technologies.

We showed here for the first time that At-ECM can be electrospun into a scaffold retaining large amounts of collagen type I and basement membrane components (collagen type IV, elastic fibers, and glycosaminoglycan-based ECM), while further supporting human ASCs. Interestingly, the amount of VVG staining for proteoglycans, glycosaminoglycans, and glycoproteins was extensive on electrospun At-ECM. This result may have been expected as these ECM materials are found tightly bound through covalent cross-linking in connective tissue ECM and are ECM components also found in fat shown to integrate in electrospun At-ECM.

Characterization of the At-ECM extracted, however, remains incomplete. Western blot analysis on At-ECM as compared to Matrigel and to purified matrix standards of collagens I-XII, laminin and fibronectin and potentially other ECM components likely present in At-ECM is required to better characterize the material composition of adipose tissue ECM. Alternatively, MALDI-TOF mass-spec would be another highly useful, perhaps superior tool to determine the fat ECM composition both after extraction and post-electrospinning. As the electrospinning process likely recombines the various ECM polymers in a unique fashion, it may prove informative to assay both At-ECM and fibrinogen both pre- and post-electrospinning to characterize their composition, as well as testing for the availability of various cell and integrin

binding sites present on native ECM that may or may not be presented on other electrospun analogues.

While we showed cell attachment to electrospun At-ECM and At-ECM:PDO, additional studies may prove highly informative and valuable for further supporting the significance of this material in basic research and for therapeutic purposes. For instance, we could determine proliferation of ASCs on these scaffolds (PCNA, Ki67), assessing differentiation potential and the immunophenotype of ASCs cultured on this material, determine the immunophenotype of ASCs cultured on electrospun At-ECM as compared to tissue culture plastic, and assess the immune response of electrospun At-ECM with *in vivo* animal models

SUMMARY

In summary, we show that ASCs can be isolated in a traditional and expedited manner, and they differentiate into fat, cartilage, and bone and are nearly indistinguishable from BMSCs with respect to these important, established stem cell markers. We show that immunophenotype alone is not sufficient to identify MSCs from fibroblast. We further show ASCs can grow into electrospun scaffolds of fibrinogen and a fibrinogen:PDO blend, while further supporting osteogenic differentiation, as determined by mineral, nucleic acid and protein analyses. Also we have engineered the derivation of an entirely novel material for tissue engineering purpose in electrospun adipose tissue ECM, which was found to be largely composed of collagen type I and basement membrane components (collagen type IV, elastic fibers, and glycosaminoglycans), and also capable of supporting adipose stem cells. The data generated in these studies provides the

framework and working model for combining both potentially autologous stem cells and biomimetic extracellular matrices from patient-derivable sources, with future clinical applications including, yet not limited to, the repair, replacement, and regeneration of bone.

Literature Cited

Abberton KM, Bortolotto SK, Woods AA, Findlay M, Morrison WA, Thompson EW, Messina A. Myogel, a novel, basement membrane-rich, extracellular matrix derived from skeletal muscle, is highly adipogenic in vivo and in vitro. Cells Tissues Organs. 2008;188(4):347-58. Epub 2008 Mar 20.

Achyuthan K E, Mary A, Greenberg C S 1988 The Binding Sites on Fibrin(ogen) for Guinea Pig Liver Transglutaminase Are Similar to Those of Blood Coagulation Factor XIII *The Journal of Biological Chemistry* 263 14296-14301.

Adams JC, Watt FM. 1993; Regulation of development and differentiation by the extracellular-matrix. Development 117(4): 1183–1198.

Ahmed TA, Dare EV, Hincke M. Fibrin: a versatile scaffold for tissue engineering applications. Tissue Eng Part B Rev. 2008 Jun;14(2):199-215.

Arai, F., Hirao, A., Ohmura, M., Sato, H., Matsuoka, S., Takubo, K., Ito, K., Koh, G. Y. and Suda, T. (2004). Tie2/angiopoietin-1 signaling regulates hematopoietic stem cell quiescence in the bone marrow niche. Cell 118, 149-161.

Arinzeh TL, Peter SJ, Archambault MP, van den Bos C, Gordon S, Kraus K, Smith A, Kadiyala S. 2003. Allogeneic mesenchymal stem cells regenerate bone in a critical-sized canine segmental defect. J Bone Joint Surg 85-A:1927–1935.

Arthur A, Zannettino A, Gronthos S. The therapeutic applications of multipotential mesenchymal/stromal stem cells in skeletal tissue repair. J Cell Physiol. 2009 Feb;218(2):237-45.

Badami AS, Kreke MR, Thompson MS, Riffle JS, Goldstein AS. Effect of fiber diameter on spreading, proliferation, and differentiation of osteoblastic cells on electrospun poly(lactic acid) substrates. Biomaterials. 2006 Feb;27(4):596-606. Epub 2005 Jul 15.

Badylak, S.F., *Modification of natural polymers: Collagen*, in *Methods of TissueEngineering*, A. Atala and R. Lanza, Editors. 2002, Academic Press: San Diego, CA. p. 505-514.

Baer PC, Schubert R, Bereiter-Hahn J, Plösser M, Geiger H. Expression of a functional epidermal growth factor receptor on human adipose-derived mesenchymal stem cells and its signaling mechanism. Eur J Cell Biol. 2009 May;88(5):273-83.

Baker BM, Gee AO, Metter RB, Nathan AS, Marklein RA, Burdick JA, Mauck RL. The potential to improve cell infiltration in composite fiber-aligned electrospun scaffolds by the selective removal of sacrificial fibers. Biomaterials. 2008 May;29(15):2348-58.

Barnes, C.P. *Feasibility study of electrospun collagen type III*. In *8th Annual Meeting of Tissue Engineering Society International*. 2005. Shanghai, China.

Barnes C P, Pemble C W, Brand D D, Simpson D G, Bowlin G L 2007 Cross-Linking Electrospun Type II Collagen Tissue Engineering Scaffolds with Carbodiimide in Ethanol *Tissue Engineering* 13 1593-1605.

Barnes CP, Sell SA, Boland ED, Simpson DG, Bowlin GL. Nanofiber technology: designing the next generation of tissue engineering scaffolds. Adv Drug Deliv Rev. 2007 Dec 10;59(14):1413-33. Epub 2007 Aug 25. Review.

Becker AJ, McCulloch EA, Till JE (1963). Cytological demonstration of the clonal nature of spleen colonies derived from transplanted mouse marrow cells. Nature 197: 452–4.

Bielby R, Jones E, McGonagle D. 2007. The role of mesenchymal stem cells in maintenance and repair of bone. Injury 38:S26–S32.
Bissell MJ, Barcellos-Hoff MH. The influence of extracellular matrix on gene expression: Is structure the message? J Cell Sci Suppl 1987;8:327–343.
Boland ED, Coleman BD, Barnes CP, Simpson DG, Wnek GE, Bowlin GL. Electrospinning polydioxanone for biomedical applications. Acta Biomater. 2005 Jan;1(1):115-23.
Boquest AC, Shahdadfar A, Frønsdal K, Sigurjonsson O, Tunheim SH, Collas P, Brinchmann JE. Isolation and transcription profiling of purified uncultured human stromal stem cells: alteration of gene expression after in vitro cell culture. Mol Biol Cell. 2005 Mar;16(3):1131-41. Epub 2005 Jan 5.
Campbell A, Wicha MS, Long M. Extracellular matrix promotes the growth and differentiation of murine hematopoietic cells in vitro. J Clin Invest 1985;75:2085–2090.
Carlisle CR, Coulais C, Namboothiry M, Carroll DL, Hantgan RR, Guthold M. The mechanical properties of individual, electrospun fibrinogen fibers. Biomaterials. 2009 Feb;30(6):1205-13. Epub 2008 Dec 6.
Chamberlain G, Fox J, Ashton B, Middleton J. Concise review: mesenchymal stem cells: their phenotype, differentiation capacity, immunological features, and potential for homing. Stem Cells. 2007 Nov;25(11):2739-49. Epub 2007 Jul 26. Review.
Chan CK, Liao S, Li B, Lareu RR, Larrick JW, Ramakrishna S, Raghunath M. Early adhesive behavior of bone-marrow-derived mesenchymal stem cells on collagen electrospun fibers. Biomed Mater. 2009 Jun;4(3):35006. Epub 2009 May 14.
Chen CS, Mrksich M, Huang S, et al. 1997; Geometric control of cell life and death. Science 276(5317): 1425–1428.
Choi JS, Yang HJ, Kim BS, Kim JD, Lee SH, Lee EK, Park K, Cho YW, Lee HY. Fabrication of Porous Extracellular Matrix (ECM) Scaffolds from Human Adipose Tissue. Tissue Eng Part C Methods. 2009 Jul 14. [Epub ahead of print]
Choi JS, Yang HJ, Kim BS, Kim JD, Kim JY, Yoo B, Park K, Lee HY, Cho YW. Human extracellular matrix (ECM) powders for injectable cell delivery and adipose tissue engineering. J Control Release. 2009 Oct 1;139(1):2-7. Epub 2009 May 28.
Clarke JD, Jayasinghe SN. Bio-electrosprayed multicellular zebrafish embryos are viable and develop normally. Biomed Mater. 2008 Mar;3(1):11001. Epub 2008 Feb 6.
Collet JP, Park D, Lesty C, Soria J, Soria C, Montalescot G, Weisel JW. Influence of fibrin network conformation and fibrin fiber diameter on fibrinolysis speed: dynamic and structural approaches by confocal microscopy. Arterioscler Thromb Vasc Biol. 2000 May;20(5):1354-61.
Crawford BJ, Burke RD. TEM and SEM methods. Methods Cell Biol. 2004;74:411-41.
Crisan M, Yap S, Casteilla L, Chen CW, Corselli M, Park TS, Andriolo G, Sun B, Zheng B, Zhang L, Norotte C, Teng PN, Traas J, Schugar R, Deasy BM, Badylak S, Buhring HJ, Giacobino JP, Lazzari L, Huard J, Péault B. A perivascular origin for mesenchymal stem cells in multiple human organs. Cell Stem Cell. 2008 Sep 11;3(3):301-13
Daley WP, Peters SB, Larsen M. Extracellular matrix dynamics in development and regenerative medicine. J Cell Sci. 2008 Feb 1;121(Pt 3):255-64. Review
Dellatore SM, Garcia AS, Miller WM. Mimicking stem cell niches to increase stem cell expansion. Curr Opin Biotechnol. 2008 Oct;19(5):534-40. Epub 2008 Sep 8. Review.

Dickneite G, Metzner H J, Kroez M, Hein B, Nicolay U 2002 The Importance of Factor XIII as a Component of Fibrin Sealants *Journal of Surgical Research* 107 186-195.

Dimri GP, Lee X, Basile G, Acosta M, Scott G, Roskelley C, Medrano EE, Linskens M, Rubelj I, Pereira-Smith O. "A biomarker that identifies senescent human cells in culture and in aging skin in vivo". Proc. Natl. Acad. Sci. U.S.A.1995. 92 (20): 9363–7.

DiPersio CM, Jackson DA, Zaret KS. The extracellular matrix coordinately modulates liver transcription factors and hepatocyte morphology. Mol Cell Biol 1991;11:4405–4414.

Dominici M, Le Blanc K, Mueller I, Slaper-Cortenbach I, Marini F, Krause D, Deans R, Keating A, Prockop Dj, Horwitz E. Minimal criteria for defining multipotent mesenchymal stromal cells. The International Society for Cellular Therapy position statement. Cytotherapy. 2006;8(4):315-7.

Ekaputra AK, Zhou Y, Cool S, Hutmacher DW. Composite electrospun scaffolds for engineering tubular bone grafts. Tissue Eng Part A. 2009 Jun 15. [Epub ahead of print]

Exposito JY, Cluzel C, Garrone R, Lethias C. 2002. Evolution of collagens. Anat. Rec. 268:302–16

Flaim CJ, Chien S, Bhatia SN. An extracellular matrix microarray for probing cellular differentiation. Nat Methods 2005;2:119 –125.

Flanagan, L. A., Rebaza, L. M., Derzic, S., Schwartz, P. H. and Monuki, E. S. (2006). Regulation of human neural precursor cells by laminin and integrins. J. Neurosci. Res. 83, 845-856.

Francis MP, Sachs PC, Elmore LW, Holt SE. Isolating adipose-derived mesenchymal stem cells from lipoaspirate blood and saline fraction. Organogenesis. 2010 Jan;6(1):10-14.

Friedenstein AJ, Deriglasova UF, Kulagina NN, Panasuk AF, Rudakowa SF, Luria EA, Ruadkow IA (1974). "Precursors for fibroblasts in different populations of hematopoietic cells as detected by the in vitro colony assay method". Exp Hematol 2 (2): 83–92.

Friedenstein AJ, Gorskaja JF, Kulagina NN (1976). "Fibroblast precursors in normal and radiated mouse hematopoietic organs". Exp Hematol 4 (5): 267–74.

Geach TJ, Mongkoldhumrongkul N, Zimmerman LB, Jayasinghe SN. Bio-electrospraying living Xenopus tropicalis embryos: investigating the structural, functional and biological integrity of a model organism. Analyst. 2009 Apr;134(4):743-7. Epub 2009 Jan 23.

Giannini G, Valbonesi M, Tel A et al. Use of autologous fibrin platelet glue and bone fragments in maxillofacial surgery. Transfus Apheresis Sci 2004; 30: 139–144.

Gilbert TW, Sellaro TL, Badylak SF. Decellularization of tissues and organs. Biomaterials. 2006 Jul;27(19):3675-83. Epub 2006 Mar 7.

Gimble JM, Katz AJ, Bunnell BA. Adipose-derived stem cells for regenerative medicine. Circ Res. 2007 May 11;100(9):1249-60. Review.

Gupta D, Venugopal J, Mitra S, Giri Dev VR, Ramakrishna S. Nanostructured biocomposite substrates by electrospinning and electrospraying for the mineralization of osteoblasts. Biomaterials. 2009 Apr;30(11):2085-94. Epub 2009 Jan 23.

Gupta, P., Oegema, T. R., Jr, Brazil, J. J., Dudek, A. Z., Slungaard, A. and Verfaillie, C. M. (1998). Structurally specific heparan sulfates support primitive human hematopoiesis by formation of a multimolecular stem cell niche. Blood 92, 4641-4651.

Haaralson MA, Hassell JR. Extracellular Matrix: A Practica Approach. Oxford University IRL Press Inc., New York, 1995.

Hall RP, Ogilvie CM, Aarons E, Jayasinghe SN. Genetic, genomic and physiological state studies on single-needle bio-electrosprayed human cells. Analyst. 2008 Oct;133(10):1347-51. Epub 2008 Jul 2.

Han B, Schwab IR, Madsen TK et al. A fibrin-based bioengineered ocular surface with human corneal epithelial stem cells. Cornea 2002; 21: 505–510.

Haylock DN, Nilsson SK. Stem cell regulation by the hematopoietic stem cell niche. Cell Cycle 2005;4:1353–1355.

Hofmann A, Ritz U, Hessmann MH, Schmid C, Tresch A, Rompe JD, Meurer A, Rommens PM. Cell viability, osteoblast differentiation, and gene expression are altered in human osteoblasts from hypertrophic fracture non-unions. Bone. 2008 May;42(5):894-906. Epub 2008 Feb 9

Hoogduijn MJ, Crop MJ, Peeters AM, Van Osch GJ, Balk AH, Ijzermans JN, Weimar W, Baan CC. Human heart, spleen, and perirenal fat-derived mesenchymal stem cells have immunomodulatory capacities. Stem Cells Dev. 2007 Aug;16(4):597-604.

Horwitz EM. 2001. Marrow mesenchymal cell transplantation for genetic disorders of bone. Cytotherapy 3:399–401.

Horwitz EM, Prockop DJ, Fitzpatrick LA, Koo WW, Gordon PL, Neel M, Sussman M, Orchard P, Marx JC, Pyeritz RE, Brenner MK. 1999. Transplantability and therapeutic effects of bone marrow-derived mesenchymal cells in children with osteogenesis imperfecta. Nat Med 5:309–313.

Horwitz EM, Prockop DJ, Gordon PL, Koo WW,Fitzpatrick LA, Neel MD, McCarville ME, Orchard PJ, Pyeritz RE, Brenner MK. 2001. Clinical responses to bone marrow transplantation in children with severe osteogenesis imperfecta. Blood 97:1227–1231.

Horwitz EM, Gordon PL, Koo WK, Marx JC, Neel MD, McNall RY, Muul L, Hofmann T. 2002. Isolated allogeneic bone marrow-derived mesenchymal cells engraft and stimulate growth in childrenwith osteogenesis imperfecta: Implications for cell therapy of bone. Proc Natl Acad Sci USA 99:8932–8937.

Hutter H, Vogel BE, Plenefisch JD, Norris CR, Proenca RB, et al. 2000. Conservation and novelty in the evolution of cell adhesion and extracellular matrix genes. Science 287:989–94

Ikuyo Nakajima, Takahiro Yamaguchi, Kyouhei Ozutsumi, Hisashi Aso. Adipose tissue extracellular matrix:newly organized by adipocytes during differentiation. Differentiation (1998) 63:193–200.

Izadpanah R, Trygg C, Patel B, Kriedt C, Dufour J, Gimble JM, Bunnell BA. Biologic properties of mesenchymal stem cells derived from bone marrow and adipose tissue. J Cell Biochem. 2006 Dec 1;99(5):1285-97.

Jayakrishnan, A. and S.R. Jameela, *Glutaraldehyde as a fixative in bioprostheses and drug delivery matrices.* Biomaterials, 1996. 17(5): p. 471-484.

Jayakrishnan A, Jameela S R 1996 Glutaraldehyde as a fixative in bioprostheses and drug delivery matrices *Biomaterials* 17 471.

Jensen, U. B., Lowell, S. and Watt, F. M. (1999). The spatial relationship between stem cells and their progeny in the basal layer of human epidermis: a new view based on whole-mount labelling and lineage analysis. Development 126, 2409-2418.

Kanczler JM, Oreffo RO. 2008. Osteogenesis and angiogenesis: The potential for engineering

bone. Eur Cells Mater 15:100–114.
Katz AJ, Tholpady A, Tholpady SS, Shang H, Ogle RC. Cell surface and transcriptional characterization of human adipose-derived adherent stromal (hADAS) cells. Stem Cells. 2005 Mar;23(3):412-23.
Kern S, Eichler H, Stoeve J, Klüter H, Bieback K. Comparative analysis of mesenchymal stem cells from bone marrow, umbilical cord blood, or adipose tissue. Stem Cells. 2006 May;24(5):1294-301. Epub 2006 Jan 12.
Khan Y, Yaszemski MJ, Mikos AG, Laurencin CT. Tissue engineering of bone: material and matrix considerations. J Bone Joint Surg Am. 2008 Feb;90 Suppl 1:36-42.
Khor E. Methods for the treatment of collagenous tissues for bioprostheses. Biomaterials. 1997 Jan;18(2):95-105. Review.
Kihara T, Hirose M, Oshima A et al. Exogenous type I collagen facilitates osteogenic differentiation and acts as a substrate for mineralization of rat marrow mesenchymal stem cells in vitro. Biochem Biophys Res Commun 2006;341:1029 –1035.
Kim HW, Yu HS, Lee HH. Nanofibrous matrices of poly(lactic acid) and gelatin polymeric blends for the improvement of cellular responses. J Biomed Mater Res A. 2008 Oct;87(1):25-32.
Klees, R. F., Salasznyk, R. M., Kingsley, K., Williams, W. A., Boskey, A. and Plopper, G. E. (2005). Laminin-5 induces osteogenic gene expression in human mesenchymal stem cells through an ERK-dependent pathway. Mol. Biol. Cell 16, 881-890.
Kon E, Muraglia A, Corsi A, Bianco P, Marcacci M, Martin I, Boyde A, Ruspantini I, Chistolini P, Rocca M, Giardino R,Cancedda R, Quarto R. 2000. Autologous bone marrow stromal cells loaded onto porous hydroxyapatite ceramic accelerate bone repair in critical-size defects of sheep long bones. J Biomed Mater Res 49:328–337.
Koob, T.J., *Collagen fixation*, in *Encyclopedia of Biomaterials and Biomedical Engineering*, G.E. Wnek and G.L. Bowlin, Editors. 2004, Marcel Dekker: New York. p. 335-347.
Kramer JM. Basement membranes. WormBook. 2005 Sep 1:1-15. Review.
Langer R, Vacanti JP. Tissue engineering. Science. 1993 May 14;260(5110):920-6. Review
Langer RS, Vacanti JP. Tissue engineering: the challenges ahead. Sci Am. 1999 Apr;280(4):86-9.
Lapidot, T., Dar, A. and Kollet, O. (2005). How do stem cells find their way home? Blood 106, 1901-1910.
Lee JJ, Yu HS, Hong SJ, Jeong I, Jang JH, Kim HW. Nanofibrous membrane of collagen–polycaprolactone for cell growth and tissue regeneration J Mater Sci: Mater Med (2009) 20:1927–1935.
Lendeckel S, Jödicke A, Christophis P, Heidinger K, Wolff J, Fraser JK, Hedrick MH, Berthold L, Howaldt HP. Autologous stem cells (adipose) and fibrin glue used to treat widespread traumatic calvarial defects: case report. J Craniomaxillofac Surg. 2004 Dec;32(6):370-3.
Leone, D. P., Relvas, J. B., Campos, L. S., Hemmi, S., Brakebusch, C., Fassler, R., French-Constant, C. and Suter, U. (2005). Regulation of neural progenitor proliferation and survival by beta1 integrins. J. Cell Sci. 118, 2589-2599.
Li C, Vepari C, Jin H-, Kimand H J and Kaplan D Electrospun silk-BMP-2 scaffolds for bone tissue engineering. Biomaterials 2006 27 3115–24.

Li WJ, Cooper JA Jr, Mauck RL, Tuan RS. Fabrication and characterization of six electrospun poly(alpha-hydroxy ester)-based fibrous scaffolds for tissue engineering applications. Acta Biomater. 2006 Jul;2(4):377-85. Epub 2006 May 6.

Liebschner and Wettergreen. Optimization of Bone Scaffold Engineering for Load Bearing Applications. Topics in Tissue Engineering 2003.

Lin K, Matsubara Y, Masuda Y, Togashi K, Ohno T, Tamura T, Toyoshima Y, Sugimachi K, Toyoda M, Marc H, Douglas A. Characterization of adipose tissue-derived cells isolated with the Celution system. Cytotherapy. 2008;10(4):417-26.

Liu G, Zhao L, Zhang W, Cui L, Liu W,Cao Y. 2008a. Repair of goat tibial defects with bone marrow stromal cells and beta-tricalcium phosphate. J Mater Sci Mater Med 19:2367–2376.

Lozito TP, Kuo CK, Taboas JM, Tuan RS. Human mesenchymal stem cells express vascular cell phenotypes upon interaction with endothelial cell matrix. J Cell Biochem. 2009 Jul 1;107(4):714-22.

Lozito TP, Taboas JM, Kuo CK, Tuan RS. Mesenchymal stem cell modification of endothelial matrix regulates their vascular differentiation. J Cell Biochem. 2009 Jul 1;107(4):706-13.

Lorenz K, Sicker M, Schmelzer E, Rupf T, Salvetter J, Schulz-Siegmund M, Bader A. Multilineage differentiation potential of human dermal skin-derived fibroblasts. Exp Dermatol. 2008 Nov;17(11):925-32. Epub 2008 Jun 14.

Lozito TP, Taboas JM, Kuo CK, Tuan RS. Mesenchymal stem cell modification of endothelial matrix regulates their vascular differentiation. J Cell Biochem. 2009 Jul 1;107(4):706-13.

Lutolf MP, Hubbell JA. Synthetic biomaterials as instructive extracellular microenvironments for morphogenesis in tissue engineering. Nat Biotechnol. 2005 Jan;23(1):47-55. Review.

Madurantakam PA, Rodriguez IA, Cost CP, Viswanathan R, Simpson DG, Beckman MJ, Moon PC, Bowlin GL. Multiple factor interactions in biomimetic mineralization of electrospun scaffolds. Biomaterials. 2009 Oct;30(29):5456-64.

Maeng YJ, Choi SW, Kim HO, Kim JH. Culture of human mesenchymal stem cells using electrosprayed porous chitosan microbeads. J Biomed Mater Res A. 2009 Mar 11. [Epub ahead of print].

Martin GR, Timpl R. Laminin and other basement membrane components. Annu Rev Cell Biol. 1987;3:57-85. Review.

Mastrogiacomo M, Corsi A, Francioso E, Di Comite M, Monetti F, Scaglione S, Favia A,
Crovace A, Bianco P, Cancedda R. 2006. Reconstruction of extensive long bone defects in sheep using resorbable bioceramics based on silicon stabilized tricalcium phosphate.Tissue Eng 12:1261–1273.

Matthews JA, Wnek GE, Simpson DG, Bowlin GL. Electrospinning of collagen nanofibers. Biomacromolecules. 2002 Mar-Apr;3(2):232-8

Mavis B, Demirtaş TT, Gümüşderelioğlu M, Gündüz G, Colak U. Synthesis, characterization and osteoblastic activity of polycaprolactone nanofibers coated with biomimetic calcium phosphate Acta Biomaterialia 5 (2009) 3098–3111.

McBeath, R., Pirone, D. M., Nelson, C. M., Bhadriraju, K. and Chen, C. S. (2004). Cell shape, cytoskeletal tension, and RhoA regulate stem cell lineage commitment. Dev. Cell 6, 483-495.

McClure M J, Sell S A, Barnes C P, Bowen W C, Bowlin G L 2007 Cross-linking Electrospun Polydioxanone-Soluble Elastin Blends: Material Characterization *Journal of Engineered Fibers and Fabrics* In Press.

McCullen SD, Zhu Y, Bernacki SH, Narayan RJ, Pourdeyhimi B, Gorga RE, Loboa EG. Electrospun composite poly(L-lactic acid)/tricalcium phosphate scaffolds induce proliferation and osteogenic differentiation of human adipose-derived stem cells. Biomed Mater. 2009 Jun;4(3):35002. Epub 2009 Apr 24.

McManus M, Boland E, Sell S, Bowen W, Koo H, Simpson D, et al. 2007 Electrospun nanofibre fibrinogen for urinary tract tissue reconstruction *Biomedical Materials* In Press.

McManus M C, Boland ED, Koo HP, Barnes CP, Pawlowski KJ, Wnek GE, Simpson DG, Bowlin GL 2006 Mechanical properties of electrospun fibrinogen structures *Acta Biomater* 2 19-28.

McManus MC, Boland ED, Simpson DG, Barnes CP, Bowlin GL. Electrospun fibrinogen: feasibility as a tissue engineering scaffold in a rat cell culture model. J Biomed Mater Res A. 2007 May;81(2):299-309.

McManus M C, Sell S A, Bowen W C, Koo H P, Bowlin G L 2007 Electrospun Fibrinogen-Polydioxanone Composite Matrix: Potential for In Situ Urologic Tissue Engineering *Journal of Engineered Fibers and Fabrics* In Press .

Meane A, Iglesias J, Del Rio M et al. Large surface of cultured human epithelial obtained in a dermal matrix based on live fibroblast-containing fibrin gels. Burns 1998; 24: 621–630.

Meng X, Ichim TE, Zhong J, Rogers A, Yin Z, Jackson J, Wang H, Ge W, Bogin V, Chan KW, Thébaud B, Riordan NH. Endometrial regenerative cells: a novel stem cell population. J Transl Med. 2007 Nov 15; 5:57.

Menicanin D, Bartold M, Shi S, Gronthos S. 2007. Stem cells in dental structural regeneration. J Stomatol Investig 1:3–13.

Miner JH, Yurchenco PD. Laminin functions in tissue morphogenesis. Annu Rev Cell Dev Biol. 2004;20:255-84.

Moen JL, Gorkun OV, Weisel JW, Lord ST. Recombinant BbetaArg14His fibrinogen implies participation of N-terminus of Bbeta chain in desA fibrin polymerization. Blood. 2003 Oct 1;102(7):2466-71. Epub 2003 Jun 12.

Molea, G., et al., Comparative study on biocompatibility and absorption times of three absorbable monofilament suture materials (Polydioxanone, Poliglecaprone 25, Glycomer 631). British Journal of Plastic Surgery, 2000. 53(2): p. 137-141.

Mongkoldhumrongkul N, Best S, Aarons E, Jayasinghe SN. Bio-electrospraying whole human blood: analysing cellular viability at a molecular level. J Tissue Eng Regen Med. 2009 Jun 25. [Epub ahead of print].

Moore, K. A. and Lemischka, I. R. (2006). Stem cells and their niches. Science 311, 1880-1885.

Mosesson MW. Fibrinogen and fibrin structure and functions. J Thromb Haemost. 2005 Aug;3(8):1894-904. Review.

Mosesson M W, Siebenlist K R 1995 The Covalent Structure of Factor XIIIa Crosslinked Fibrinogen Fibrils *Journal of Structural Biology* 115 88-101.

Muneoka K, Han M, Gardiner DM. Regrowing human limbs. Sci Am. 2008 Apr;298(4):56-63.

Naugle JE, Olson ER, Zhang X et al. Type VI collagen induces cardiac myofibroblast differentiation: Implications for postinfarction remodeling. Am J Physiol Heart Circ Physiol 2006;290:H323–H330.

Nilsson, S. K., Johnston, H. M., Whitty, G. A., Williams, B., Webb, R. J., Denhardt, D. T., Bertoncello, I., Bendall, L. J., Simmons, P. J. and Haylock, D. N. (2005). Osteopontin, a key component of the hematopoietic stem cell niche and regulator of primitive hematopoietic progenitor cells. Blood 106, 1232-1239.

Nakajima I, Yamaguchi T., Ozutsumi K., Aso H. Adipose tissue extracellular matrix: newly organized by adipocytes during differentiation. (1998). Differentiation Volume 63 Issue 4, Pages 193 – 200.

Nakajima I., Muroya S., Tanabe R. and Chikuni K. Extracellular matrix development during differentiation into adipocytes with a unique increase in type V and VI collagen. Biology of the Cell (2002) 94, (197–203).

Noël D, Caton D, Roche S, Bony C, Lehmann S, Casteilla L, Jorgensen C, Cousin B. Cell specific differences between human adipose-derived and mesenchymal-stromal cells despite similar differentiation potentials. Exp Cell Res. 2008 Apr 15;314(7):1575-84. Epub 2008 Jan 12.

Nussbaum J, Minami E, Laflamme MA, Virag JA, Ware CB, Masino A, Muskheli V, Pabon L, Reinecke H, Murry CE. Transplantation of undifferentiated murine embryonic stem cells in the heart: teratoma formation and immune response. FASEB J. 2007 May;21(7):1345-57. Epub 2007 Feb 6.

Olde Damink L H H, Dijkstra P J, van Luyn M J A, van Wachem P B, Nieuwenhuis P, Feijen J 1996 Cross-linking of dermal sheep collagen using a water-soluble carbodiimide *Biomaterials* 17 765-773.

Palsson, B.O., and Sangeeta N. Bhatia, *Tissue Engineering*. 2004, Upper Sadle River, New Jersey: Pearson Prentice Hall.

Pittenger MF, Mackay AM, Beck SC, Jaiswal RK, Douglas R, Mosca JD, Moorman MA, Simonetti DW, Craig S, Marshak DR. Multilineage potential of adult human mesenchymal stem cells. Science. 1999 Apr 2;284(5411):143-7.

Powell M. and Segal D.David. In New York, a Grisly Traffic in Body Parts Illegal Sales Worry Dead's Kin, Tissue Recipients. Washington Post Staff Writers. Saturday, January 28, 2006; Page A03.

Prabhakaran MP, Venugopal J, Ramakrishna S. Electrospun nanostructured scaffolds for bone tissue engineering. Acta Biomater. 2009 May 15. [Epub ahead of print].

Quarto R, Mastrogiacomo M, Cancedda R, Kutepov SM, Mukhachev V, Lavroukov A, Kon E, Marcacci M. 2001. Repair of large bone defects with the use of autologous bonemarrow stromal cells. N Engl J Med 344:385–386.

Rapraeger, A.C. In *Molecular and cellular aspects of baement membranes* (ed. D.R. Rohrbach and R. Timple), pp. 267-88, Academic Press, San Diego.

Rebelatto CK, Aguiar AM, Moretão MP, Senegaglia AC, Hansen P, Barchiki F, Oliveira J, Martins J, Kuligovski C, Mansur F, Christofis A, Amaral VF, Brofman PS, Goldenberg S, Nakao LS, Correa A. Dissimilar differentiation of mesenchymal stem cells from bone marrow, umbilical cord blood, and adipose tissue. Exp Biol Med (Maywood). 2008 Jul;233(7):901-13. Epub 2008 Apr 29.

Rodriguez AM, Pisani D, Dechesne CA, Turc-Carel C, Kurzenne JY, Wdziekonski B, Villageois A, Bagnis C, Breittmayer JP, Groux H, Ailhaud G, Dani C. Transplantation of a multipotent cell population from human adipose tissue induces dystrophin expression in the immunocompetent mdx mouse. J Exp Med. 2005 May 2;201(9):1397-405.

Salasznyk, R. M., Klees, R. F., Williams, W. A., Boskey, A. and Plopper, G. E. (2007b).

Focal adhesion kinase signaling pathways regulate the osteogenic differentiation of human mesenchymal stem cells. Exp. Cell Res. 313, 22-37.

Scadden, D. T. (2006). The stem-cell niche as an entity of action. Nature 441, 1075-1079.

Schiller PC, D'Ippolito G, Balkan W, et al. 2001; Gap-junctional communication is required for the maturation process of osteoblastic cells in culture. Bone 28(4): 362–369.

Schuger L, Skubitz AP, O'Shea KS, Chang JF, Varani J. Identification of laminin domains involved in branching morphogenesis: effects of anti-laminin monoclonal antibodies on mouse embryonic lung development. Dev Biol. 1991 Aug;146(2):531-41.

Schindeler A, McDonald MM, Bokko P, Little DG. Bone remodeling during fracture repair: The cellular picture. Semin Cell Dev Biol. 2008 Oct;19(5):459-66. Epub 2008 Jul 25.

Sefcik LS, Neal RA, Kaszuba SN, Parker AM, Katz AJ, Ogle RC, Botchwey EA. Collagen nanofibres are a biomimetic substrate for the serum-free osteogenic differentiation of human adipose stem cells. J Tissue Eng Regen Med. 2008 Jun;2(4):210-20.

Sell SA, Francis MP, Garg K, McClure MJ, Simpson DG, Bowlin GL. Cross-linking methods of electrospun fibrinogen scaffolds for tissue engineering applications. Biomed Mater. 2008 Dec;3(4):45001.

Sell S, Barnes C, Simpson D, Bowlin G. Scaffold permeability as a means to determine fiber diameter and pore size of electrospun fibrinogen. J Biomed Mater Res A. 2008 Apr;85(1):115-26.

Shields KJ, Beckman MJ, Bowlin GL, Wayne JS. Mechanical properties and cellular proliferation of electrospun collagen type II. Tissue Eng. 2004 Sep-Oct;10(9-10):1510-7.

Shih YR, Chen CN, Tsai SW, Wang YJ, Lee OK. Growth of mesenchymal stem cells on electrospun type I collagen nanofibers. Stem Cells. 2006 Nov;24(11):2391-7.

Shun-ichi Harada and Gideon A. Rodan. Control of osteoblast function and regulation of bone mass. Nature 423, 349-355.

Siminovitch L, McCulloch EA, Till JE (1963). "The distribution of colony-forming cells among spleen colonies". Journal of Cellular and Comparative Physiology 62: 327–36.

Smith MJ, McClure MJ, Sell SA, Barnes CP, Walpoth BH, Simpson DG, Bowlin GL. Suture-reinforced electrospun polydioxanone-elastin small-diameter tubes for use in vascular tissue engineering: a feasibility study. Acta Biomater. 2008 Jan;4(1):58-66.

Spiegelman BM, Ginty CA. 1983; Fibronectin modulation of cell shape and lipogenic gene expression in 3T3 adipocytes. Cell 35(3): 657–666.

Song E, Yeon Kim S, Chun T, Byun HJ, Lee YM. Collagen scaffolds derived from a marine source and their biocompatibility. Biomaterials. 2006 May;27(15):2951-61.

Stankus JJ, Guan J, Fujimoto K, Wagner WR. Microintegrating smooth muscle cells into a biodegradable, elastomeric fiber matrix. Biomaterials. 2006 Feb;27(5):735-44.

Stankus JJ, Soletti L, Fujimoto K, Hong Y, Vorp DA, Wagner WR. Fabrication of cell microintegrated blood vessel constructs through electrohydrodynamic atomization. Biomaterials. 2007 Jun;28(17):2738-46.

Stier, S., Ko, Y., Forkert, R., Lutz, C., Neuhaus, T., Grunewald, E., Cheng, T., Dombkowski, D., Calvi, L. M., Rittling, S. R. et al. (2005). Osteopontin is a hematopoietic stem cell niche component that negatively regulates stem cell pool size. J. Exp. Med. 201, 1781-1791.

Steigman SA, Ahmed A, Shanti RM, Tuan RS, Valim C, Fauza DO. Sternal repair with bone grafts engineered from amniotic mesenchymal stem cells Journal of Pediatric Surgery (2009) 44, 1120–1126.

Sung H-W, Chang W-H, Ma C-Y, Lee M-H 2003 Crosslinking of biological tissues using genipin and/or carbodiimide *Journal of Biomedical Materials Research Part A* 64 427-438.

Suzuki A, Iwama A, Miyashita H et al. Role for growth factors and extracellular matrix in controlling differentiation of prospectively isolated hepatic stem cells. Development 2003;130:2513–2524.

Tholpady SS, Schlosser R, Spotnitz W, Ogle RC, Lindsey WH. Repair of an osseous facial critical-size defect using augmented fibrin sealant. Laryngoscope. 1999 Oct;109(10):1585-8.

Thomas CH, Collier JH, Sfeir CS, et al. 2002; Proc Natl Acad Sci USA 99(4): 1972–1977.

Tsai C-C, Huang R-N, Sung H-W, Liang H C 2000 *In vitro* evaluation of the genotoxicity of a naturally occurring crosslinking agent (genipin) for biologic tissue fixation *Journal of Biomedical Materials Research* 52 58-65

Valbonesi M. Fibrin glues of human origin. Best Pract Res Clin Haematol. 2006;19(1):191-203. Review

Venugopal J, Low S, Choon AT, Sampath Kumar TS, Ramakrishna S. Mineralization of osteoblasts with electrospun collagen/hydroxyapatite nanofibers. J Mater Sci Mater Med. 2008 May;19(5):2039-46. Epub 2007 Oct 24.

Vlodavski, I., Krner, G., Eldor, A., Bar-Shavit, R., Klagsbrun, M., and Fuks, Z. In *Extracellular matrix: chemistry, biology and pathobiology with emphasis on the liver* (ed. M.A. Zern and L.M. Reid), Marcel Decker, Inc., New York, New York, 1993.

Wainstein, M., J. Anderson, and J.S. Elder, Comparison of effects of suture materials on wound healing in a rabbit pyeloplasty model. Urology, 1997. 49(2): p.261-264.

Wagner W, Wein F, Seckinger A, Frankhauser M, Wirkner U, Krause U, Blake J, Schwager C, Eckstein V, Anso. Comparative characteristics of mesenchymal stem cells from human bone marrow, adipose tissue, and umbilical cord blood. Exp Hematol. 2005 Nov;33(11):1402-16.

Wang M, Crisostomo PR, Herring C, Meldrum KK, Meldrum DR. Human progenitor cells from bone marrow or adipose tissue produce VEGF, HGF, and IGF-I in response to TNF by a p38 MAPK-dependent mechanism. Am J Physiol Regul Integr Comp Physiol. 2006 Oct;291(4):R880-4.

Weissman IL, Anderson DJ, Gage F. Stem and progenitor cells: origins, phenotypes, lineage commitments, and transdifferentiations. Annu Rev Cell Dev Biol. 2001;17:387-403. Review.

Wnek GE, Carr M, Simpson DG, Bowlin GL. Electrospinning of nanofiber fibrinogen structures, Nano. Lett. 3 (2003) 213–216.

Wutticharoenmongkol P, Pavasant P and Supaphol P Osteoblastic phenotype expression of MC3T3-E1 cultured on electrospun polycaprolactone fiber mats filled with hydroxyapatite nanoparticles Biomacromolecules (2007) 8 2602–10.

Yoshimura K, Shigeura T, Matsumoto D, Sato T, Takaki Y, Aiba-Kojima E, Sato K, Inoue K, Nagase T, Koshima I, Gonda K. Characterization of freshly isolated and cultured cells derived from the fatty and fluid portions of liposuction aspirates. 31 J Cell Physiol. 2006 Jul;208(1):64-76.

Zhu, A. J., Haase, I. and Watt, F. M. (1999). Signaling via beta1 integrins and mitogenactivated protein kinase determines human epidermal stem cell fate in vitro. Proc. Natl. Acad. Sci. USA 96, 6728-6733.

Zuk PA, Zhu M, Mizuno H, Huang J, Futrell JW, Katz AJ, Benhaim P, Lorenz HP, Hedrick MH. Multilineage cells from human adipose tissue: implications for cell-based therapies. Tissue Eng. 2001 Apr;7(2):211-28

Zuk PA, Zhu M, Ashjian P, De Ugarte DA, Huang JI, Mizuno H, Alfonso ZC, Fraser JK, Benhaim P, Hedrick MH. Human adipose tissue is a source of multipotent stem cells. Mol Biol Cell. 2002 Dec;13(12):4279-95.

-Appendix A-

Cell Response to Crosslinked vs. Uncrosslinked Fibrinogen

To determine the feasibility of using ASCs and electrospun fibrinogen together as a starting template for tissue engineering mature, biomimetic tissue types, we first need to show that ASCs are 1) adherent, 2) viable long term, 3) able to penetrate the scaffold and 4) able to synthesis natural matrix *de novo* in electrospun fibrinogen (Fg) scaffolds. To test these parameters, approximately 50,000 ASCs were seeded on 10mm discs cut from electrospun fibrinogen or a fibrinogen:elastin 50:50 blend, and cultured for up to 2 weeks. The scaffolds were fixed then paraffin embedded and section for H&E and Masons Trichrome staining at days 7 and 14. Initial tests showed what appeared to be a single cell layer thick confluent sheet of ASCs atop of the electrospun fibrinogen at day 7 and 14 in culture, and with cells only on the periphery of the matrix on a fibrinogen:elastin blended scaffold **(Fig 46)**. However, the ASCs were unable to effectively penetrate the Fg scaffolds, which were genipin cross-linked for enhanced mechanical properties (Sell et al. 2008). Trichrome stains of the genipin cross-linked electrospun fibrinogen scaffolds seeded with ASCs showed few patches of new collagen synthesis with limited penetration into the scaffold up to 14 days in culture **(Fig. 47)**, putting the practice of cross-linking fibrinogen into question if a highly cellularized scaffold was a desired feature of the finished product.

Following these initial observations, we next set out to assess any phenotypic changes at the nanoscale level that cross-linking may impart on electrospun fibrinogen. SEM images of pre- and post-cross-linked fibrinogen treated with the various cross-linkers were acquired to gain

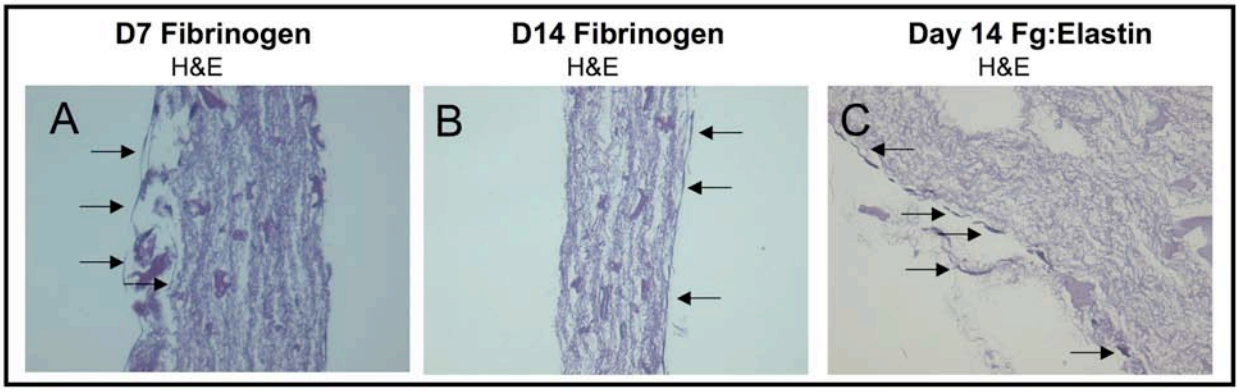

Figure 46. **Cross-linked Fibrinogen Histology**. H&E staining of ASCs seeded upon genipin cross-linked fibrinogen at day 7 (A) and day 14 (B) show viable cells yet limited scaffold penetration (arrows indicated cells). A cross-linked blend of 50:50 elastin:fibrinogen also showed a lack of ASC penetrating the scaffold at day 14 (C).

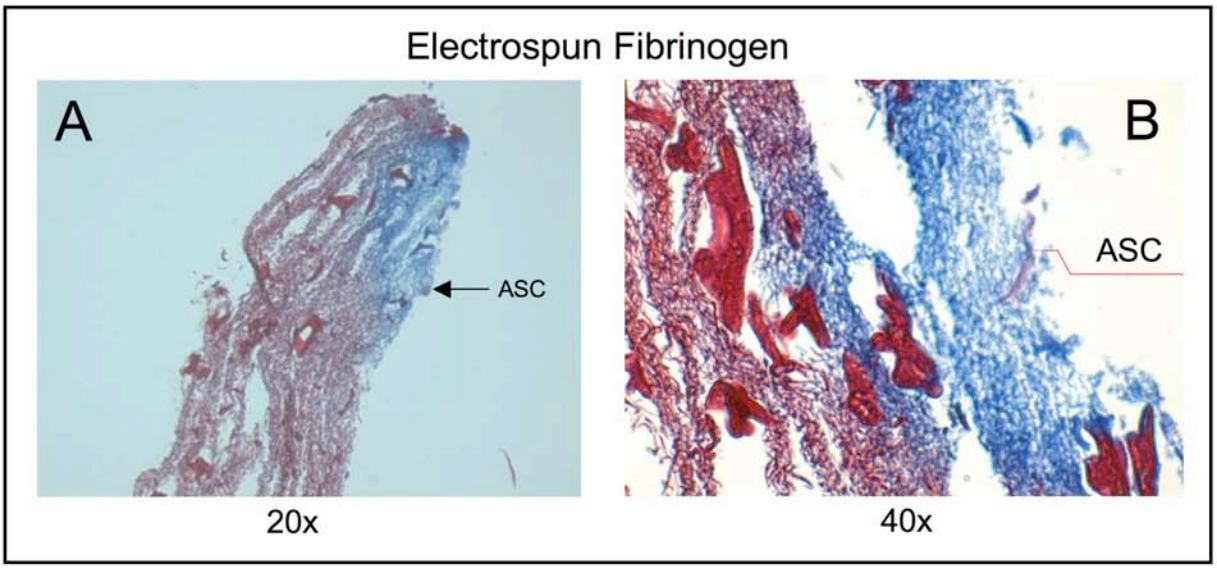

Figure 47. Limited New Collagen Production on Cross-linked Fibrinogen. Masons Trichrome stain of genipin cross-linked fibrinogen at day 14 shows limited new collagen synthesis in only spotted patches near the scaffold exterior at 20x (A) and 40x (B).

insight into any apparent alterations in the scaffold topography and fiber morphology **(Fig. 48)**. Each scaffold was ethanol soaked, dehydrated, then gold sputter coated prior to SEM analysis. The SEM images largely show an apparent extensive fusing of fibers and densification of the scaffolds from the cross-linking processes, as is to be expected with extensive cross-linking.

We next sought to measure any alteration in the scaffold porosity related to cross-linking. Much of total void space was maintained with any type of cross-linking in comparison to uncross-linked scaffolds. However, porosity decreases in control scaffolds that were unfixed or ethanol soaked, and GLUT cross-linking produced a measurable decrease mean scaffold porosity **(Table 10)**. Genipin produced a minimal difference between PBS soaked and dry discs, with minimal densification, while EDCs affect on porosity appeared insignificant.

To determine the cellular activity on cross-linked vs. non-cross-linked fibrinogen scaffolds, SEM analysis was used to provide qualitative information on cell migration across the scaffolds surface and for assessing cell viability on scaffolds with time **(Fig. 49)**. H&E and Trichrome stains show both migration into the scaffolds interior and on its surface, and the extent of new collagen production **(Fig. 50)**. BJ-GFP-hTERT fibroblast were used in these studies as fibroblasts have been the standard reference cell type in such systems, with the GFP-hTERT modified cells selected for easy cell tracking in prospective future experiments and for producing a more stable proliferative cell type. A clear increase in staining intensity is apparent atop all of the cross-linked scaffolds at 21 days of culture vs. 7 days, suggesting the persistence of cells atop of the scaffold **(Fig. 50)**. While cells were only present in spotted areas on the scaffolds at day 7, all scaffolds were highly covered over their surface by day 21, suggesting good migration atop

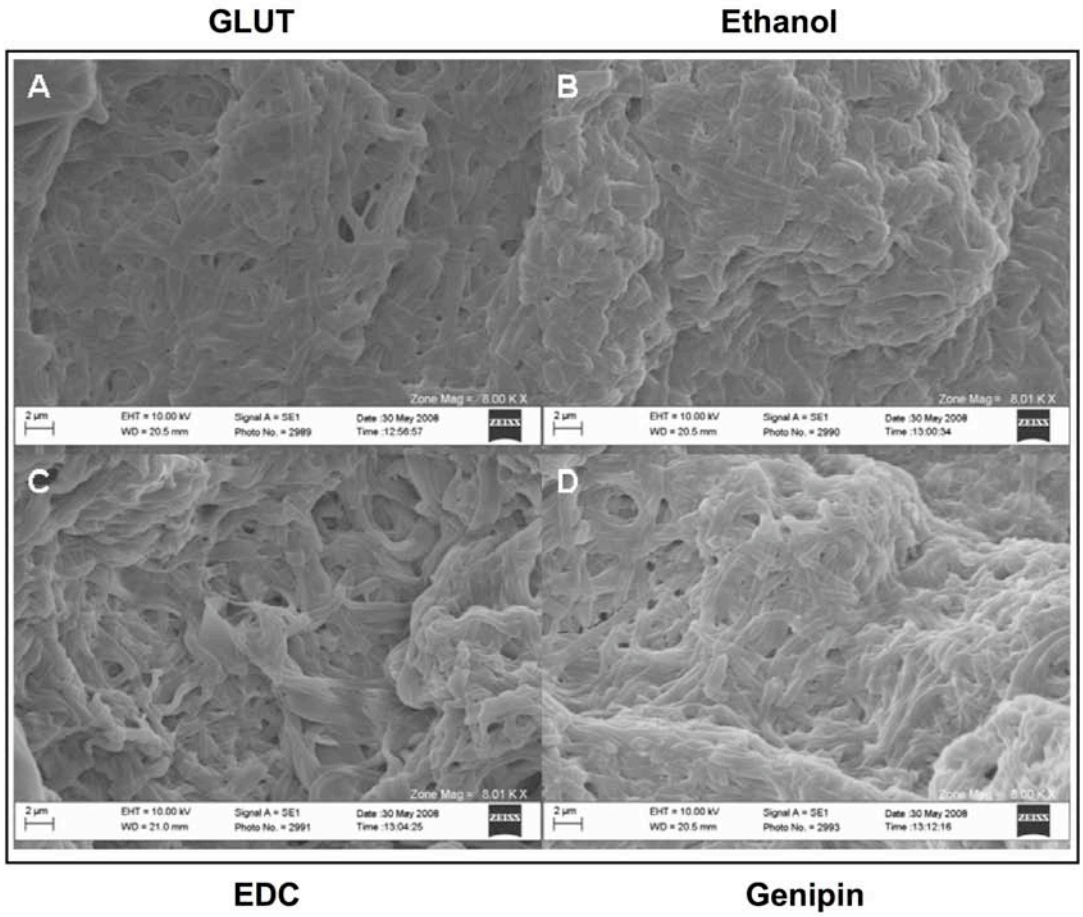

Figure 48. SEM of Fibrinogen Cross-linked by Multiple Methods. Scanning electron micrographs (8000x) of acellular electrospun fibrinogen scaffolds treated with GLUT (A), ethanol (B), EDC (C), and genipin (D) are shown (From Sell et al. 2008).

Table 11: Mean Scaffold Porosities of Cross-Linked Fibrinogen Scaffolds[#].

	Unfixed	Glut	Ethanol	EDC	Genipin
Dry	84±4%	85 ±1%	79 ±3%	84 ±2%	87 ±1%
Ethanol	82±3%	84 ±1%	77 ±4%	79 ±2%	84 ±3%
PBS	66±6%	74 ±1%	64 ±9%	79 ±3%	77 ±4%

[#](adapted from Sell et al. 2008)

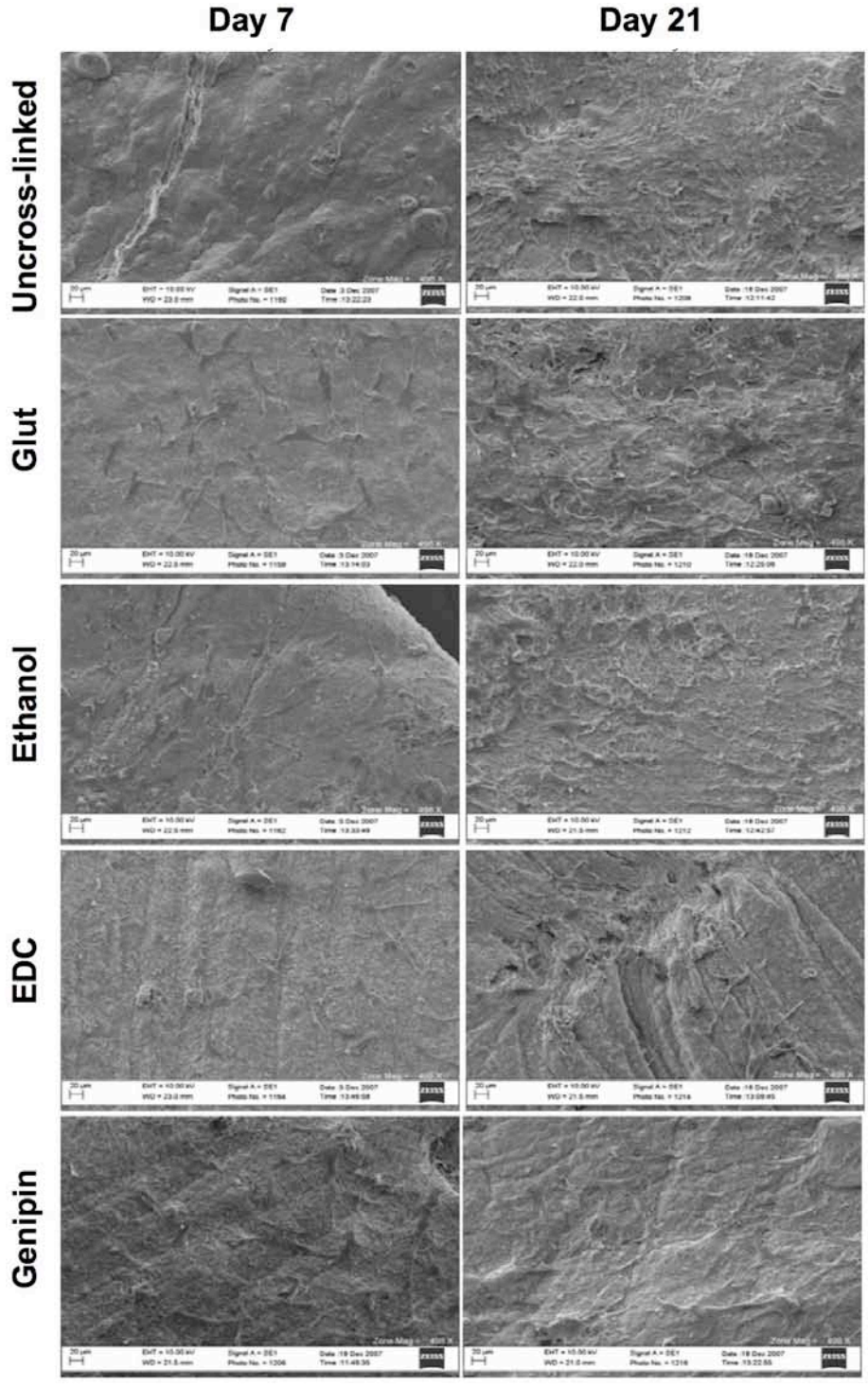

Figure 49. SEM analysis of BJ-GPF-hTERT Fibroblasts Seeded Upon Electrospun Scaffolds. SEM shows the presence of BJs on the scaffold surface with each cross-linking chemical at days 7 and 21 at 498X (from Sell et al. 2008).

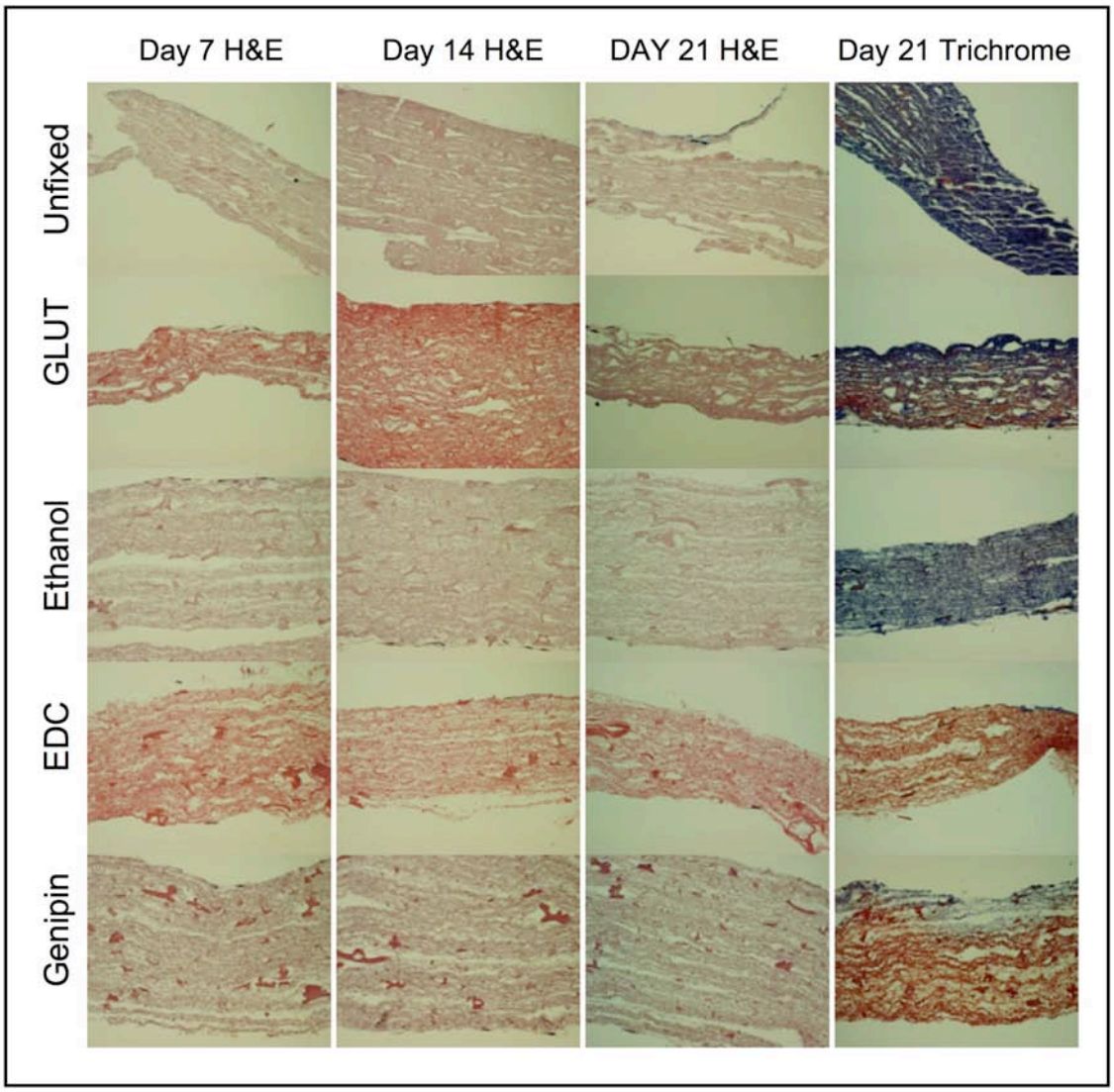

Figure 50. Cross-linked Fibrinogen Histology. H&E and Mason's Trichrome stained cross-linked fibrinogen scaffolds seeded with BJ-hTERT fibroblasts are visualized by optical light microscope at 40x. Trichrome stained samples show fibrinogen in a native red coloration, where new collagen synthesis stains appear blue (Sell et al. 2008).

the cross-linked and the native spun scaffolds. Conversely, cells did not appear to penetrate the scaffold exterior of the cross-linking specimens **(Fig. 50)**. We then followed new collagen production via Trichrome stained samples at 21 days of culture. While control and uncross-linked scaffolds were near completely composed of newly synthesized collagen (blue staining), GLUT cross-linked scaffolds exhibited only a gradual transition to new collagen, with genipin and EDC cross-linked scaffolds exhibiting little new collagen production or matrix remodeling.

Noting the deleterious affects of chemical crosslinking in these studies, we next sought to assess the ability of ASCs to attach, proliferate and migrate upon native, un-cross-linked electrospun fibrinogen. 50,000 ASCs at PD4 or approximately PD25 were seeded on 10mm electrospun fibrinogen scaffolds discs and cultured for 7, 14, 21 and 28 days. The ability for ASCs to penetrate into the interior of uncross-linked fibrinogen was determined by H&E. These un-cross-linked scaffolds had cellularity into the scaffold interior at all time points **(see chapter 4)**.

Summary:

Thus, we show here that chemical cross-linking of fibrinogen scaffolds is linked to a negative effect on the cell response for both ASCs and BJs fibroblasts, leaving the scaffolds largely impenetrable. While cells will attach to cross-linked fibrinogen, cells appear to more rapidly penetrate into the scaffold if left in a native, uncross-linked form. Noting by H&E sections that uncross-linked scaffolds showed cells inside of the scaffolds at early and late time points, cross-linking was thus avoided in all the following experiments, which are encompassed in chapter 5.

-Appendix B-

Bioelectrospinning

Our preliminary studies taught us that synthesizing a natural appearing biological tissue enriched with progenitor cells is an arduous task using conventional cell seeding methods on cross-linked electrospun scaffolds. Decreasing the time needed to cellularize an electrospun scaffold is important for producing workable research models, as well as for potentially developing a clinically relevant system. Appreciating the limitation of conventional scaffold seeding, a method for simultaneously electrosprayed ASCs and matrix material together, in a process here termed "bioelectrospinning" **(Fig. 52)**, was used to rapidly produce a highly cellularized tissue construct. This process produces sheets of cellularized scaffold material with entrapped stem cells in around 30min (instead of around 30 days), producing an evenly colored pink scaffold (pink from phenol red dye-containing media) **(Fig. 53A)**. Scaffolds produced by this bioelectrospinning process show large numbers of apparent cell clusters visible under light microscopy **(Fig. 53B-C, D-I)**.

After optimizing many critical parameters in the bioelectrospinning process, as described in the main methods section, the bioelectrospun constructs created remained moist throughout the bioelectrospinning process and cells remained viable for up to a month after the bioelectrospinning process. Initial "test" or acellular control bioelectrospun scaffold sheets were formed by electrospraying media alone into the spinning matrix, used to setup the intricate electrospraying parameters, and also for use as a negative, acellular control in later experiments **(Fig. 53D).**

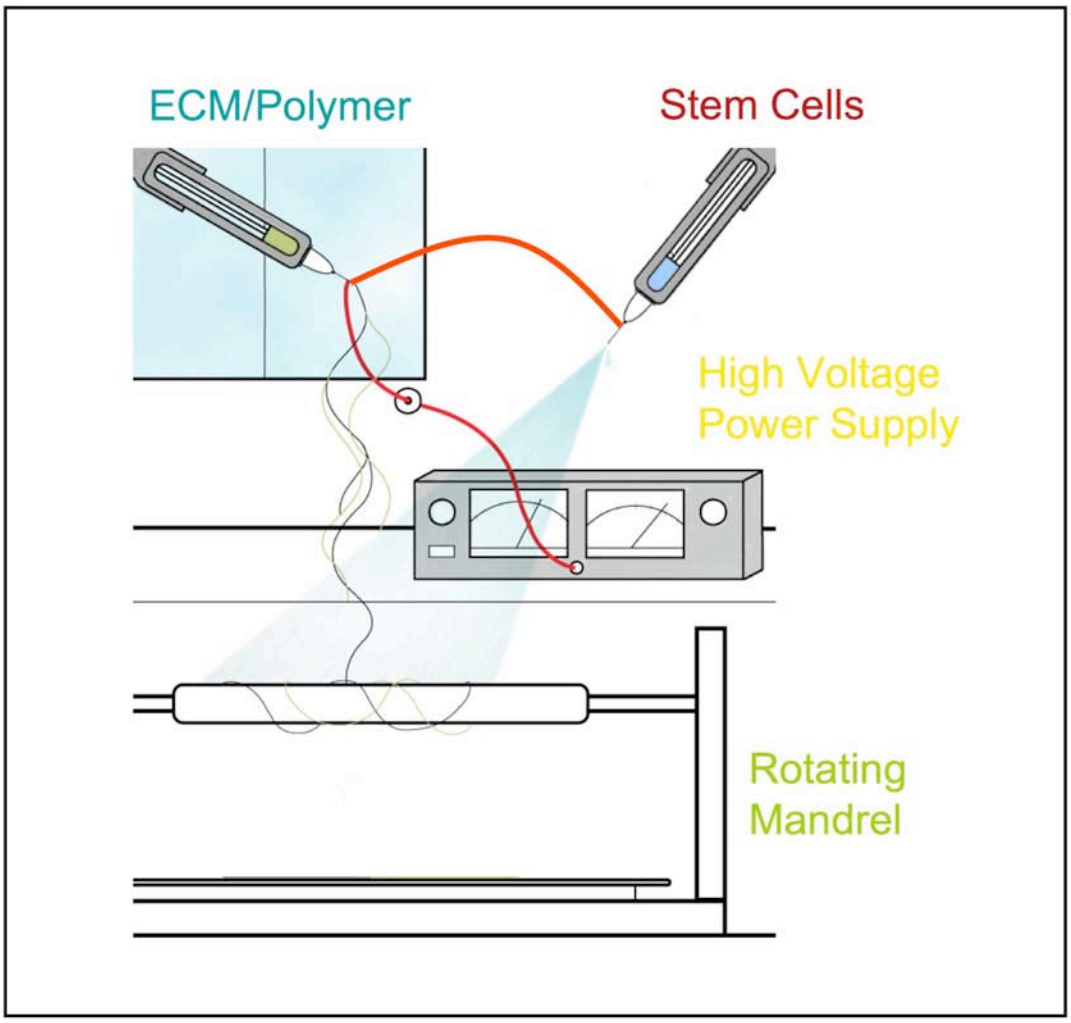

Figure 51. Bioelectrospinning Illustration. Modifying the standard electrospinning apparatus, a syringe filled with cells and media each placed on a syringe pump, is "jumpered" to a syringe containing an extracellular matrix polymer solution, thereby connecting both syringes to a high voltage power supply. With the syringes slowly presenting polymer/ECM and cells/media the high voltage power supply draws nanofibers out of the polymer that deposit in the rotating mandrel scaffold collection target, while the voltage creates an electrospraying effect. The stem cells, with media, are concurrently sprayed into the spinning fibrous scaffold.

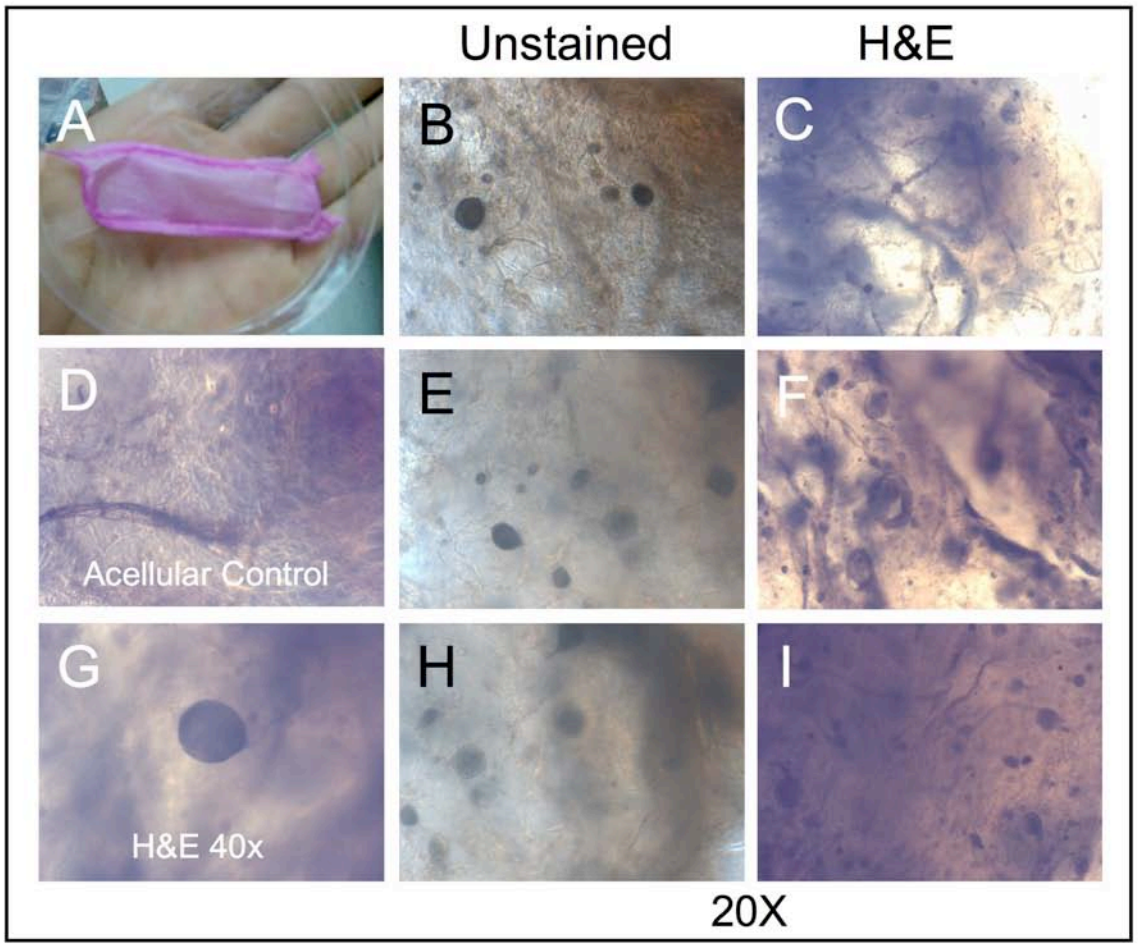

Figure 52. Bioelectrospun ASCs in Fibrinogen:PDO Histology. ASCs concurrently spun within spinning Fg:PDO are shown at the macroscopic level, with a wet, evenly pink sheet of tissue construct formed from the process (A). An acellular control was spun for reference (D). Scaffolds created by this process are shown unstained under phase microscopy (B, E, H) and as H&E stained (C, F, G, I).

In developing the bioelectrospinning process, ASCs were initially encapsulated in alginate, a viscous gum derived from brown algae and widely used in tissue engineering for cell immobilization and cell encapsulation, to protect cells from possible harm endured from the electric field and organic solvent, and to keep the cells moist during the electrospraying process. However, the alginate, mixed at the predetermined ideal 25% concentration for spraying the cells/media (with ABAM), produced scaffolds with poor mechanical properties. Scaffolds with alginate-encapsulated cells quickly dissolved in static culture in 5-7 days, and these scaffolds did not last more than 72 hours in bioreactor cultures before disintegrating. A 50:50 fibrinogen:PDO scaffold was used in all bioelectrospinning experiments as the electrospun fibrinogen alone dissolved on the mandrel when electrosprayed with media/cells, and the PDO alone had proven a poor substrate for ASC growth and differentiation by this point.

We proceeded to concurrently spray ASCs in media without alginate or other protectant into the electrospinning fibrinogen:PDO, which faired more stable in culture then alginate-containing scaffolds. Cells sprayed into the spinning matrix remained viable within the solid, stable construct for at least 6 weeks. Bioelectrospun ASCs were readily dissociated from the 2 week old scaffolds with vigorous pipetting agitation. These released cells were able to be re-cultured and expanded on plastic where they maintained a normal morphology, growth rate and maximum cumulative PD, suggesting that the process did not damage the cells.

After optimizing the intricate electrospraying/bioelectrospinning process, the ability of the scaffolds to support differentiating stem cells within the construct was next tested. $2x10^7$ ASCs (both ASC-8 and ASC-9) were spun in 50:50 fibrinogen:PDO blended scaffold sheets, from which 10mm punches were collected and left in static culture for 12 hours to promote cell

attachment and proliferation. The next day, punches where placed in 4 separate rotating vessel bioreactors filled with either normal growth media, osteogenic differentiation media, adipogenic media, or treated for 24hrs with 5-azacytidine, a global demethylating agent shown to induce cardiomyocyte differentiation in MSCs. Adipogenic and myogenic differentiation were included to validate the multipotential differentiation capacity of ASCs in bioelectrospinning process. A bioreactor with an acellular bioelectrospun sheet of fibrinogen:PDO and osteogenic media was included for a negative control.

Preliminary SEM work showed promising results, particularly in stimulating bone synthesis. While a control cell-free scaffold had a familiar acellular fibrinogen:PDO appearance under SEM **(Fig 54F)**, only scaffolds with cells grown in osteogenic media produced distinct, porous, honeycomb-like structures **(Fig. 54A-E)**. Bone induced scaffolds at 3 weeks of differentiation were phenotypically hard and brittle, while the control scaffolds remained pliable. Scaffolds in adipogenic and myogenic media also showed a pronounced change in topography under SEM analysis as shown in **Figure 55**. At this point, equipment issues, notably the loss of the electrospinning translator apparatus and the power supplies requisite for the process, precluded any further experiments and no further lines of research could be explored using this bioelectrospinning process.

SUMMARY:

While cells are typically seeded upon electrospun matrices on the outside, with days to weeks or months of time given for cells to penetrate throughout the construct, it has recently been shown that myocytes, fibroblasts and zebrafish eggs can be concurrently sprayed into

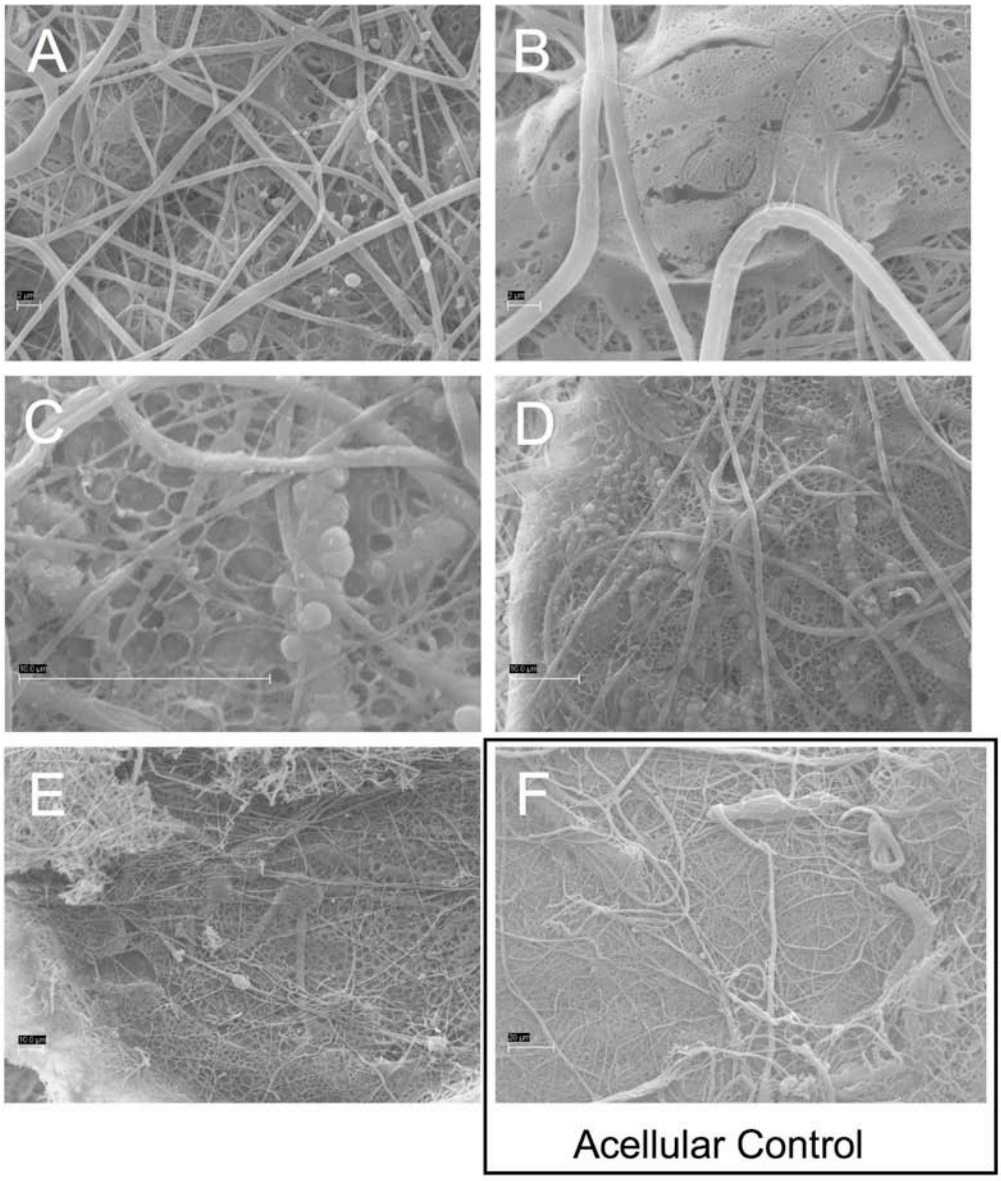

Figure 53. Topography of Osteo-Induced ASC Seeded within Fibrinogen. ASCs were bioelectrospun into Fg:PDO and placed in bioreactor culture for 21 days (A-E) with osteogenic differentiation media, then visualized under SEM. An acellular control was also formed and grown in a bioreactor with osteogenic media (F).

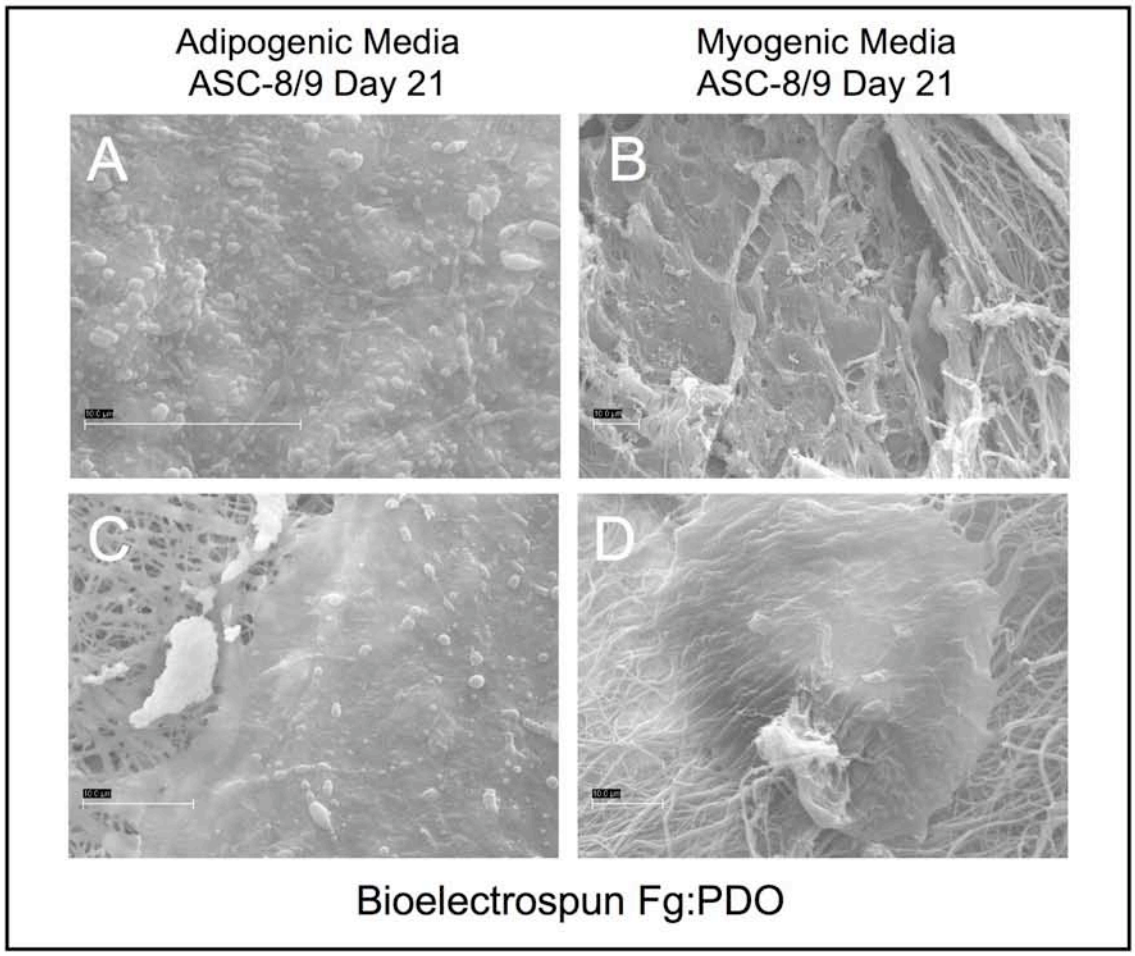

Figure 54. Topography of Bioelectrospun ASC Differentiated to Fat and Muscle. ASCs were bioelectrospun into Fg:PDO and placed in bioreactor culture for 21 days with adipogenic (A, C) or myogenic (B,D) differentiation media, then visualized under SEM for unique topographical features.

electrospinning fibers, thereby rapidly producing a highly cellularized tissue analogue rich with cells entrapped in a biomimetic nanofibrous mesh (Stankus et al, 2006 & 2007). Bioelectrospinning has gained considerable popularity since our studies have been conducted. Remarkably, the bioelectrospraying process appears not to affect karyotypic stability or alter the normal development of electrosprayed cells, and also allows robust mesenchymal stem cell differentiation in the bioelectrospun scaffold (Gupta et al. 2009, Mongkoldhumrongkul et al. 2009, Geach et al. 2009, Maeng et al., 2009, Hall et al. 2008). Clarke et al. (2008) were even able to electrospray zebrafish embryos and show that viable, normally developed adult fish are produced even after being subjected to the high voltage electrostatic field. Electrospraying can also be useful for material deposition, such as spraying a scaffold with hydroxyapatite to speed or even induce the osteogenesis process.

With the importance of the ECM in development and the stem cell niche in mind, entwining cells in a true 3D scaffold rather then seeding cells on one side of a scaffold may prove highly important in directing the cell bioactivity, for changes in cell metabolism, migratory and proliferative activity, and even in altering a cells differentiation potential, its rate of differentiation and gene expression, all of which should be further explored in this process. Following this path, the next step in advancing electrospun tissue engineered scaffolds will be applying highly proliferative, karyotypically stable yet potent stem cells, such as ASCs, to this matrix.

APPENDIX METHODS

Cross-linking

Glutaraldehyde Cross-linking. Scaffolds were placed in 50% glutaraldehyde (GLUT) (Fisher Scientific) vapor chamber at RT for 1 hour. For constructing the vapor chamber, 2ml of GLUT in an open 35mm Petri dish was situated inside a 100mm diameter Petri dish, with scaffolds laid inside the large dish, then parafilm sealed. After the 1hr incubation, the scaffolds were removed and allowed to degas for an additional hour.

EDC Cross-linking. The 1-ethyl-3-(3-dimethyl aminopropyl) carbodiimide (EDC) (Sigma) cross-linking protocol used in this study was modified from a similar protocol used to cross-link electrospun type II collagen (Barnes et al. 2007). Based on the molecular weight of fibrinogen (340kDa), the molarity of the electrospun fibrinogen solution was determined to be 0.35mM. From this, an EDC solution at a 50-fold molar excess (17.6mM) was created by dissolving the cross-linker in pure ethanol (Fisher Scientific). Electrospun scaffolds were placed in 50ml of cross-linking solution for 18hr at RT, followed by a 2hr rinse in 0.1M sodium phosphate to hydrolyze any unreacted *O*-isoacylurea intermediates.

Genipin Cross-linking. The genipin cross-linking protocol used was similar to that of the EDC cross-linking protocol and was modified from a published protocol to cross-link porcine pericardia (Sung et al. 1998). Genipin powder (Wako Pure Chemical Industries, Ltd., Osaka, Japan) was dissolved in pure ethanol to a concentration of 30mM. Fibrinogen scaffolds were placed in 50ml of cross-linking solution for 72hrs at RT. It has been reported that when the genipin cross-linking process is complete, the cross-linked material transitions to a dark blue or a brownish color (Ferretti et al. 2006). As such, it was noted that the electrospun fibrinogen

scaffolds gradually changed color over the 3-day period, eventually reaching dark blue near the end of day 3. Scaffolds were removed from the cross-linker solution at the completion of the time course.

Controls. As both the EDC and genipin cross-linkers were dissolved in ethanol for 72hrs, a pure ethanol solution left on discs for an equal duration served as a control to ensure that the cross-linking effects were a result of the cross-linkers rather than the ethanol.

Bioelectrospinning

To simultaneously electrospray stem cells within a concurrently spinning Fibrinogen:PDO matrix, the matrix needle air gap to receiver mandrel distance was set at 10-12cm. The cell and media containing needle air gap to receiver mandrel distance was set to precisely 4.5cm. Cell/media flow rate was set at 12-15ml/hr, while the rate of matrix expulsion of 3ml/hr was found to be ideal. At least $2x10^7$ stem cells were used per 500mg of scaffold for good cellularity throughout. The use of two 10ml syringes on a dual syringe pump for electrospraying cells and 4 or more 5ml syringes of fibrinogen/PDO was required to form the scaffold rapidly (under 20min), in order to prevent scaffold drying and improve cell viability. A round 10cm diameter receiver mandrel was used to avoid turbulence induced by rectangular mandrels, which also improved cell and media deposition on the bioelectrospun construct. Constructs produced an evenly pink colored media distribution, made without electrical arching from the needles, allowing good matrix/cell deposition for a rapid synthesis, keeping the construct moist throughout the bioelectrospinning process. For all experiments, an initial "test" sheet was formed with only electrospraying media into spinning matrix, which was used to

pretest the delicate setup parameters and as a negative or acellular control.

Bioreactor Cultures

Forty-eight 10mm scaffold discs were punched from the sheet formed with cells in the bioelectrospinning process, with 12 being punched from the control acellular sheet. A total of 12 scaffolds were destined for 5 separate bioreactors. Four autoclaved 55ml Slow Turning Lateral Vessel (STLV) bioreactor chambers were setup on the Rotary Cell Culture System (RCCS) (Synthecon^{TM}). The vessels were conditioned prior to use and tested for leaks by filling with PBS to check for major leakage, then drained and filled with media and the vessels allowed to rotate for 2hrs to check for minor leaks. 12 scaffolds were placed in each bioreactor under sterile conditions, with one reactor containing the acellular bioelectrospun scaffold and osteogenic induction media, and 4 vessels containing bioelectrospun scaffold, one filled with basic ASC growth media, one containing osteogenic induction media, one with adipogenic media, and the fourth with myogenic induction media containing 5-Azacytadine. These 5 bioreactors used 4 distinct medias, and half of the media was changed every 2 days for 3 weeks. Cultures were performed under the standard conditions of 37ºC at 5% CO_2 in a humidified incubator. The rates of rotation required for suspending the scaffold discs in a perpetual freefall in the vessels was determined experimentally and adjusted as needed at each media change. In general, 17 RPM was sufficient to maintain the discs in freefall throughout the tissue development, except for osteogenic media containing vessel with cells, which required 27 RPM after a week of culture.

Fiber Diameter and Pore Size Measurement of Dry Scaffolds

SEM images of pore morphologies, fiber orientation and fibers size of dry electrospun sheets were captured using a Zeiss Evo50 scanning electron microscope using ImageJ64 (NIH shareware) to measure fiber diameter and pore size. 50 separate fiber diameter and 40 pore area measurements were used to determine the mean and standard deviation, with calibration for each image made with a corresponding scale bar.

Scaffold Porosity Measurement

Previous work has shown that electrospun fibrinogen scaffolds will contract and densify when placed in an aqueous solution (Barnes et al., 2007). For determining what effects cross-linking in GLUT, ethanol soaking, EDC, and genipin had on scaffold densification, the scaffold porosity was determined for each cross-linker and compared to uncross-linked fibrinogen samples. For each sample, 21mm diameter discs were punched from uncross-linked electrospun fibrinogen scaffolds in their dry state. The thickness and dry mass of the scaffolds were recorded, with the porosity or void fraction of the disc determined by as before (Sell et al., 2002):

$$Void\ Fraction = 1 - \left[\frac{Calculated\ Scaffold\ Density}{Known\ Material\ Density} x100\right]$$

Calculated scaffold density was determined by dividing the disc mass by the discs total volume, using 1.38g/cm^3 as the known dry density of fibrinogen (McManus et al., 2006). Discs were cross-linked as previously described with punches rinsed in PBS three times to remove any remaining cross-linker and soaked in PBS for 24hrs at RT. The next day, the thickness and diameter of the discs were recorded to determine the wet total volume after the PBS soak and following ethanol rinses. Using the void fraction equation, the hydrated void fraction was determined. By dividing the disk dry mass by the determined altered total volume of the hydrated

discs the hydrated calculated scaffold density was determined, which was then divided by the dry density of fibrinogen. Dry density and mass were used based on the assumption that the presence of water or ethanol in the void spaces would account for the difference in mass, as the actual electrospun fibers are unlikely to lose or gain mass.

VITA

Michael Francis was born on February 25, 1978 in Akron, Ohio. He attended Ellet High School, from which he graduated in 1996. He attended the University of Akron where he worked for 4 years in the genetics and hypertension research labs of Dr. Monte Turner and Dr. Amy Milsted. Michael received a Bachelor of Arts degree in Philosophy with a concentration in biomedical ethics, concurrently receiving a Bachelors of Science in Biology with molecular biology and genetics concentrations, both in 2001 from the University of Akron. Michael then moved to Houston, TX to work on Type II Diabetes research as a technician for Dr. Peter O'Connell at Baylor College of Medicine. In 2002, he moved to Richmond, Virginia with Dr. O'Connell where he worked on models of breast cancer as a lab manager at VCU. In 2004, Michael entered the Molecular Medicine and Systems Biology PhD graduate program at the University of Virginia in Charlottesville, VA, concentrating didactic studies in stem cell and developmental biology coursework, while working in various labs and experimenting on embryonic, germline, mesenchymal and hematopoietic stem cell systems. In 2006 he transferred to Virginia Commonwealth University to complete his PhD studies. He plans to resume his education at LifeNet in Virginia Beach with Dr. Roy Ogle.